SYSTEMATIC GROUND MOTION OBSERVATIONS IN THE CANTERBURY EARTHQUAKES AND REGION-SPECIFIC NON-ERGODIC EMPIRICAL GROUND MOTION MODELLING

Brendon A. Bradley

Research report 2013-03

Department of Civil Engineering
University of Canterbury
Christchurch
New Zealand

28 May 2013

Table of Contents

Executive Summary

Ground motion observations from the most significant 10 events in the 2010-2011 Canterbury earthquake sequence at near-source sites are utilized to scrutinize New Zealand (NZ)-specific pseudo-spectral acceleration (SA) empirical ground motion prediction equations (GMPE) (Bradley 2010, Bradley 2013, McVerry et al. 2006). Region-specific modification factors based on relaxing the conventional ergodic assumption in GMPE development were developed for the Bradley (2010) model. Because of the observed biases with magnitude and source-to-site distance for the McVerry et al. (2006) model it is not possible to develop region-specific modification factors in a reliable manner. The theory of non-ergodic empirical ground motion prediction is then outlined, and applied to this 10 event dataset to determine systematic effects in the between- and within-event residuals which lead to modifications in the predicted median and standard deviation of the GMPE. By examining these systematic effects over sub-regions containing a total of 20 strong motion stations within the Canterbury area, modification factors for use in region-specific ground motion prediction are proposed. These modification factors, in particular, are suggested for use with the Bradley et al. (2010) model in Canterbury-specific probabilistic seismic hazard analysis (PSHA) to develop revised design response, particularly for long vibration periods.

The proposed modification factors and impact on the Bradley (2010) GMPE are summarised in Table 5, Figure 7c, and Figure 17 of the main document, repeated below.

Table 5: Numerical values of the proposed design factors for CBD ground motion prediction

	Median modification			St. dev. modification		
Period, T (s)	$\delta L2L$	$\delta S2S$	MAF	SRF_{τ}	SRF_{σ}	SRF_{σ_T}
0	-0.06	0.05	0.99	0.87	0.80	0.80
0.01	-0.06	0.03	0.97	0.87	0.80	0.80
0.02	-0.06	0.02	0.96	0.87	0.80	0.80
0.03	-0.06	0.01	0.95	0.87	0.80	0.80
0.05	-0.06	-0.02	0.93	0.87	0.80	0.80
0.1	-0.06	-0.08	0.87	0.87	0.80	0.80
0.15	-0.06	-0.15	0.81	0.87	0.80	0.80
0.2	-0.04	-0.06	0.91	0.87	0.80	0.80
0.25	0.01	0.03	1.05	0.87	0.80	0.80
0.3	0.07	0.13	1.21	0.87	0.80	0.80
0.4	0.12	0.31	1.54	0.87	0.80	0.80
0.5	0.13	0.40	1.70	0.87	0.80	0.80
0.7	0.14	0.40	1.71	0.87	0.78	0.78
1.0	0.16	0.40	1.74	0.87	0.70	0.70
1.5	0.18	0.40	1.79	0.83	0.69	0.69
2.0	0.21	0.40	1.84	0.80	0.69	0.69
3.0	0.27	0.40	1.95	0.73	0.68	0.68
4.0	0.32	0.256	1.78	0.65	0.67	0.67
5.0	0.38	0.08	1.58	0.58	0.66	0.66
7.5	0.51	0.08	1.81	0.58	0.63	0.63
10.0	0.65	0.08	2.07	0.58	0.60	0.60

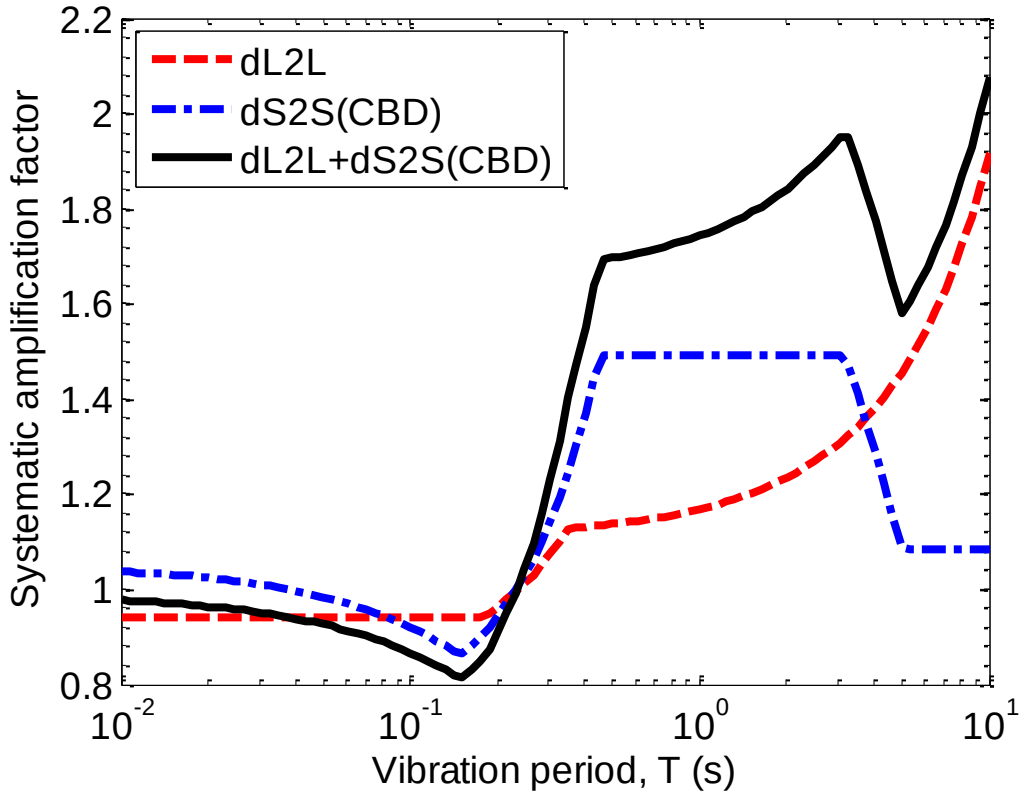

Figure 7c: Implied amplification factors in the median GMPE prediction.

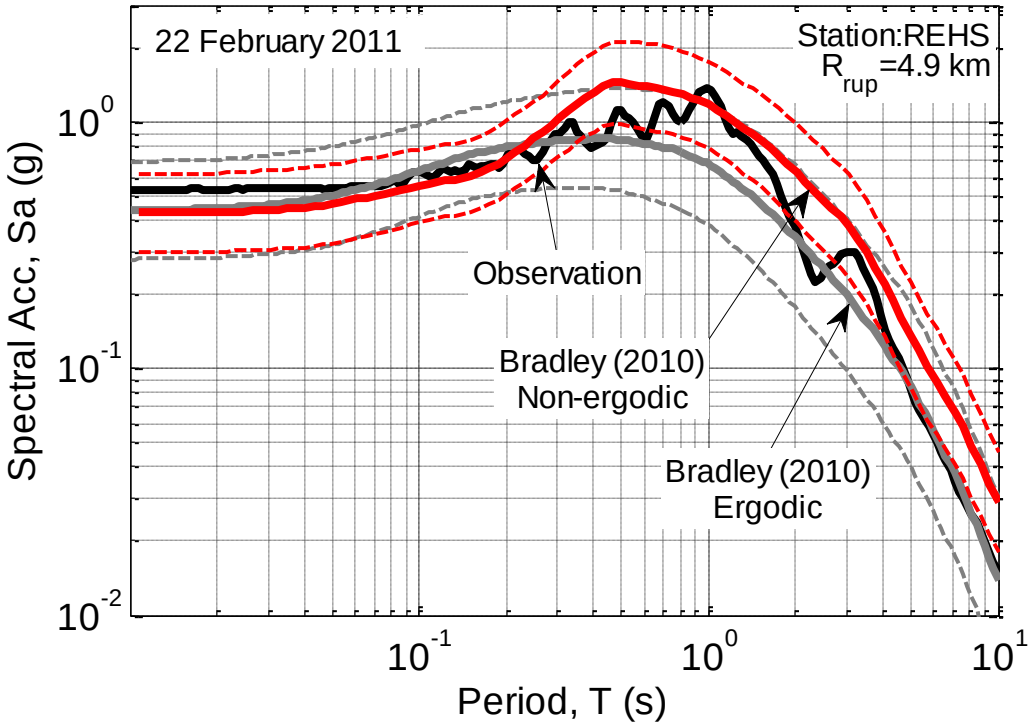

Figure 17: Comparison of the ergodic Bradley (2010) model and the CBD-specific non-ergodic model as compared to observations from the major Canterbury earthquakes.

1. Observed ground motion observations and predictions

Before embarking on developing region-specific modification factors for an empirical ground motion prediction equation (GMPE) it is necessary to first examine the performance of the GMPE against observed ground motions. Such an examination seeks to illustrate that it is unbiased in a global sense, and that the observed variability in the observations is partially a result of systematic effects which are not accounted for in the simplified representation of the earthquake source, path, and site effects.

In this document attention is given solely to examining ground motion severity in the form of elastic pseudo-acceleration response spectral ordinates (SA), although it is noted that the methodology employed could be adopted for any general intensity measure.

1.1. Earthquake events and strong motion stations considered

In selecting the events considered a trade-off was required between the number of events and the representative size of the ground motion amplitudes produced. Considering a larger number of events provides statistically more robust estimates (i.e. larger sample sizes). However, in order to consider more events the minimum allowable event magnitude obviously has to be reduced. As a result, the overall dataset becomes increasingly dominated by smaller amplitude ground motions which are not of primary concern when GMPEs are utilized in PSHA. Furthermore, there are an abundance of studies illustrating the lack of correlation between GMPE performance for small and large magnitude events.

As a result, only events above magnitude M_w4.5, which produced ground motions of engineering significance in the urban Christchurch area, were considered. This resulted in a set of 10 events, the basic details of which are given in Table 1. Following the same logic as above, a maximum source-to-site distance for recorded ground motions was also utilized to remove those ground motions which are of low amplitude.

Table 1: Earthquake events considered

ID	Event date	Magnitude, M_w	Maximum source-to-site distance, R_{rup}^{max} (km)
1	4 September 2010 ("Darfield")	7.1	100
2	19 October 2010	4.8	30
3	26 December 2010	4.7	30
4	22 February 2011 ("Christchurch")	6.2	50
5	16 April 2011	5.0	30
6	13 June 2011 (1:01pm)	5.3	50
7	13 June 2011 (2:20pm)	6.0	50
8	21 June 2011	5.2	30
9	23 December 2011 (12:58pm)	5.8	50
10	23 December 2011 (1:18pm)	5.9	50

As already noted, the selected events produced ground motions of significance in the urban Christchurch region. A total of 20 strong motion stations were considered in this region. Table 2 provides a list of the 20 considered strong motion stations, and the values of geometric mean PGA which were recorded for each of the 10 events. It should be emphasised that for each event, strong motion stations in addition to those in Table 2 were used for computing the between-event residual (i.e. all stations which recorded ground motions within a distance of R_{rup}^{max} for a given event).

Table 2: Strong motion stations for which systematic site effects are considered and the observed geometric mean PGA values

Station	Num events, NE_s	Observed geometric mean peak ground acceleration in each event, PGA (g)									
		1	2	3	4	5	6	7	8	9	10
CACS	10	0.197	0.027	0.020	0.21	0.034	0.081	0.136	0.104	0.073	0.083
CBGS	10	0.158	0.069	0.270	0.50	0.070	0.183	0.163	0.077	0.157	0.210
CCCC	6	0.224	0.119	0.227	0.43	-	-	-	-	0.134	0.179
CHHC	10	0.173	0.089	0.162	0.37	0.146	0.199	0.215	0.115	0.174	0.222
CMHS	9	0.237	0.191	0.132	0.37	0.137	0.159	0.178	-	0.152	0.174
HPSC	10	0.147	0.041	0.049	0.22	0.148	0.180	0.256	0.068	0.199	0.264
HVSC	10	0.606	0.091	0.111	1.41	0.676	0.455	0.914	0.264	0.306	0.439
KPOC	8	0.339	0.013	0.012	0.20	0.052	0.186	0.099	0.067	-	-
LINC	10	0.437	0.034	0.020	0.12	0.028	0.026	0.065	0.114	0.062	0.073
LPCC	9	0.290	0.025	0.018	0.92	0.294	0.146	0.639	0.068	-	0.437
NBLC	6	-	-	0.025	-	0.129	0.232	0.214	0.040	0.201	-
NNBS	8	0.206	0.042	0.039	0.67	0.156	0.239	0.198	0.070	-	-
PPHS	10	0.221	0.048	0.091	0.21	0.062	0.118	0.122	0.074	0.116	0.138
PRPC	9	0.214	0.054	0.087	0.63	0.223	0.299	0.341	0.089	0.290	-
REHS	10	0.252	0.081	0.245	0.52	0.101	0.188	0.264	0.086	0.204	0.254
RHSC	9	0.210	0.282	-	0.28	0.075	0.083	0.194	0.202	0.159	0.159
ROLC	10	0.340	0.013	0.022	0.18	0.013	0.036	0.045	0.111	0.102	0.062
SHLC	10	0.175	0.072	0.156	0.33	0.116	0.245	0.184	0.076	0.262	0.275
SMTC	10	0.176	0.020	0.034	0.16	0.034	0.132	0.085	0.078	0.066	0.148
TPLC	10	0.266	0.058	0.032	0.11	0.024	0.037	0.065	0.250	0.068	0.081

1.2. Comparison of NZ-specific GMPEs with the Canterbury earthquakes

The representation of (pseudo) spectral acceleration (SA), from event e, at a single location s, for the purposes of ground motion prediction, is generally given by:

$$lnSA_{es} = f_{es}(Site, Rup) + \delta B_e + \delta W_{es} \quad (1)$$

where $lnSA_{es}$ is the (natural) logarithm of the observed SA; $f_{es}(Site, Rup)$ is the median of the predicted logarithm of SA as given by an empirical ground motion prediction equation (GMPE), which is a function of the site and earthquake rupture considered; δB_e is the between-event (or inter-event) residual with zero mean and variance τ^2; and δW_{es} is the within-event (or intra-event) residual with zero mean and variance σ^2. Based on equation (1), empirical ground motion prediction equations can provide the distribution of SA as:

$$lnSA_{es} \sim N(f_{es}, \tau^2 + \sigma^2) \quad (2)$$

where $X \sim N(\mu_X, \sigma_X^2)$ is short-hand notation for X having a normal distribution with mean μ_X and variance σ_X^2.

Two GMPEs are currently employed for ground motion prediction within seismic hazard analyses performed by GNS Science. The "McVerry et al. (2006) model" (McVerry et al. 2000, McVerry et al. 2006) was developed in 1997 and has been subsequently utilized in NZ PSHA for over a decade. The "Bradley (2010) model" (Bradley 2010, Bradley 2013) is a more recent model, developed on the basis of foreign GMPEs, and has been employed in NZ PSHA by GNS following the Canterbury earthquakes. Below a comparison of these two models with data from the Canterbury earthquakes is illustrated as a starting point for the subsequent non-ergodic considerations.

1.2.1. The Bradley (2010) model

Figure 18-Figure 27 in Appendix 1 illustrate the SA observations at periods of 0.0 (i.e. PGA), 0.2, 1.0, and 3.0 for the 10 considered events as compared to the site class D prediction of Bradley (2010). An elaborate discussion of the Bradley (2010) model performance for these events in the Canterbury earthquake sequence is not given here, however, the following general points are noted:

- Across the 40 plots shown in Figure 18-Figure 27 the model exhibits good scaling of SA amplitudes with distance, even for very near-source distances – i.e. the R_{rup} scaling is unbiased (see Figure 18 of Bradley (2013) for further details).
- The model provides a consistent prediction of ground motions from events of different magnitudes. Obviously for individual events there will be non-zero values of the between-event residual, δB_e (as noted in the top right of each plot), however, these values are centered around zero, and do not display any apparent trends with event magnitude (as illustrated later).
- There is a slight systematic bias in the model predictions at long vibration periods (i.e. $T \geq 3s$). This could be a result of the fact that GMPEs are generally least constrained for such long periods because a significantly lower number of empirical ground motion data which is useable at these long periods. It could also be the result of Christchurch-specific wave propagation due to the stratigraphy of surficial and deep geological sediments. This is elaborated upon further in the subsequent sections.

- Some large events occurred in quick succession of each other. For example, on 13 June 2011 and 23 December 2011 two large events ($M_w 5.3/6.0$ and $M_w 5.8/5.9$, respectively) occurred approximately 80mins apart. Both of these events occurred near the east of Christchurch, which has soft surficial soil deposits. As a result, it is speculated that the ground motions recorded in the latter event of these two sequences were affected by the surficial soils having elevated pore water pressures from the strong shaking in the earlier event. Such speculation would be expected to result in a general over prediction of short period SA amplitudes and under prediction of long period SA amplitudes because of the reduced stiffness of the soft surficial soils due to elevated pore pressures. The plots in Figure 24 and Figure 27 (with the exception of Figure 27d) all provide quantitative evidence in accordance with this speculation. Effective stress analyses, which account for this effect, should be conducted in order to confirm this apparent influence in the observations. No effect is accounted for this in the subsequent analyses.
- Although not shown explicitly in Figure 18-Figure 27, the standard deviation of the within-event residuals for each event is consistent with the model standard deviation (see Figure 18 of Bradley (2013) for further details).
- The results presented here are for the site class-based version of the Bradley (2010) model without the explicit inclusion of near-source directivity.

Figure 18-Figure 27, and the above comments, illustrate that the Bradley (2010) model provides an unbiased prediction of the 10 considered events as a function of various model parameters. However, clearly these figures also point to the significant variability in the observations for a given set of model parameters. A large portion of this variability arises due to systematic features of the specific sites at which the ground motions were recorded, features which are not adequately captured in the simple parameterization used in GMPEs. The subsequent sections therefore examine the between- and within-event residuals obtained for the Bradley (2010) GMPE in order to ascertain these site specific systematic effects.

1.2.2. The McVerry et al (2006) model

Figure 28-Figure 37 in Appendix 1 illustrate the SA observations at periods of 0.0 (i.e. PGA), 0.2, 1.0, and 3.0 for the 10 considered events as compared to the site class D prediction of McVerry et al. (2006). An elaborate discussion of the McVerry et al. (2006) model performance for these events in the Canterbury earthquake sequence is not given here, such details have been discussed at length in Bradley (2012a). The performance of the McVerry et al. (2006) model with respect to another recent NZ-wide dataset is also given in Bradley (Bradley 2010, Bradley 2013). From Figure 28-Figure 37 the following general points are briefly noted:

- The model exhibits quite different scaling of SA amplitudes with distance than is observed in data. This is particularly the case at medium to long vibration periods (i.e. $T = 1\text{s},3s$). As a result, (i) the amplitudes of near-source ground motions are often under-estimated; and (ii) the between-event residual can no longer give a reasonable indication of overall model over- or under-prediction, because it will depend on the proportion of observations at near and far distances.
- The model generally provides a poor representation of the observed SA values for small magnitude events (i.e. $M_w < 6$), typically significantly over-predicting the observed SA amplitudes.

- In terms of the performance of the model at different vibration periods, it can be stated that, relatively speaking: (i) the model is most robust for the estimation of PGA; (ii) the model generally over predicts the ground motion SA(0.2s) amplitudes; (iii) the model generally under predicts SA(1.0) and SA(3.0) amplitudes. However, the other competing biases with R_{rup} and M_w noted above have an additional effect on these three noted period dependencies.

Figure 28-Figure 37, the above comments, and other references (Bradley 2010, Bradley 2012a, Bradley 2013), illustrate that the McVerry et al. (2005) model contains several biases (M_w, R_{rup}, T). As a result, the deviations between the model prediction and observations (as represented by the between- and within-event residuals) using this model cannot be possibly attributed to systematic effects of the ground motion recording sites. Hence, systematic features of the residuals using the McVerry et al. (2006) model are not considered in the subsequent sections.

It is also noted, in addition, that the aim of this work is to develop Canterbury-specific ground motion prediction over a broad range of vibration periods (specifically PGA and SA for $T = 0.01s$ to $10s$). As the McVerry et al. (2006) model only provides predictions for $T \leq 3s$ it means that it could not be utilized for this broad range of periods in any case.

2. Non-ergodic ground motion prediction

The representation of SA GMPE's given in the previous section is based on the ergodic assumption, i.e. the time-averaged behaviour of a random process at a given location is the same as the space-averaged behaviour at given instants in time. Practically speaking, the ergodic assumption is invoked when ground motion records from different locations around the globe are combined for the purposes of ground motion prediction at a single location. Several studies have illustrated that the ergodic assumption generally leads to an over-prediction of ground motion uncertainties because it combines variability in source, path and site effects from different tectonic regions and sites, and some of this variability may in fact be systematic in a site-specific context. Further technical details on the ergodic assumption in ground motion prediction is given elsewhere (Anderson and Brune , Atik et al. 2010, Lin et al. 2011, Rodriguez-Marek et al. 2011, Walling 2009).

The ergodic assumption can be relaxed by considering that the between- and within-event residuals, given in Equation (1), are no longer purely random variables with zero-mean, but systematically depart from this for a given earthquake source (or source region) and given site of interest. In general, systematic effects due to source, path and site effects can be considered.

One possible methodology for considering such effects is given by Lin et al. (2011) and Walling (2009), which will be employed here. Firstly, the between-event residual, δB_e, is separated into a systematic event location-to-location (here simply 'location-to-location') residual (for location *l*), $\delta L2L_l$, and a 'remaining' between-event residual, δB_{el}^0 (i.e. $\delta B_e = \delta L2L_l + \delta B_{el}^0$). Secondly, the within-event residual, δW_{es}, is separated into a systematic 'site-to-site' (or 'station-to-station' (Rodriguez-Marek et al. 2011)) residual (for site *s*), $\delta S2S_s$, and a 'remaining' within-event residual, δW_{es}^0 (i.e. $\delta W_{es} = \delta S2S_s + \delta W_{es}^0$). As a result, Equation (1) can be re-written as:

$$lnSA_{es} = f_{es}(Site, Rup) + (\delta L2L_l + \delta B_{el}^0) + (\delta S2S_s + \delta W_{es}^0) \quad (3)$$

It should be noted that no consideration has been given to a path-specific effect in the within-event residual, as done so by Lin et al. (2011), for example. The principal reason for this omission is that only near-source recordings from moderate-to-large magnitude earthquakes are considered. As a result, ray paths from different sub-faults in the idealized rupture plane can be quite different. This makes determination of the specific ray path to be used in consideration of spatial correlation and path-specific effects non-unique.

In addition it is noted that the all 10 earthquake events considered here are taken to be from the same 'Canterbury' region so that all events are considered to have the same location-to-location residual, $\delta L2L_l$. Subsequent analyses examine that this residual is not a function of event magnitude.

The subsequent two sections discuss these two sub-components of δB_e and δW_{es}, how they can be estimated, and how the non-ergodic standard deviations of the four residuals can be determined to obtain the total model residual.

2.1. Between-event residual and its components

As noted in Equation (3), the between-event residual, δB_e, is considered to be comprised of two parts. The systematic location-to-location residual can be computed as the average value of δB_e from all the events considered:

$$\delta L2L_l = \frac{1}{NE}\sum_{e=1}^{NE} \delta B_e \tag{4}$$

where NE is the number of events (i.e. $NE = 10$ in this study). For each event the 'remaining' portion of the between-event residual, δB_e^0, can then be computed from:

$$\delta B_{el}^0 = \delta B_e - \delta L2L_l \tag{5}$$

By definition, since $\delta L2L_l$ is the average of δB_e, δB_{el}^0 has zero mean. In addition to their mean values, both $\delta L2L_l$ and δB_{el}^0 are uncertain. The uncertainty in $\delta L2L_l$ results from the fact that it is computed from a finite number of events, and hence its variance can be computed from:

$$Var[\delta L2L_l] = \tau_{L2L}^2 = \frac{\tau^2}{NE} \tag{6}$$

where τ^2 is the variance in the between-event residual, δB_e. The variance in the 'remaining' between-event residual can be computed simply from statistical inference of the values of δB_{el}^0:

$$\tau_0^2 = Var[\delta B_{el}^0] = \frac{1}{NE-1}\sum_{e=1}^{NE} (\delta B_{el}^0)^2 \tag{7}$$

2.2. Within-event residual and its components

As noted in Equation (3), the within-event residual, δW_{es}, is considered to be comprised of two parts. The systematic site-to-site residual can be computed for each site (i.e. strong motion station) as the average value of δW_{es} from all the events considered:

$$\delta S2S_s = \frac{1}{NE_s}\sum_{e=1}^{NE_s} \delta W_{es} \tag{8}$$

where NE_s is the number of events at site s. Since not all events are recorded at the same set of locations then $NE_s \leq NE$, and the value of NE_s for each site is given in Table 2. Once $\delta S2S_s$ has been computed, the 'remaining' within-event residual can be computed as:

$$\delta W_{es}^0 = \delta W_{es} - \delta S2S_s \tag{9}$$

By definition, since $\delta S2S_s$ is the average of δW_{es}, δW_{es}^0 has zero mean. In addition to their mean values, both $\delta S2S_s$ and δW_{es}^0 are uncertain. The uncertainty in $\delta S2S_s$ results from

the fact that it is computed from a finite number of events, and hence its variance can be computed from:

$$Var[\delta S2S_s] = \sigma_{S2Ss}^2 = \frac{\sigma^2}{NE_s} \tag{10}$$

where σ^2 is the variance in the within-event residual, δW_{es}. The variance in the 'remaining' within-event residual can be computed simply from statistical inference of the values of δW_{es}^0:

$$\sigma_0^2 = Var[\delta W_{es}^0] = \frac{1}{NE_s - 1}\sum_{e=1}^{NE_s}(\delta W_{es}^0)^2 \tag{11}$$

2.3. Non-ergodic prediction

Having characterized the components of the between- and within-event residuals and their sub-components in the previous section it is now possible to obtain the mean and variance of the non-ergodic GMPE. The mean value of $lnSA_{es}$ is given by:

$$E[lnSA_{es}] = f_{es} + \delta L2L_l + \delta S2S_s \tag{12}$$

since $E[\delta B_{el}^0] = E[\delta W_{es}^0] = 0$. Because SA_{es} has a lognormal distribution then it follows that the median value of SA_{es} can be obtained as the exponential of the mean of $lnSA_{es}$:

$$Median[SA_{es}] = exp\{E[lnSA_{es}]\} \tag{13}$$

In examining the two systematic effects, $\delta L2L_l$ and $\delta S2S_s$, it is useful to consider a 'median modification factor'(MMF) which is the ratio of the non-ergodic to ergodic median GMPE predictions. Taking the ratio of Equations (12) and the median from Equation (2) gives:

$$MMF = \frac{Median[SA_{es}]_{nonergodic}}{Median[SA_{es}]_{ergodic}} = exp(\delta L2L_l + \delta S2S_s) \tag{14}$$

Making the conventional, and adequate, assumption that the different residuals are uncorrelated, the variance of the non-ergodic prediction can be obtained as:

$$Var[lnSA_{es}] = (\tau_{L2L}^2 + \tau_0^2) + (\sigma_{S2Ss}^2 + \sigma_0^2) \tag{15}$$

For each of the between-event, within-event, and total residuals, a standard deviation modification factor can be computed for the ratio of the non-ergodic and ergodic standard deviations:

$$SMF_\tau = \sqrt{\frac{\tau_{L2L}^2 + \tau_0^2}{\tau^2}} \tag{16}$$

$$SMF_{\sigma} = \sqrt{\frac{\sigma_{S2Ss}^2 + \sigma_0^2}{\sigma^2}} \tag{17}$$

$$SMF_{\sigma_T} = \sqrt{\frac{(\tau_{L2L}^2 + \tau_0^2) + (\sigma_{S2Ss}^2 + \sigma_0^2)}{\tau^2 + \sigma^2}} \tag{18}$$

It is these variables: MMF, SMF_{τ}, SMF_{σ}, SMF_{σ_T} for which parametric relationships will be provided to develop Christchurch-specific modification factors for various regions in Christchurch.

3. Observed systematic effects from the Canterbury earthquakes

Using the methodology presented in section 2, and the ground motion observations and Bradley (2010) model discussed in section 1, systematic ground motion effects were examined in this section.

3.1. Between-event residual

Figure 1 illustrates the computed values for δB_e as a function of SA vibration period for the 10 events considered. Also shown is the systematic location-to-location residual, $\delta L2L$. It can be seen that for short vibration periods ($T \sim < 0.3s$) the value of $\delta L2L$ is approximately zero, illustrating that the Bradley (2010) is, on average, unbiased for these short vibration periods, across the events and strong motion stations considered. However, as the vibration period increases the value of $\delta L2L$ increases.

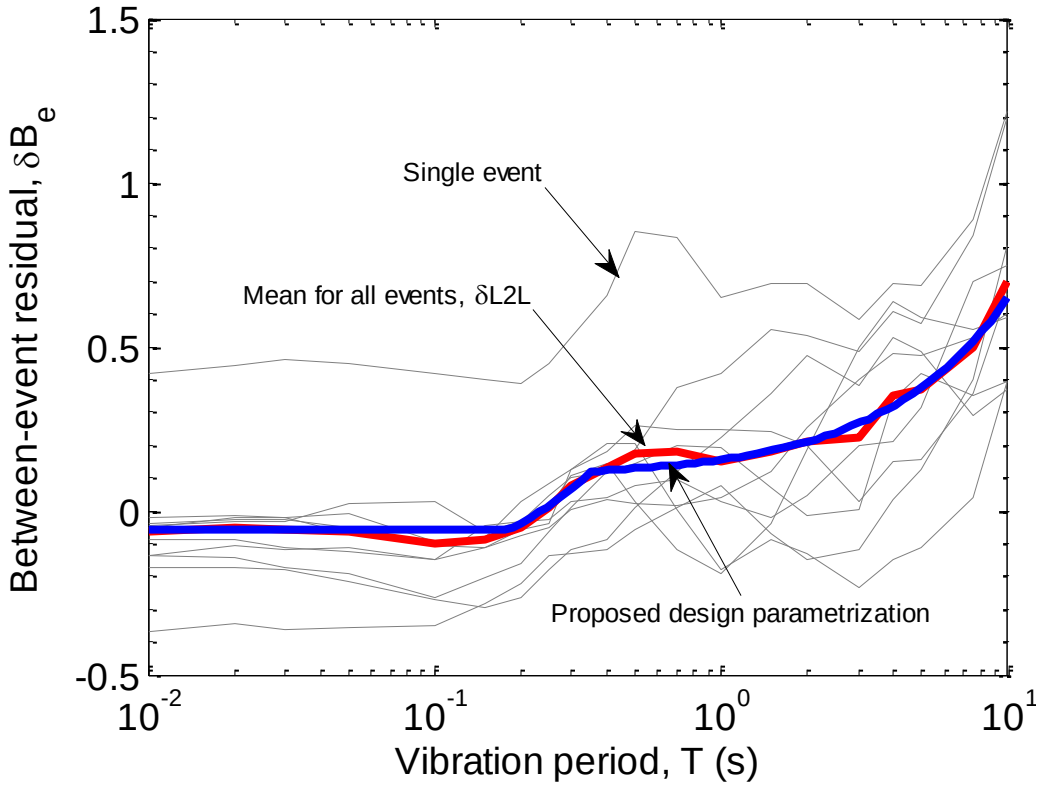

Figure 1: Computed between-event residuals, δB_e, for the considered 10 events, the location-to-location residual, $\delta L2L$, and the proposed design parametrization.

Bradley and Cubrinovski (2011) and Bradley (2012b) have suggested that greater than predicted SA amplitudes at long periods could be the result of: (i) near-source forward directivity; (ii) nonlinear response of soft surficial soils; (iii) basin-induced surface waves; and (iv) inherent model bias as a result of a limited amount of reliable ground motion records at long vibration periods. While all these points are plausible on a single ground motion observation by observation basis, noting that the observations in Figure 1 are based on sites in the Canterbury region located at various azimuths from 10 different earthquake events it can be said:

- (i) Forward directivity effects would not systematically affect sites at the range of azimuths considered, and such effects would not be significant for smaller magnitude events;
- (ii) As the majority of the stations considered are located on the Canterbury alluvial deposits nonlinear response of surficial soils may be of importance, since only ground motions from moderate-to-large magnitude earthquakes at close distances were considered (e.g. the average PGA in Table 2 is 0.183g).
- (iii) Again, as the majority of the stations considered are located on the Canterbury alluvial deposits, basin-induced surface waves may be of importance.
- (iv) Inherent model bias is a possibility for very long periods (i.e. $T > 5s$), but is unlikely at shorter periods.

The dependence of the between-event residuals as a function of event magnitude for five different vibration periods is illustrated in Figure 2. It can be seen that there is no apparent (or statistically significant) trends in δB_e as a function of event magnitude. The only noteworthy observation is the relatively large δB_e values from the $M_w 5.0$ event on 16 April 2011. Without further investigation, the reason for this is not immediately apparent.

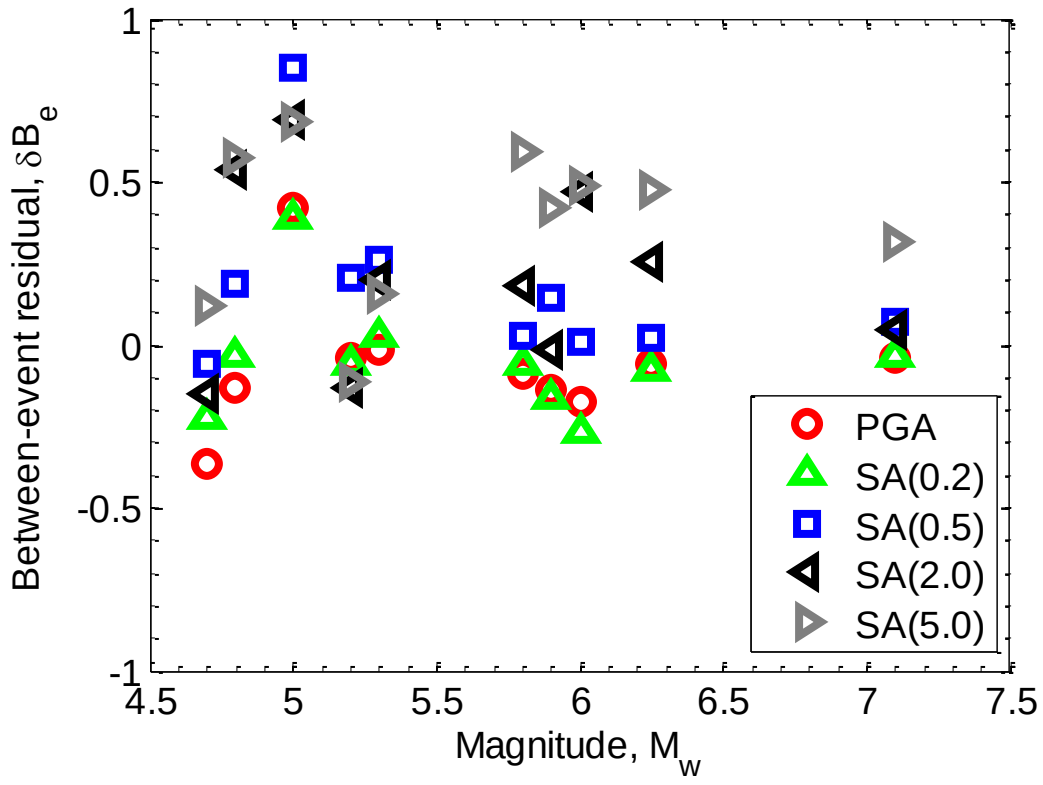

Figure 2: Variation in between-event residuals with magnitude for five different vibration periods.

While it is not possible to further investigate the cause of the systematic value of $\delta L2L$ in Figure 1, clearly it is a systematic feature of the observations in ground motion SA values for these sites in the Canterbury region, and therefore can be corrected for via non-ergodic modification factors. Nonetheless, the long period ground motion resulting from sources (ii) and (iii) above has been examined via 1D site response analysis simulations of the surficial and deep geotechnical stratigraphy beneath Christchurch as elaborated in Appendix 2.

The proposed design parameterization for the systematic effect in the between-event residual, $\delta L2L_l$, is a multi-linear interpolation of vibration period as depicted in Figure 1. The 'pinch points' which define the points within which the linear interpolation is applied are given in Table 3. The generic linear interpolation equation is given by:

$$y(T) = y_i + \frac{y_{i+1} - y_i}{T_{i+1} - T_i}(T - T_i) \tag{19}$$

where $T_i \leq T < T_{i+1}$, and y is a generic variable to be interpolated, in this case the location-to-location residual, $\delta L2L_l$. Note that the linear interpolation with T, appears as an exponential variation when a logarithmic axis is used for plotting T, such as in Figure 1. Numerical values of this proposed equation are given in Table 5 presented in section 3.3.

Table 3: Linear interpolation 'pinch points' for the proposed design parameterization of the location-to-location systematic effect, $\delta L2L_l$

Period, T_i	$\delta L2L_l$ (i.e. "y_i")
0.0	-0.06
0.18	-0.06
0.35	0.12
10.0	0.65

3.2. Within-event residuals

For each ground motion recorded during the 10 events a within-event residual is computed. By considering the within-event residuals at each strong motion station site during the 10 events, systematic site effects can be ascertained. Appendix 2 provides the within-event residuals as a function of vibration period for all 20 strong motion station sites considered here. Figure 3-Figure 5 illustrate, as examples from Appendix 2, the within-event residuals and the systematic site effect at CBGS, LINC, and HVSC, respectively. It can be seen that the ground motions observed at the CBGS (Canterbury Botanic Gardens) site are largely that predicted by the median of the Bradley (2010) model, with $\delta S2S_s$ being close to zero for all vibration periods. LINC (Lincoln) generally has ground motion observations which are lower than that predicted by the Bradley (2010) model with $\delta S2S_s$ generally slightly less than zero. Finally, HVSC (Heathcote Valley) generally has ground motion observations which are significantly greater than predicted at short periods and less than predicted at long periods, consistent with the identified basin-edge effects at this location (Bradley 2012a, Bradley and Cubrinovski 2011).

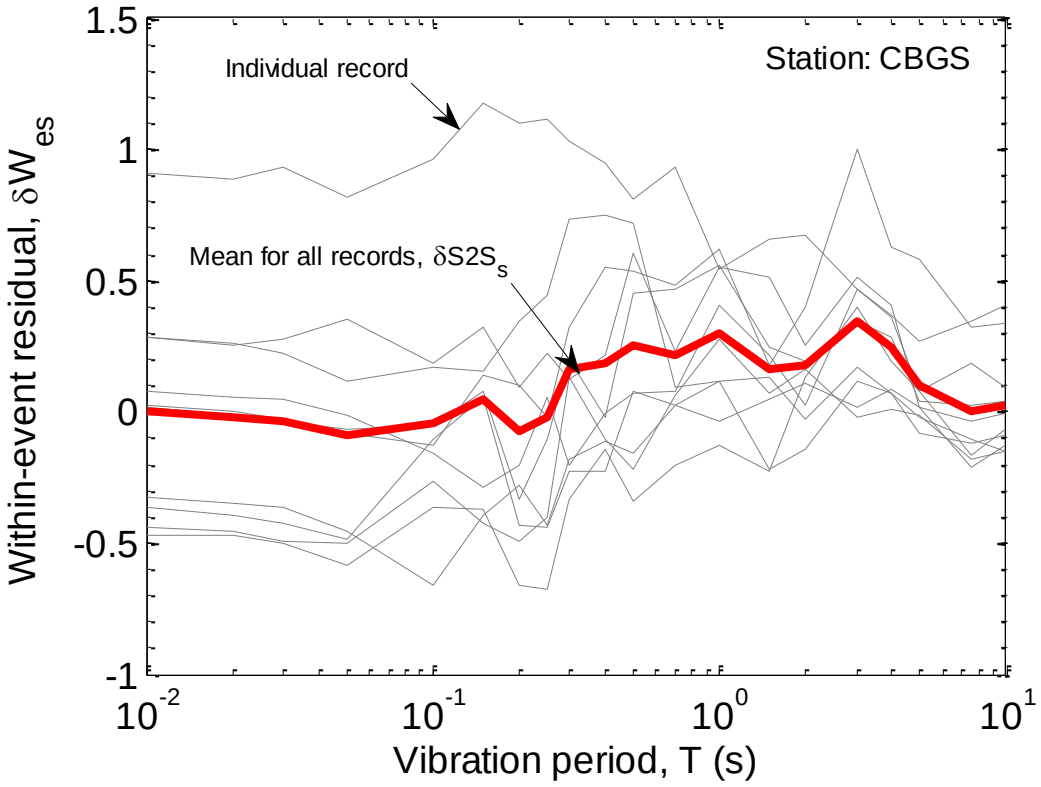

Figure 3: Within-event residuals at CBGS (Christchurch Botanical Gardens) and the site specific effect, $\delta S2S$.

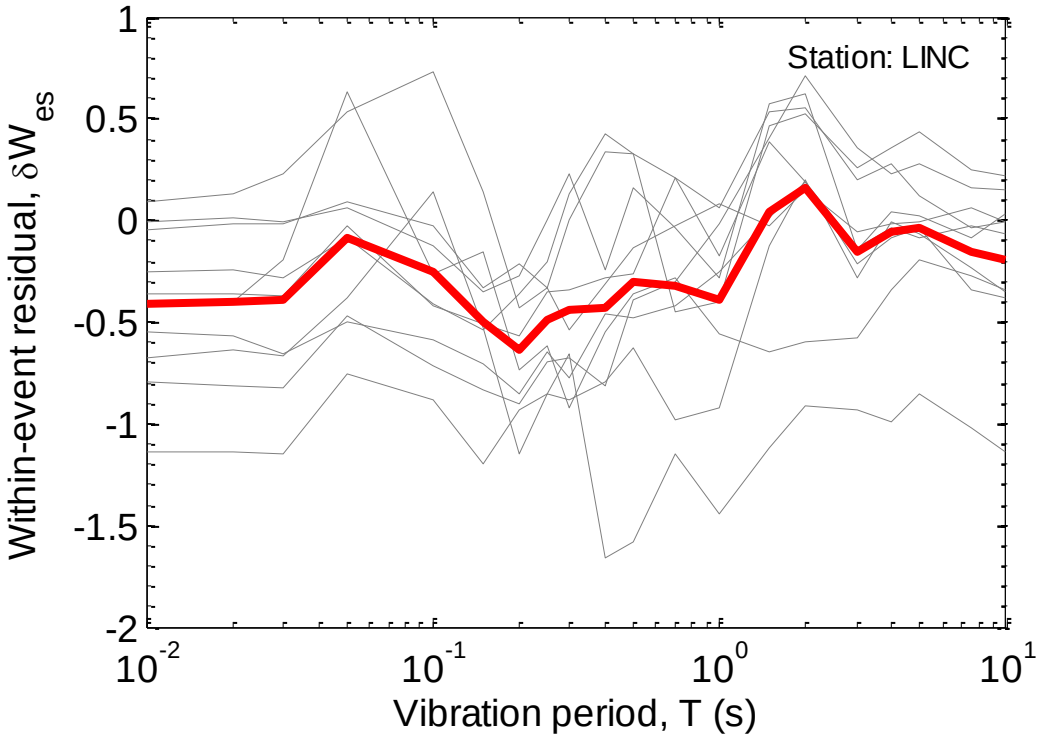

Figure 4: Within-event residuals at LINC (Lincoln) and the site specific effect, $\delta S2S$.

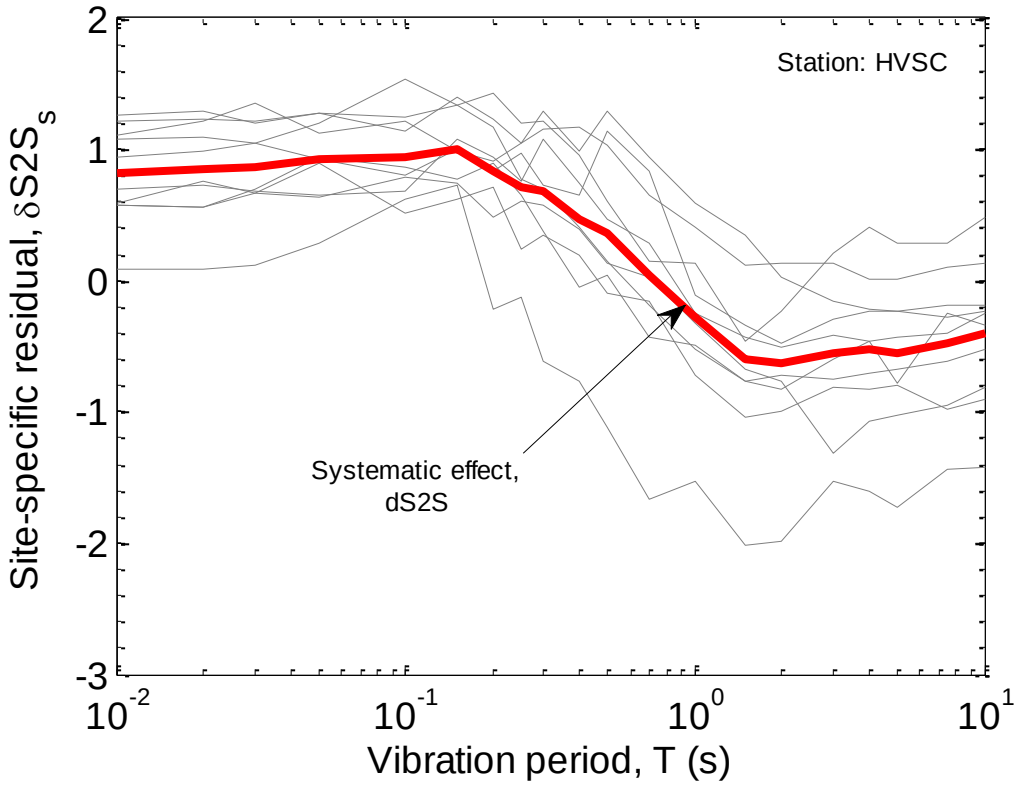

Figure 5: Within-event residuals at HVSC (Heathcote Valley) and the site specific effect, $\delta S2S$.

Figure 3-Figure 5 illustrate that different strong motion stations have systematic site specific residuals, $\delta S2S_s$, which depart from zero. Figure 6 illustrates these site-to-site residuals for all 20 strong motion stations considered, as well as the median, 16th and 84th percentiles of these $\delta S2S_s$ values. It can be seen that, on average, the values of $\delta S2S_s$ are very close to zero. This is largely expected, given that the between-event residual is used to give a within-event residual which is random with approximately zero mean. However, it serves to again illustrate that while the ergodic Bradley (2010) model is unbiased, a significant amount of the observed variability is the result of systematic site effects.

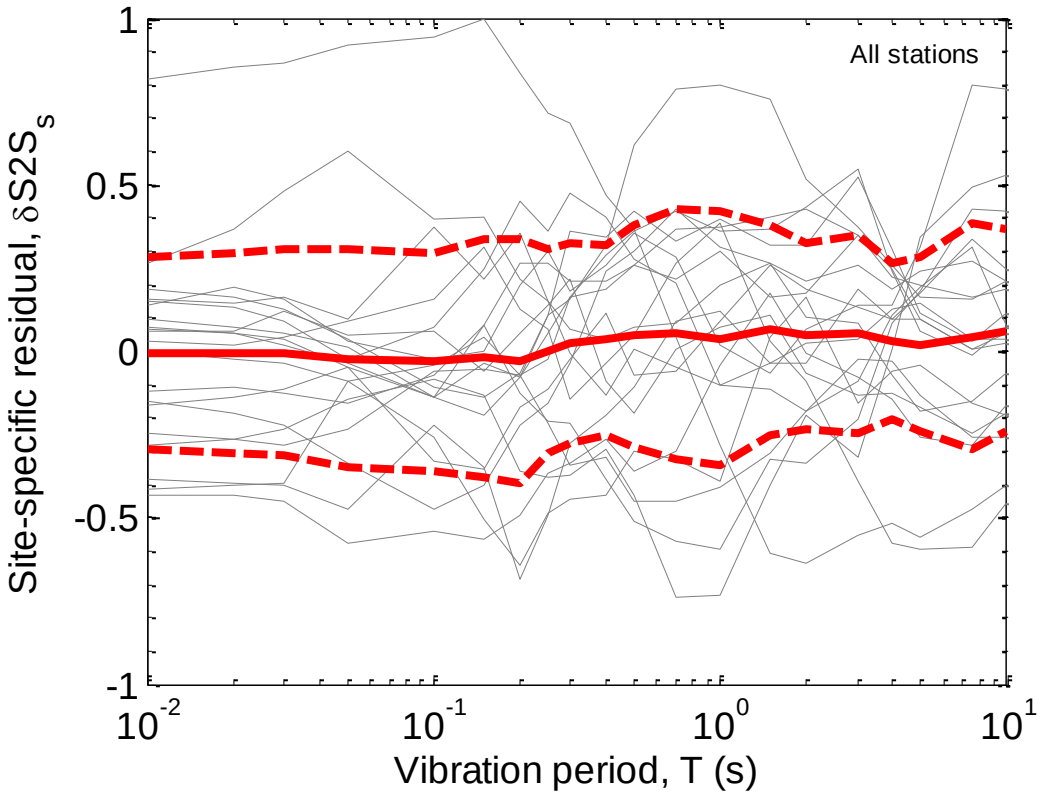

Figure 6: Site-to-site residuals, $\delta S2S_s$, for all stations considered

3.3. Proposed systematic modifications to GMPE for specific sub-regions in Christchurch

The location-to-location and site-to-site residuals ($\delta L2L_l$ and $\delta S2S_s$, respectively) presented in the previous two sections in combination with Equation (12) allows for non-ergodic median site-specific prediction of ground motions at the 20 strong motion stations from earthquakes in the Canterbury region. However, for the purposes of design ground motions for the Christchurch region it is more desirable to develop modification factors which can be utilized over a broad region of Christchurch. This section develops such factors, while the subsequent two sections examine the non-ergodic standard deviations.

3.3.1. Christchurch Central Business District

There are four strong motion stations located in the Christchurch CBD: CBGS, CCCC, CHHC, REHS. The site-to-site residuals, $\delta S2S_s$, for these four stations are shown in Figure 7a. It can be seen that all four stations have $\delta S2S_s$ values which vary similarly with vibration period, with the exception being over the period range of 0.5-2.0 seconds, in which the REHS site has a larger residual that those others. The proposed parameterization of this site-specific residual is a multi-linear interpolation which approximately follows the mean value of $\delta S2S_s$ for the CBD sites. The specific parameterization of this relationship follows Equation (19) with the 'pinch point' values given in Table 4.

Figure 7b illustrates the parameterization of $\delta S2S_s$ along with that for $\delta L2L_l$ and their summation, while Figure 7c illustrates their implied amplification of the median ground motion prediction (i.e. the amplification is equal to the exponential of the residual values), the numerical values of which are given in Table 5 for a range of periods). It can be seen that this 'CBD-specific' modification is nearly 1.0 for $T \leq 0.3s$ (i.e. within $\pm 20\%$), which then

increases in magnitude to factors of approximately 2.0. It is noted in particular that the 'total' amplification factor, which is based solely on a simple parameterization of the non-ergodic methodology presented previously, provides a relatively narrowband amplification of the predicted SA values around the $T = 2 - 4s$ region which has been systematically observed to have large amplitudes across multiple events. Table 5 also provides values of the reduction factors for the standard deviation which are presented later.

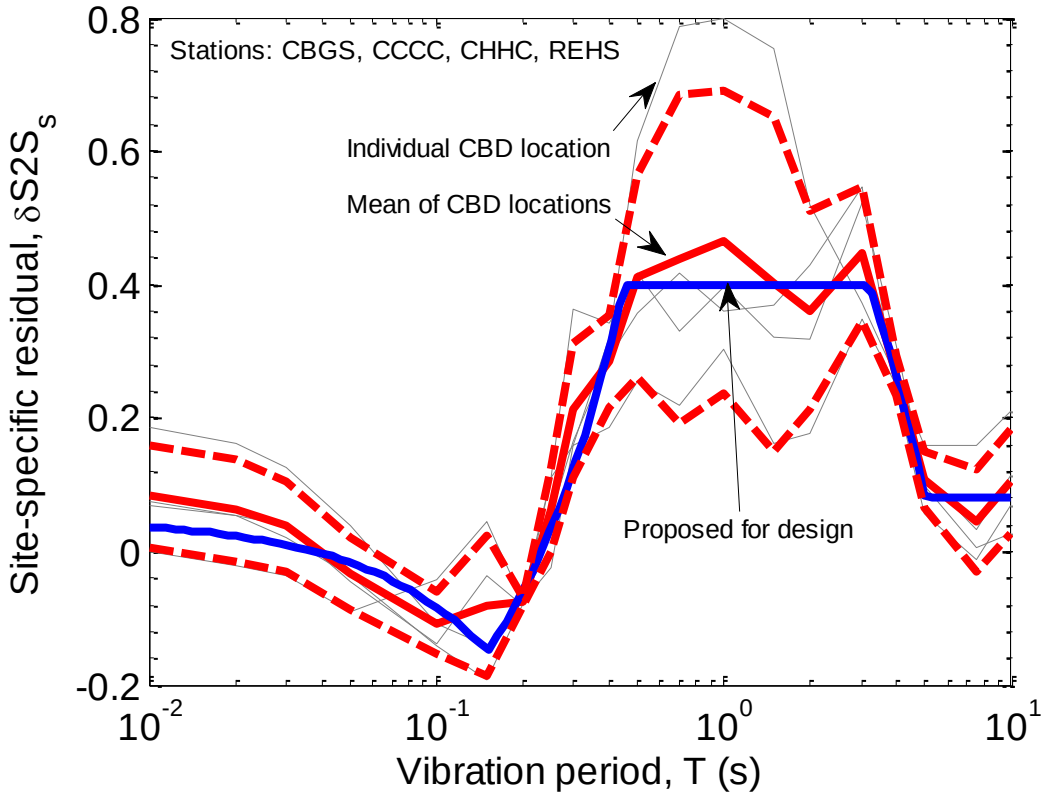

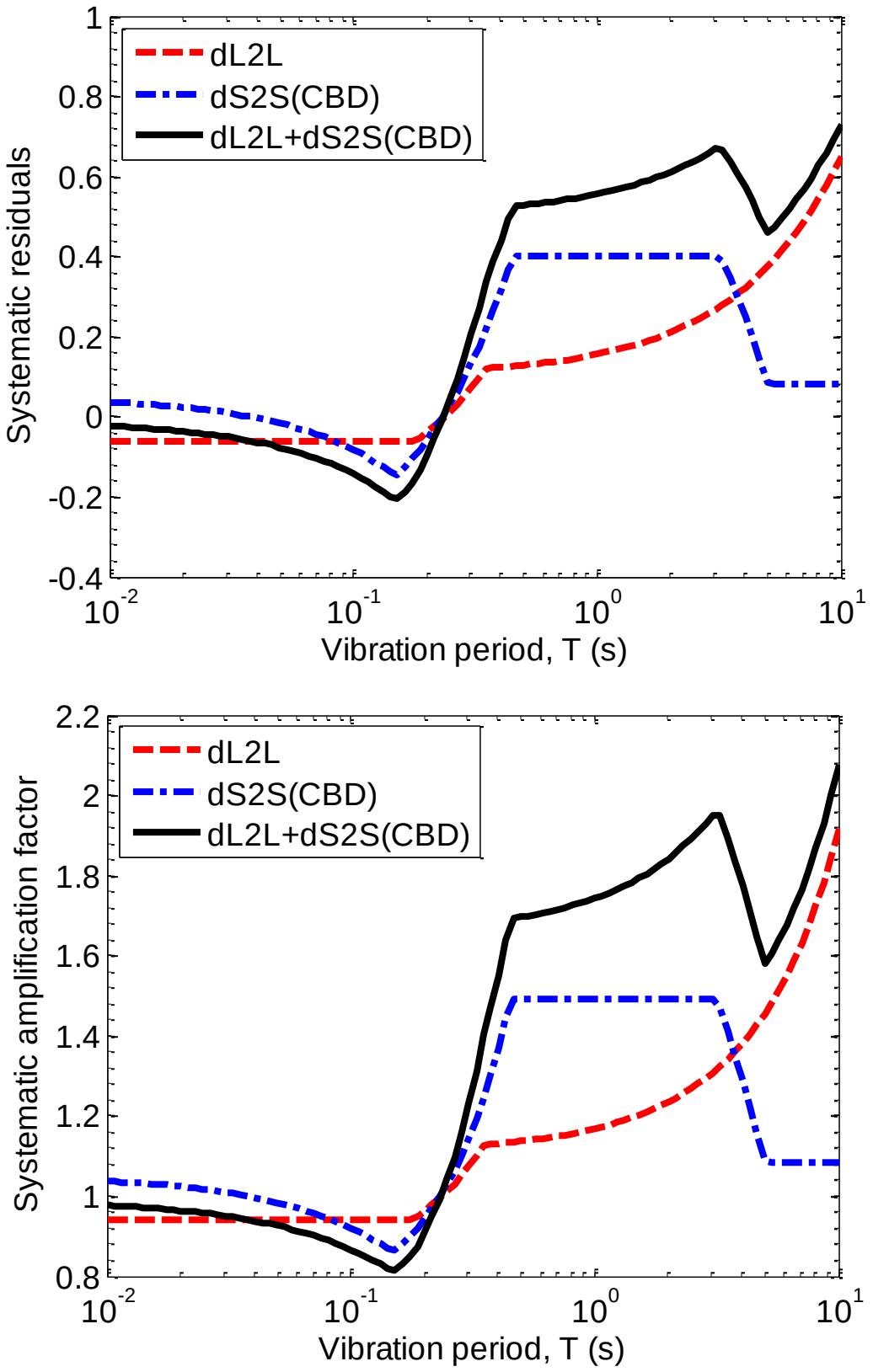

Figure 7: Systematic site effects for the CBD sub-region: (a) site-specific residuals observed and proposed parametric model; (b) parametric models for the systematic location-to-location, site-to-site residuals and then summation; and (c) implied amplification factors in the median GMPE prediction.

Table 4: Linear interpolation 'pinch points' for the proposed design parameterization of the site-specific systematic effect, $\delta S2S_s$ for the CBD

Period, T_i	$\delta S2S_s$ (i.e. "y_i")
0.0	0.05
0.15	-0.15
0.45	0.40
3.2	0.40
5.0	0.08
10.0	0.08

Table 5: Numerical values of the proposed design factors for CBD ground motion prediction

	Median modification			St. dev. modification		
Period, T (s)	$dL2L$	$dS2S$	MAF	SRF_τ	SRF_σ	SRF_{σ_T}
0	-0.06	0.05	0.99	0.87	0.80	0.80
0.01	-0.06	0.034	0.9769	0.87	0.80	0.80
0.02	-0.06	0.02	0.96	0.87	0.80	0.80
0.03	-0.06	0.01	0.95	0.87	0.80	0.80
0.05	-0.06	-0.02	0.93	0.87	0.80	0.80
0.1	-0.06	-0.08	0.87	0.87	0.80	0.80
0.15	-0.06	-0.15	0.81	0.87	0.80	0.80
0.2	-0.04	-0.06	0.91	0.87	0.80	0.80
0.25	0.01	0.03	1.05	0.87	0.80	0.80
0.3	0.07	0.13	1.21	0.87	0.80	0.80
0.4	0.12	0.31	1.54	0.87	0.80	0.80
0.5	0.13	0.40	1.70	0.87	0.80	0.80
0.7	0.14	0.40	1.71	0.87	0.78	0.78
1.0	0.16	0.40	1.74	0.87	0.70	0.70
1.5	0.18	0.40	1.79	0.83	0.69	0.69
2.0	0.21	0.40	1.84	0.80	0.69	0.69
3.0	0.27	0.40	1.95	0.73	0.68	0.68
4.0	0.32	0.256	1.78	0.65	0.67	0.67
5.0	0.38	0.08	1.58	0.58	0.66	0.66
7.5	0.51	0.08	1.81	0.58	0.63	0.63
10.0	0.65	0.08	2.07	0.58	0.60	0.60

3.3.2. The extended western suburbs of Christchurch

There are four strong motion stations located at the western extents of Christchurch's urban area: CACS, TPLC, ROLC, LINC. The site-to-site residuals, $\delta S2S_s$, for these four stations are shown in Figure 8a. It can be seen that all four stations have $\delta S2S_s$ values which vary similarly with vibration period. The proposed parameterization of this site-specific residual is a multi-linear interpolation which approximately follows the mean value of $\delta S2S_s$ for the sites. Figure 8b illustrates the parameterization of $\delta S2S_s$ along with that for $\delta L2L_l$ and their summation, while Figure 8c illustrates their implied amplification of the median ground motion. It can be seen that this modification is less than 1.0 for $T \leq 2.0s$, and then increases significantly in magnitude at very long periods.

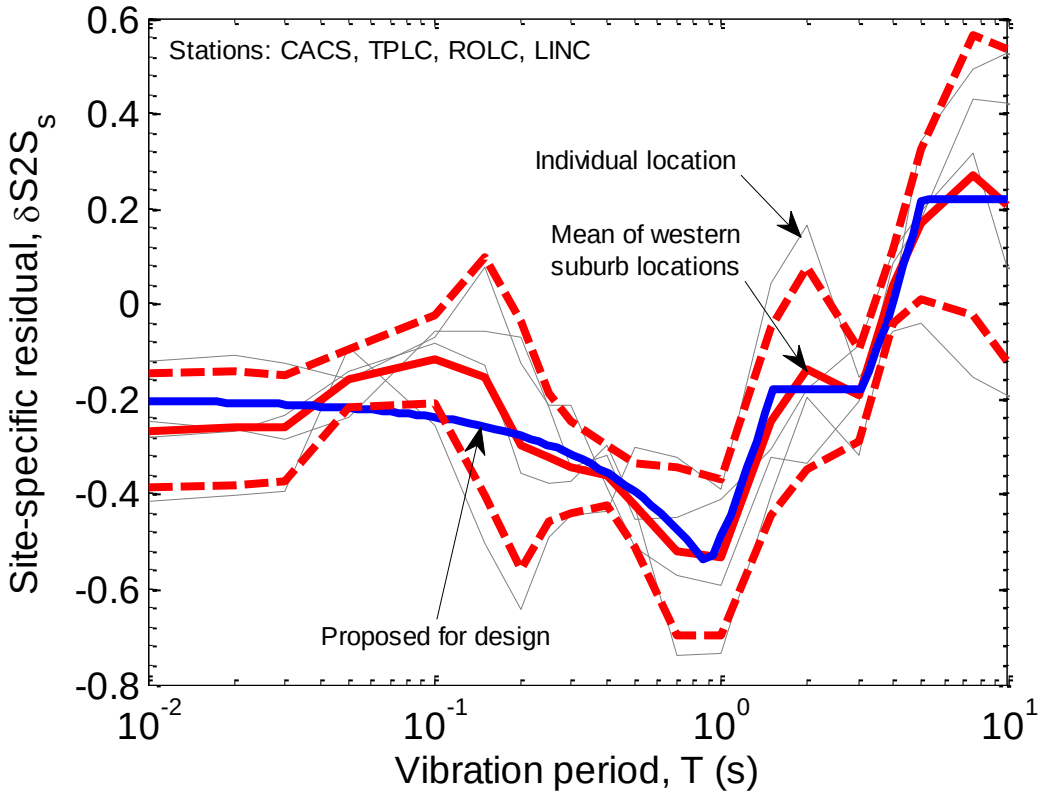
Stations: CACS, TPLC, ROLC, LINC
Individual location
Mean of western suburb locations
Proposed for design
Site-specific residual, δS2S_s
Vibration period, T (s)

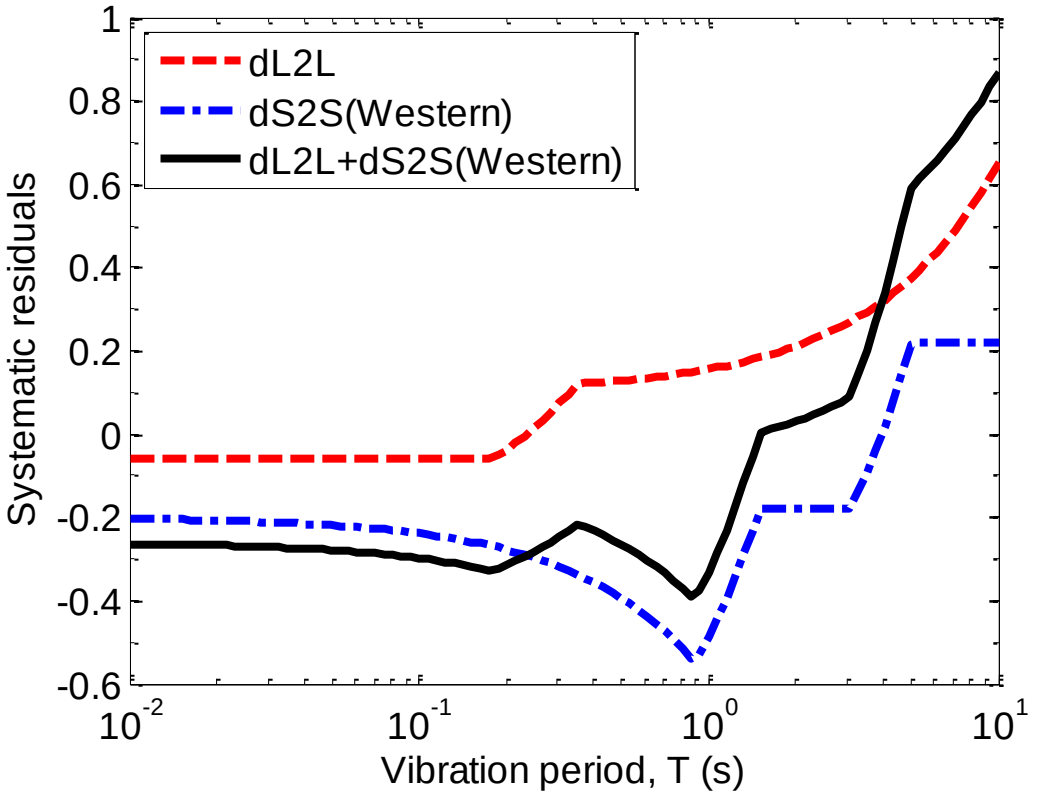
dL2L
dS2S(Western)
dL2L+dS2S(Western)
Systematic residuals
Vibration period, T (s)

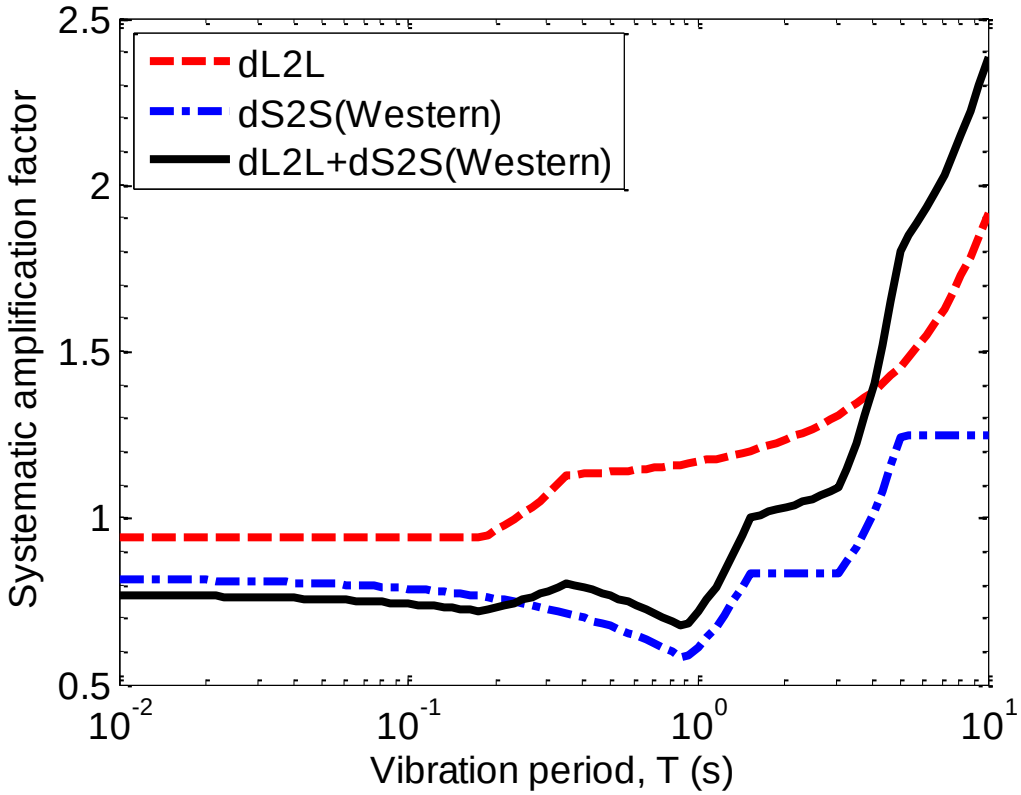

Figure 8: Systematic site effects for the 'Western Suburbs' sub-region: (a) site-specific residuals observed and proposed parametric model; (b) parametric models for the systematic location-to-location, site-to-site residuals and then summation; and (c) implied amplification factors in the median GMPE prediction.

3.3.3. Eastern suburbs of Christchurch (and Kaiapoi)

There are five strong motion stations located at the eastern extents of Christchurch's urban area which exhibit similar site effects: SHLC, PRPC, HPSC, NNBS, KPOC (the other station, NBLC, is discussed separately subsequently). The site-to-site residuals, $\delta S2S_s$, for these stations are shown in Figure 9a. It can be seen that all stations have $\delta S2S_s$ values which vary similarly with vibration period. The proposed parameterization of this site-specific residual is a multi-linear interpolation which approximately follows the mean value of $\delta S2S_s$ for the sites. Figure 9b illustrates the parameterization of $\delta S2S_s$ along with that for $\delta L2L_l$ and their summation, while Figure 9c illustrates their implied amplification of the median ground motion.

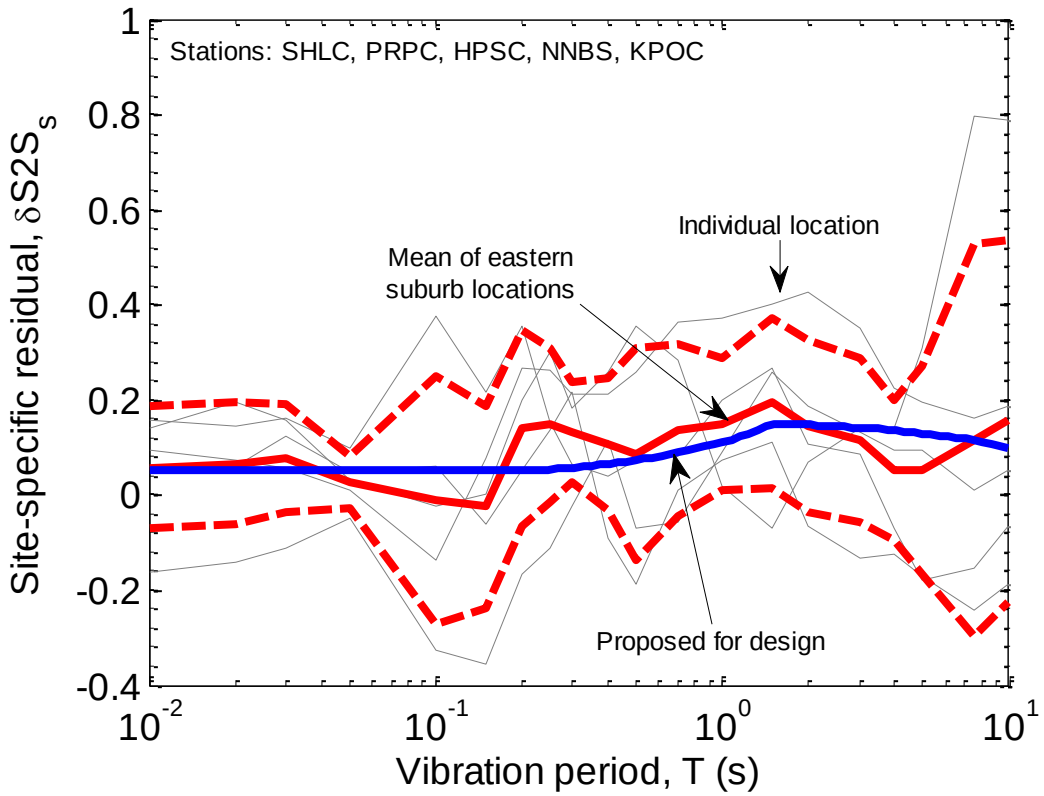
Stations: SHLC, PRPC, HPSC, NNBS, KPOC
Individual location
Mean of eastern
suburb locations
Proposed for design
Site-specific residual, δS2S_s
Vibration period, T (s)

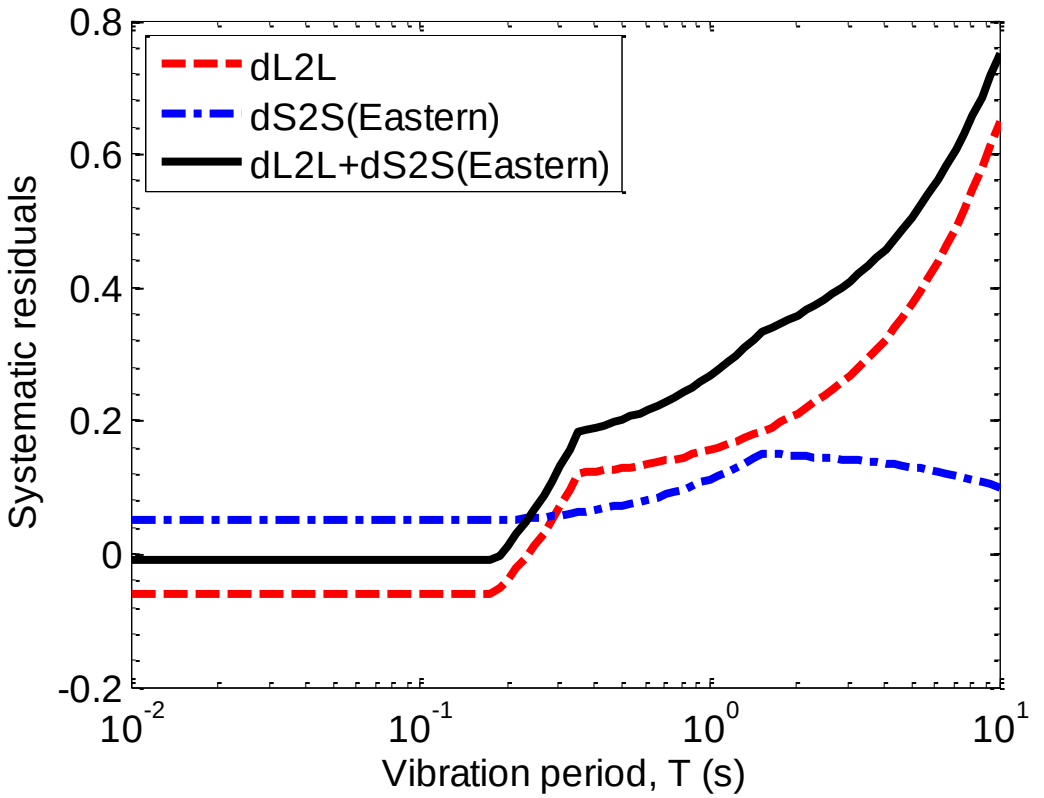
dL2L
dS2S(Eastern)
dL2L+dS2S(Eastern)
Systematic residuals
Vibration period, T (s)

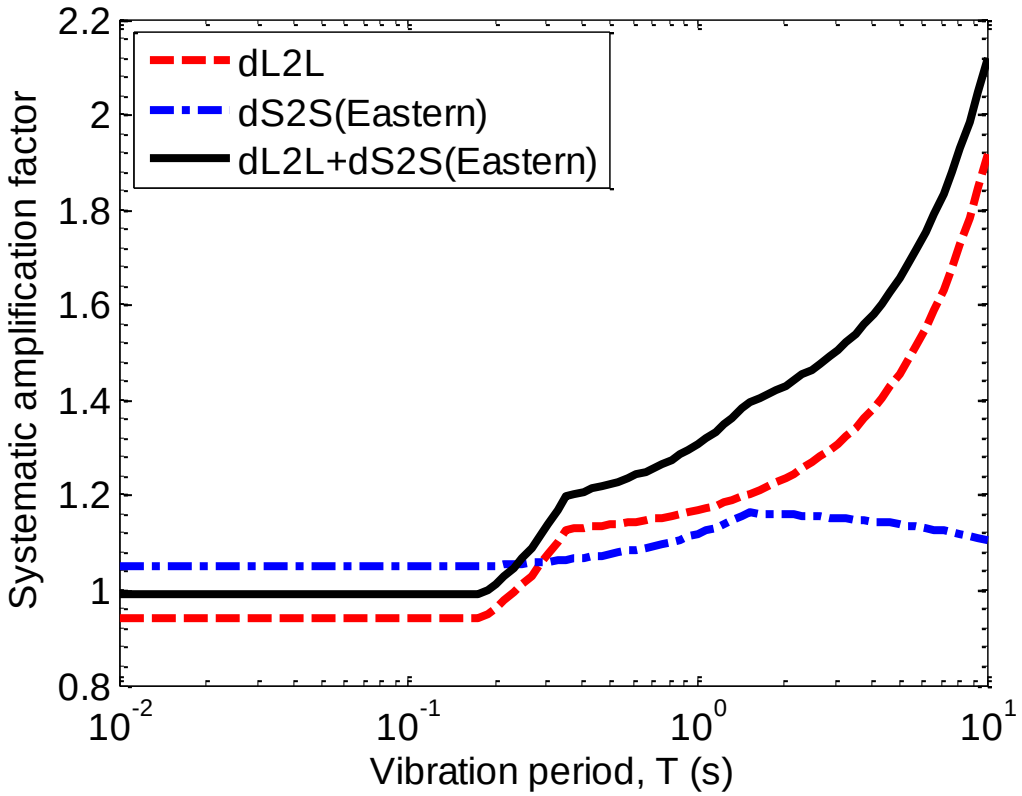

Figure 9: Systematic site effects for the 'Eastern Suburbs' sub-region: (a) site-specific residuals observed and proposed parametric model; (b) parametric models for the systematic location-to-location, site-to-site residuals and then summation; and (c) implied amplification factors in the median GMPE prediction.

3.3.4. Northern Suburbs of Christchurch

There are two strong motion stations located at the northern extents of Christchurch's urban area: PPHS and SMTC. The site-to-site residuals, $\delta S2S_s$, for these stations are shown in Figure 10a. It can be seen that all stations have $\delta S2S_s$ values which vary similarly with vibration period. The proposed parameterization of this site-specific residual is a multi-linear interpolation which approximately follows the mean value of $\delta S2S_s$ for the sites. Figure 10b illustrates the parameterization of $\delta S2S_s$ along with that for $\delta L2L_l$ and their summation, while Figure 10c illustrates their implied amplification of the median ground motion.

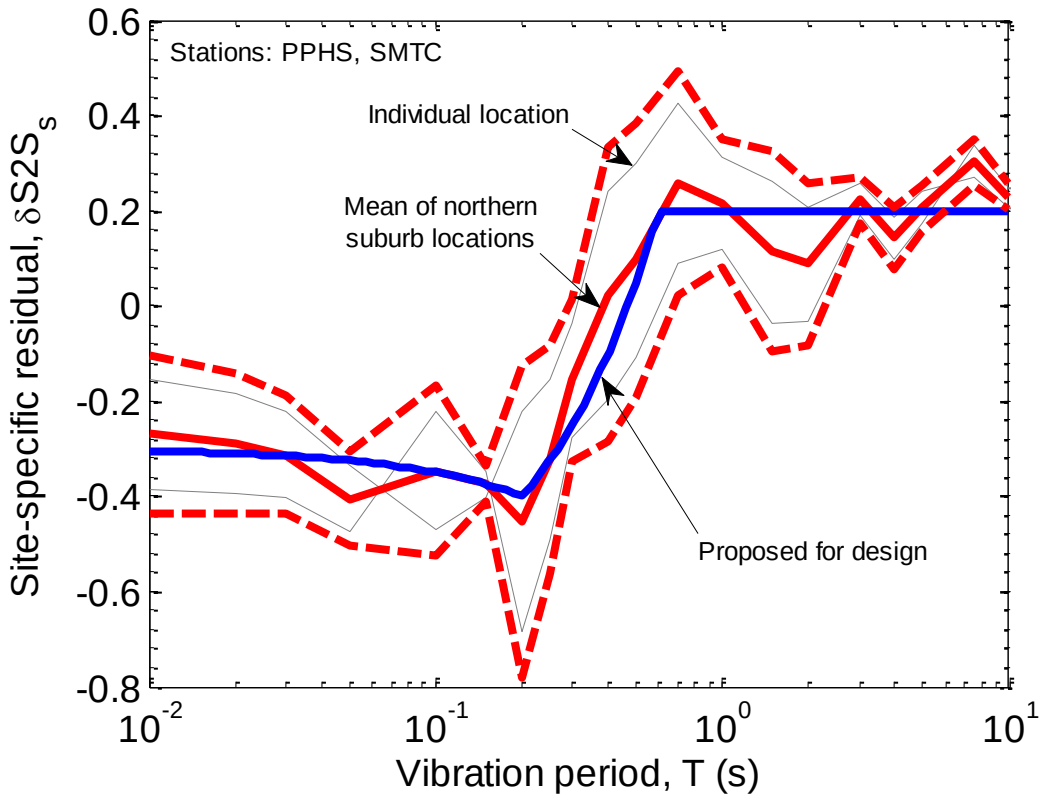
Stations: PPHS, SMTC
Individual location
Mean of northern suburb locations
Proposed for design
Site-specific residual, δS2S_s
Vibration period, T (s)
0.6
0.4
0.2
0
-0.2
-0.4
-0.6
-0.8
10^-2
10^-1
10^0
10^1

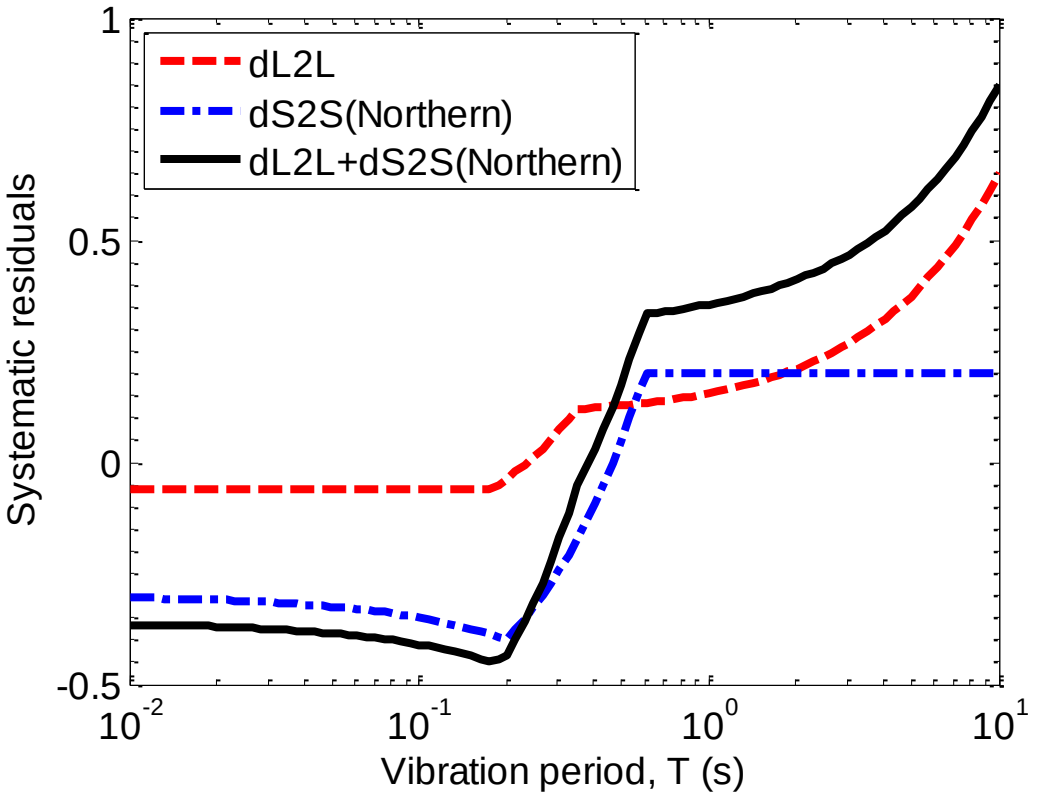
dL2L
dS2S(Northern)
dL2L+dS2S(Northern)
Systematic residuals
Vibration period, T (s)
1
0.5
0
-0.5
10^-2
10^-1
10^0
10^1

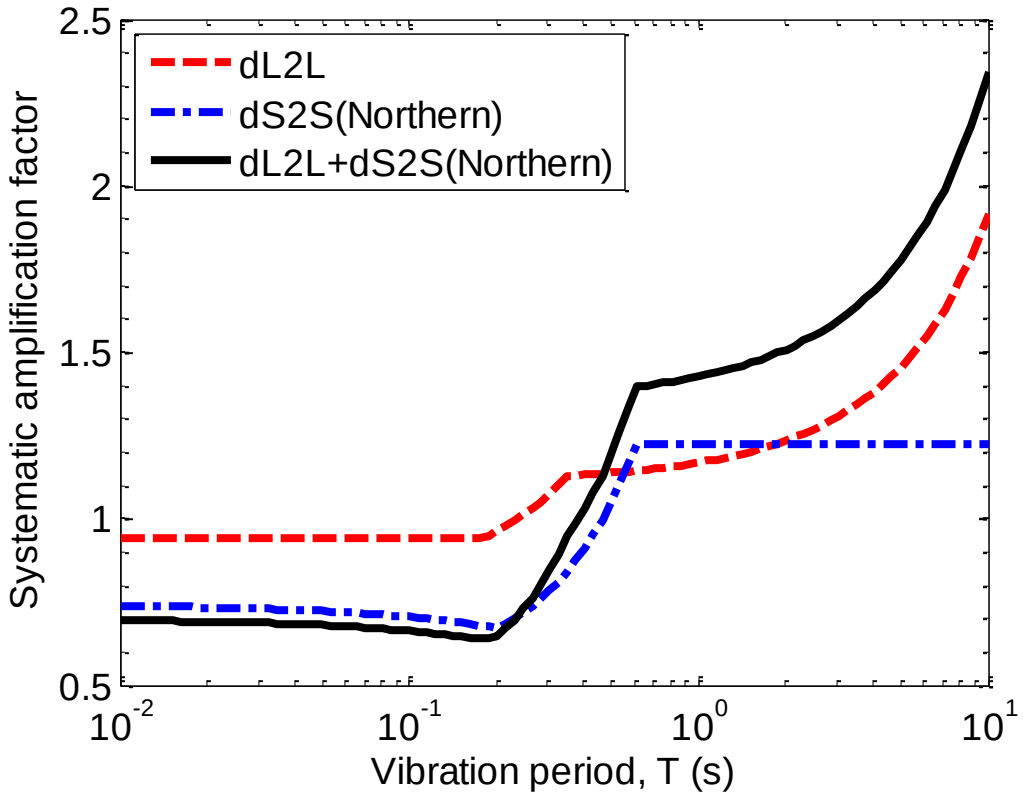

Figure 10: Systematic site effects for the 'Northern Suburbs' sub-region: (a) site-specific residuals observed and proposed parametric model; (b) parametric models for the systematic location-to-location, site-to-site residuals and then summation; and (c) implied amplification factors in the median GMPE prediction.

3.3.5. Other notable locations which don't conform to other categories

Of the 20 strong motion stations investigated, 15 fall into the previously discussed 4 catergories (CBD, and Western, Eastern, and Northern Suburbs). The remaining 5 stations are: RHSC, CMHS, LPCC, HVSC, NBLC. Appendix 3 provides the within-event residuals for these sites as well as the site-to-site residual. The RHSC (Riccarton High School) station is a relatively standard site class D site, but with relatively strong SA amplitudes in the range $T = 0.2 - 0.4s$, which is approximately the natural period of the site's shallow surficial soils. The CMHS (Cashmere High School), HVSC (Heathcote Valley), and LPCC (Lyttelton Port) stations are all affected by the local sub-surface topography of the Banks Peninsula volcanics beneath them and respond in ways that cannot be generalized among them. Finally, the NBLC site, while being located in the eastern suburbs, is actually located on a sand dune region, and therefore exhibits the performance more a-kin to a stiff soil site.

3.3.6. Comparison of all sub-regions

Figure 11 illustrates the variation in site-to-site residuals and the resulting median GMPE amplification factors for four main sub-regions of Christchurch. Figure 12 provides the same results as Figure 11, with the addition of the HVSC, LPCC, CMHS, and RHSC stations which don't conform to these main four sub-regions.

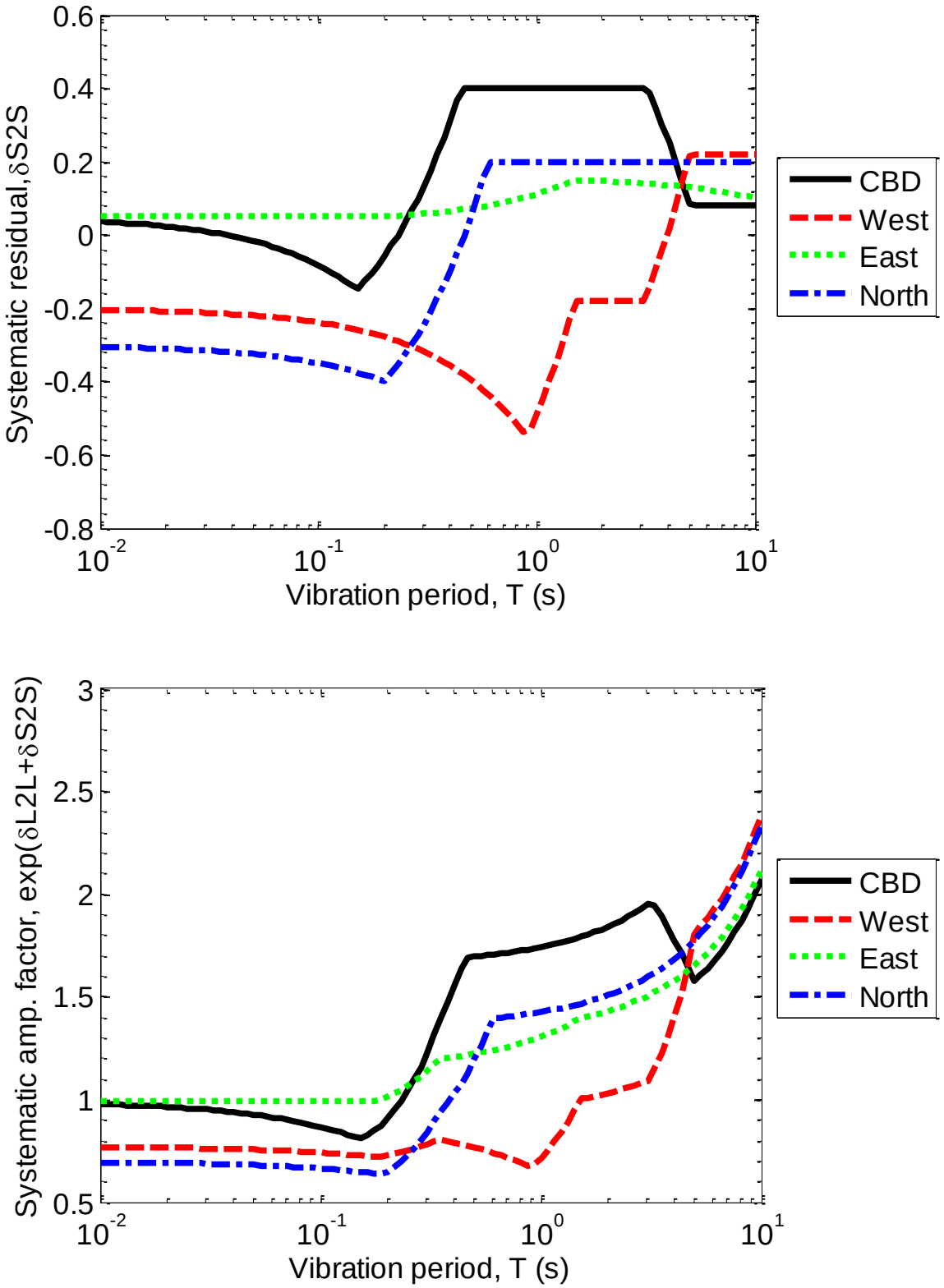

Figure 11: Comparison of: (a) site-to-site residuals; and (b) the systematic amplification factors from systematic location-to-location and site-to-site effects for the four main sub-regions in Christchurch.

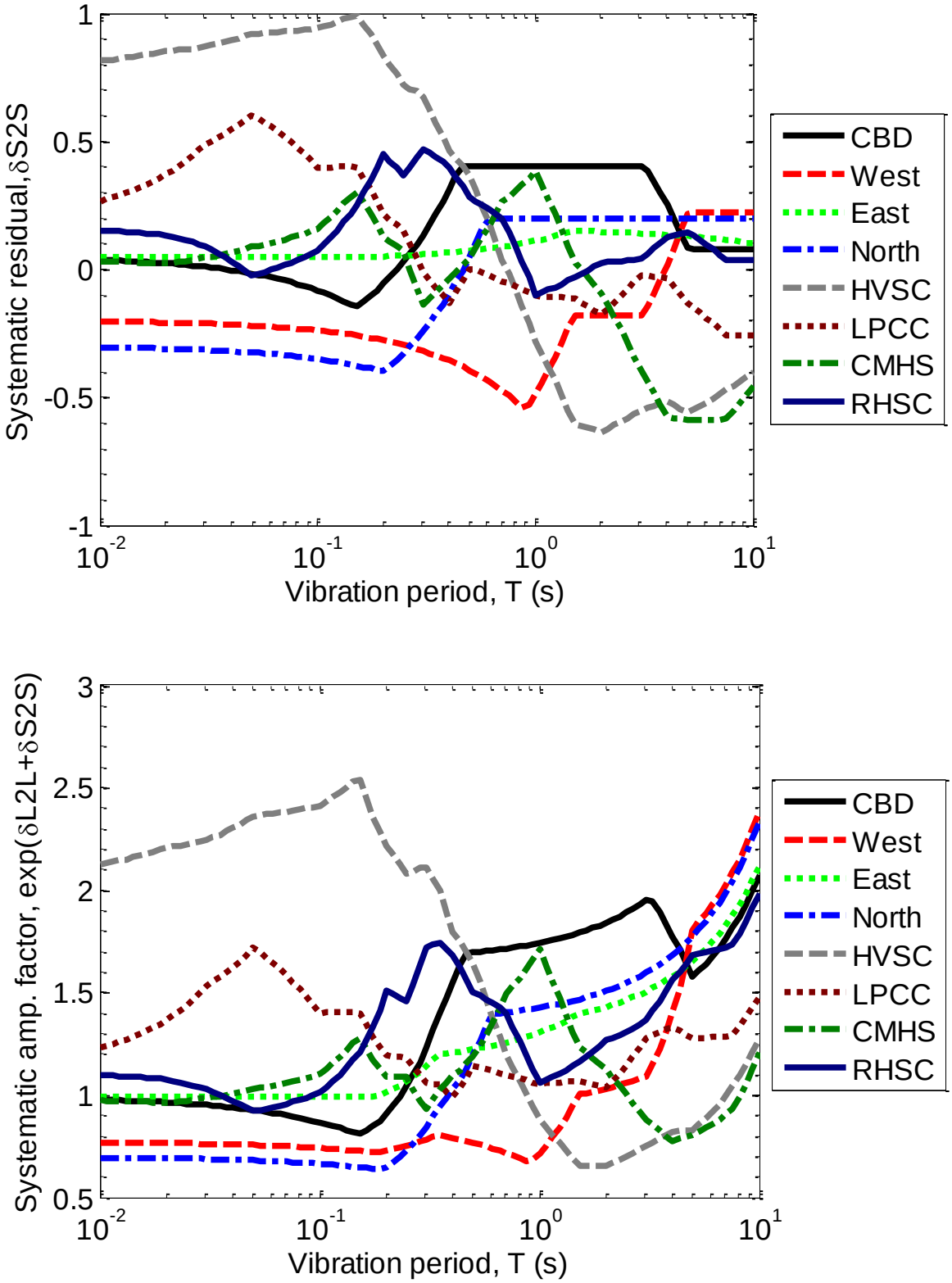

Figure 12: Comparison of: (a) site-to-site residuals; and (b) the systematic amplification factors from systematic location-to-location and site-to-site effects for various sub-regions in Christchurch.

3.4. Between-event standard deviations

In order to fully incorporate non-ergodic aspects into a GMPE it is necessary to modify both its median and its standard deviation prediction. Figure 13a presents the ergodic between-event standard deviation of the Bradley (2010) model, τ, in comparison with the observed standard deviations in the location-to-location residual, τ_{L2L}, that of the 'remaining' between-event residual, τ_0, and their SRSS combination. Figure 13b illustrates that ratio between this SRSS combination of the non-ergodic between-event standard deviation and that of the ergodic model, as well as the proposed multi-linear interpolation with vibration period. The pinch-points for this interpolation function (Equation (19)) are given in Table 6, as well as numerical values for a range of vibration periods given in Table 5. Note that the use of a smooth reduction factor is desired over utilizing the SRSS combined values in Figure 13a directly because a significant variation in standard deviation with vibration period can lead to Uniform Hazard Spectra obtained from PSHA having undesirable 'spurious' variations with period.

Table 6: Linear interpolation 'pinch points' for the proposed design parameterization of the reduction factor in the between-event standard deviation, SRF_τ

Period, T_i	SRF_τ (i.e. "y_i")
0.0	0.87
1.0	0.87
5.0	0.58
10	0.58

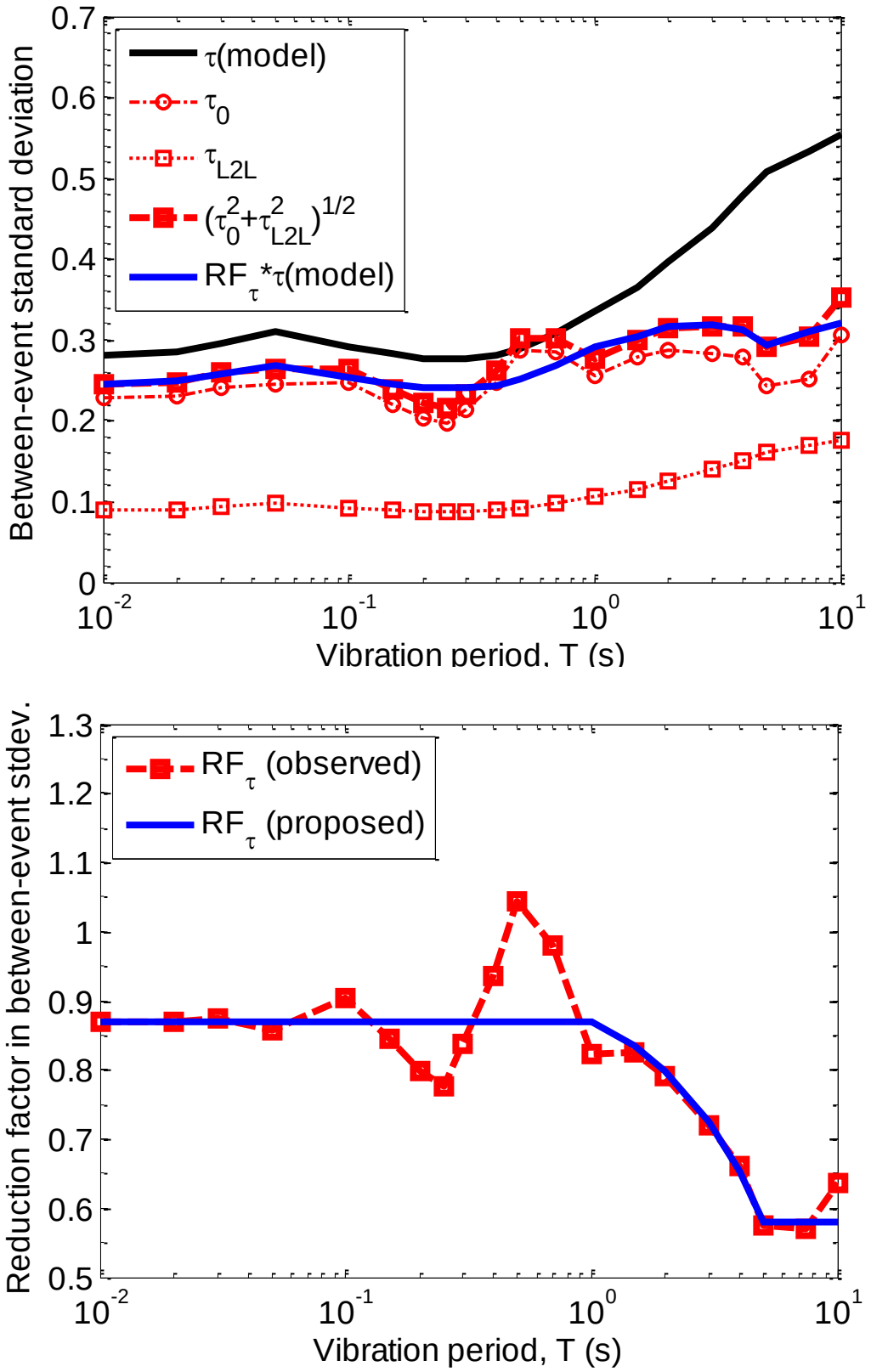

Figure 13: (a) Ergodic and non-ergodic between-event standard deviation components; and (b) proposed between-event standard deviation reduction factor, SRF_τ.

3.5. Within-event standard deviations

Figure 14 presents the reduction in the within-event standard deviation as a function of vibration period for the 20 different strong motion stations which were considered. As well as considering all of the strong motions stations, the subset of 4 strong motion stations in the CBD were also considered in particular, and are annotated separately. It can be seen that the CBD stations follow the general variation in the average of all 20 stations. A proposed multi-linear parameterization (i.e. Equation (19)) of this relationship is also illustrated in the figure, with 'pinch-point' values given in Table 7, as well as numerical values for a range of vibration periods given in Table 5

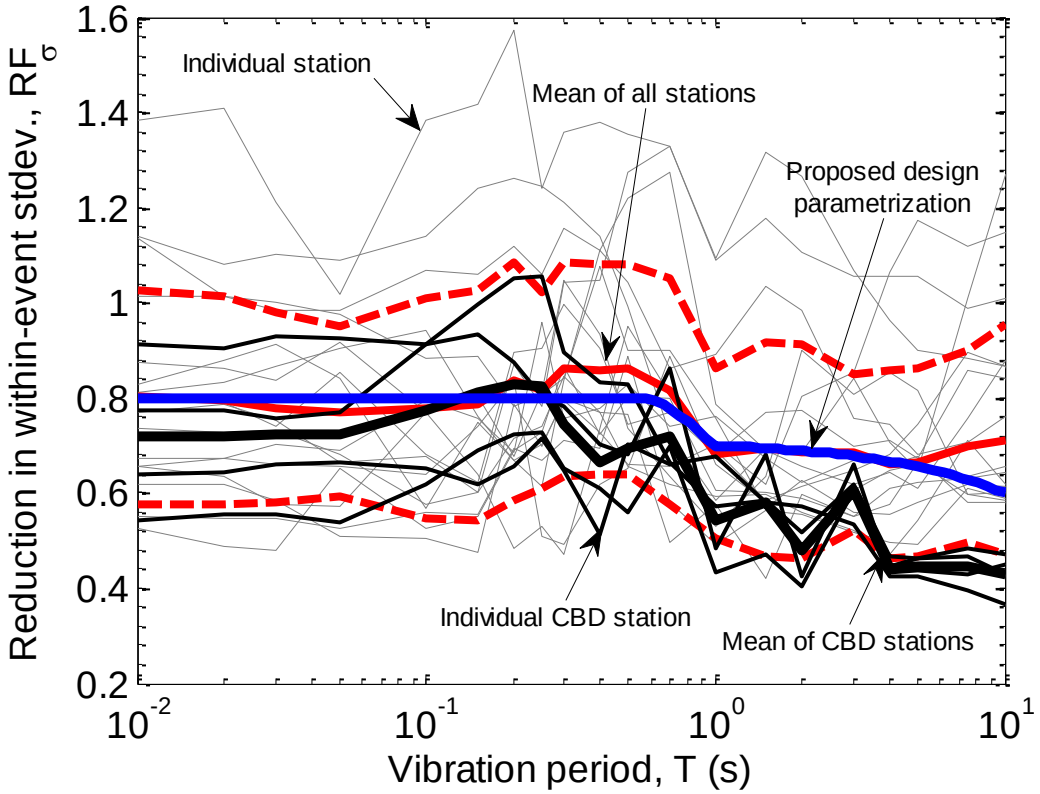

Figure 14: Reduction in the within-event standard deviation of the non-ergodic model as compared to the ergodic model for all stations, the subset of CBD stations, and the proposed design parameterization.

Table 7: Linear interpolation 'pinch points' for the proposed design parameterization of the reduction factor in the within-event standard deviation, SRF_σ

Period, T_i	SRF_σ (i.e. "y_i")
0.0	0.80
0.6	0.80
1.0	0.70
10	0.60

3.6. Total standard deviation

It is recommended that the proposed modification factors for the between- and within-event standard deviations are applied directly to the ergodic predictions of the Bradley (2010) model, and then combined in SRSS fashion to obtain the total standard deviation. This is because the between- and within-event standard deviations vary as a function of various prediction parameters (e.g. M_w, R_{rup} etc), and therefore the ratio of these two standard deviations is not constant.

However it is appreciated that some numerical software within which PSHA is performed allow only the input of the total standard deviation, rather than decomposing into the between- and within-event portions. As such, the reduction factor in the total standard deviation was also computed, and is depicted in Figure 15. It can be seen that the reduction factor values for the total standard deviation are very similar to the within-event standard deviation – a consequence that the within-event standard deviation is notable larger than the between-event standard deviation, and hence it is the dominant contributor to the total standard deviation. As a result, the same parameterization of the within-event standard deviation is also adopted for the total standard deviation. Table 8 presents the 'pinch-point' values for the total standard deviation for completeness, as well as numerical values for a range of vibration periods given in Table 5

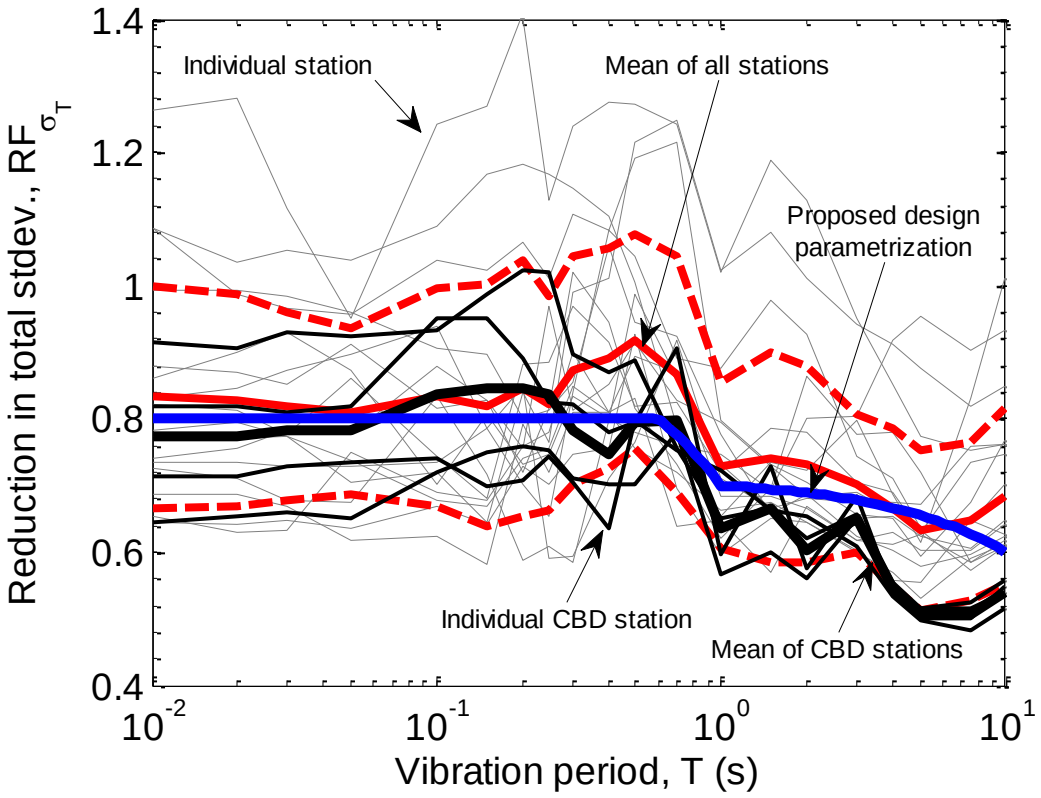

Figure 15: Reduction in the 'total' standard deviation of the non-ergodic model as compared to the ergodic model for all stations, the subset of CBD stations, and the proposed design parameterization.

Table 8: Linear interpolation 'pinch points' for the proposed design parameterization of the reduction factor in the total standard deviation, SRF_{σ_T}

Period, T_i	SRF_σ (i.e. "y_i")
0.0	0.80
0.6	0.80
1.0	0.70
10	0.60

3.7. Comparison of non-ergodic standard deviation reduction with previous studies

Figure 16 provides a comparison of the non-ergodic total standard deviation reduction obtained in this study with those of previous studies. Previous studies are classified into two types. The first are so-called 'single station' non-ergodic studies in that only the site-to-site systematic effect (i.e. $\delta S2S_s$) is considered. Naturally, such studies are seen to result in less of a reduction than this study (which also considered the location-to-location systematic effect, $\delta L2L_l$). The second are so-called 'single-path single-station' non-ergodic studies in that they consider systematic site, path and source effects. Also, as one would expect such studies are seen here to generally result in greater reductions that that observed here. This is both because of the additional systematic path effect considered, but also the use of generally small amplitude ground motions (i.e. no nonlinear soil response), recorded at generally larger source-to-site distances (for which the ray path is more uniquely defined).

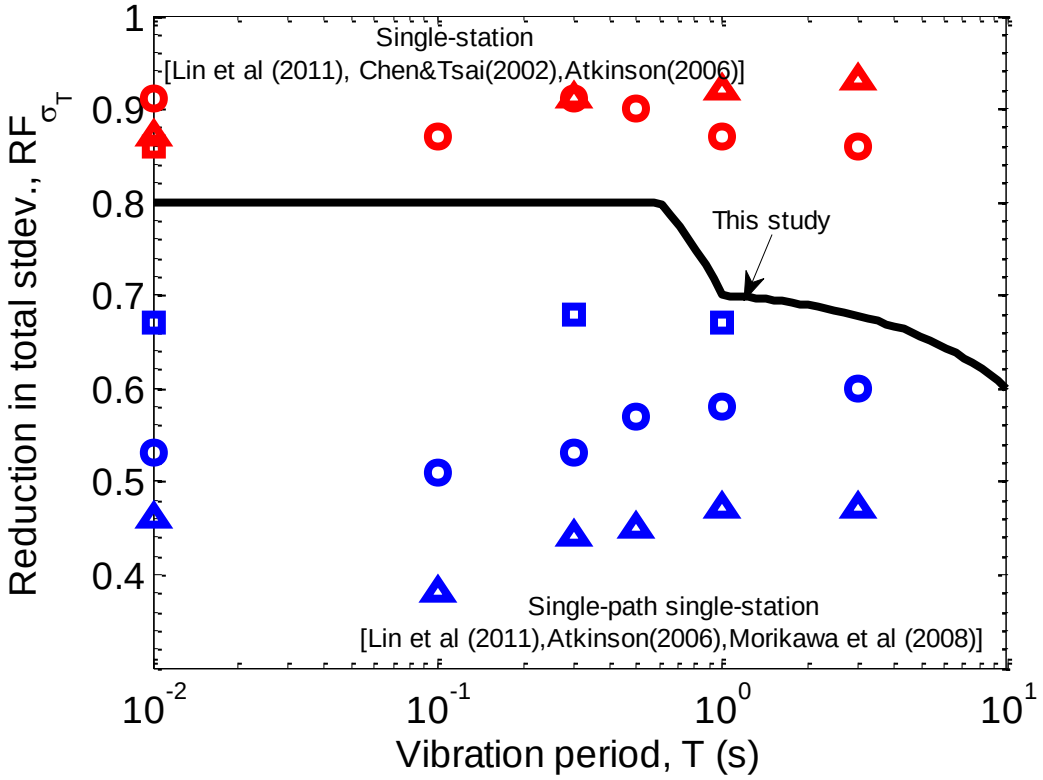

Figure 16: Comparison of the reduction in the total standard deviation from non-ergodic consideration in this study compared with previous studies. PGA results from other studies plotted at T=0.01s.

4. Comparison of ergodic and non-ergodic predictions

Figure 17 compares the difference in predictions from the ergodic Bradley (2010) model with the CBD-specific non-ergodic model based on the proposed modification factors developed in earlier sections. Across the four CBD stations and four largest events depicted in Figure 17 it can be seen that the modification leads to improved SA prediction.

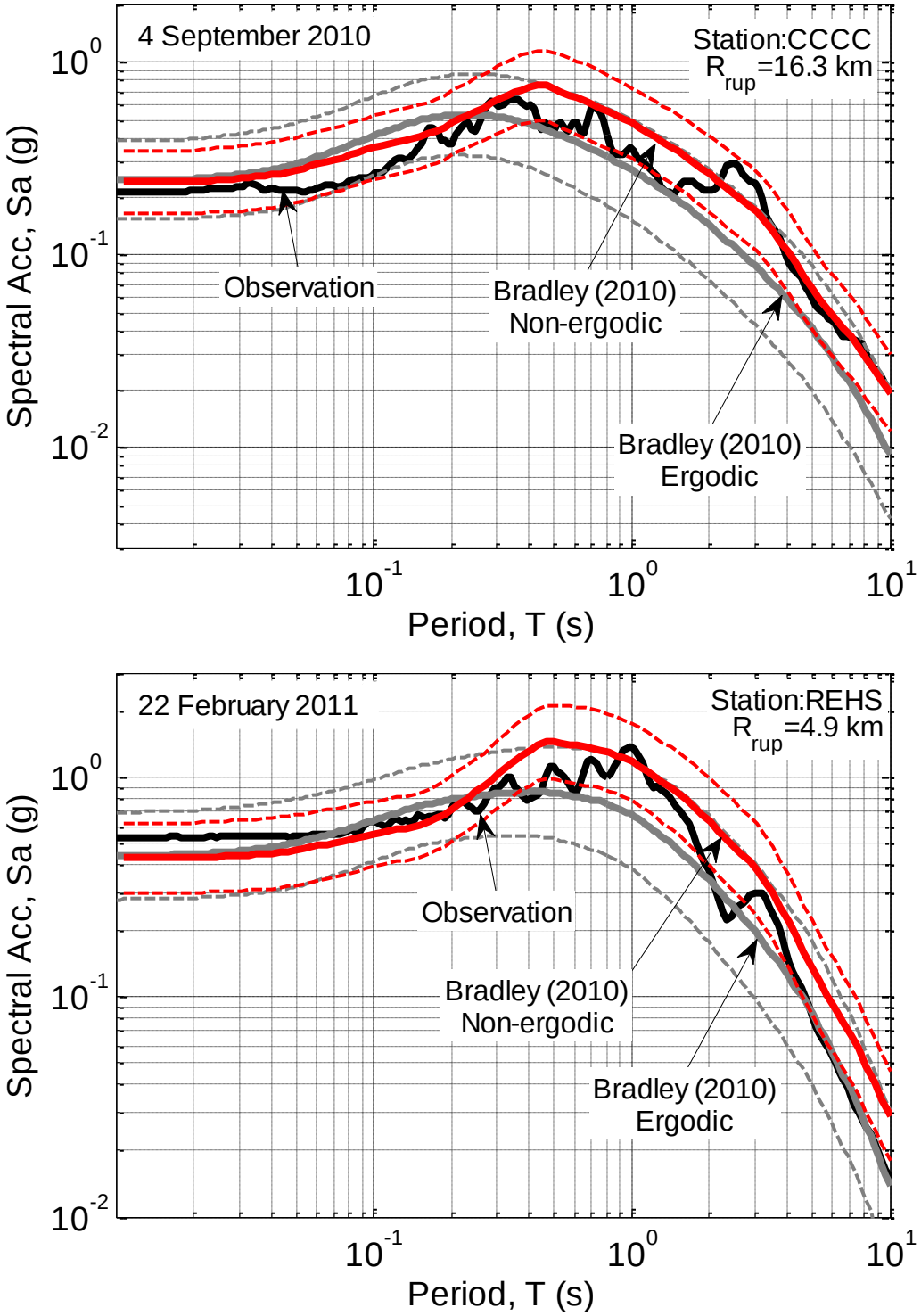

Figure 17: Comparison of the ergodic Bradley (2010) model and the CBD-specific non-ergodic model as compared to observations from the major Canterbury earthquakes.

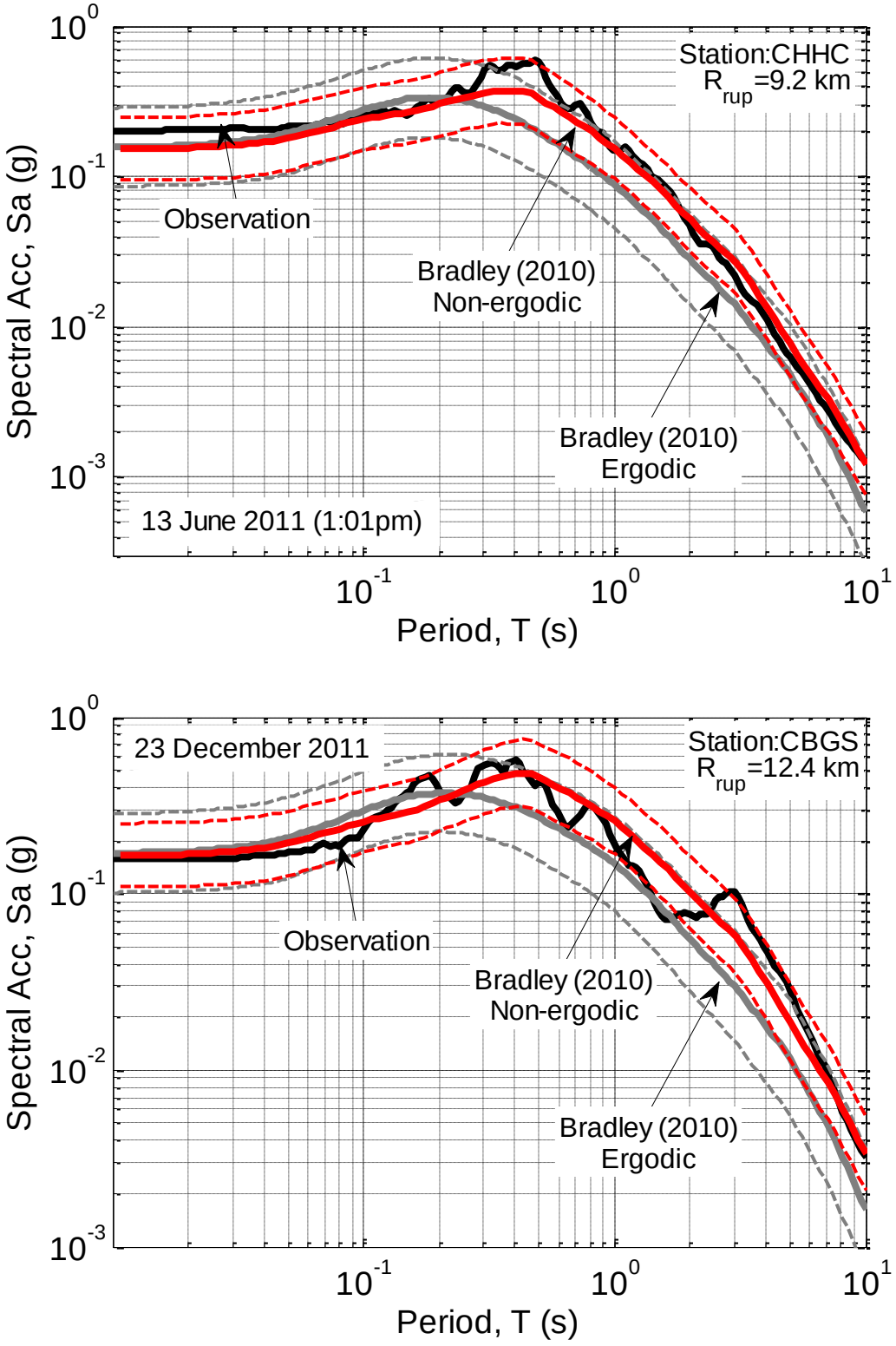

Figure 17 continued.

5. Conclusions

This study has examined ground motion observations from the most significant 10 events in the 2010-2011 Canterbury earthquake sequence at near-source sites to scrutinize New Zealand (NZ)-specific pseudo-spectral acceleration (SA) empirical ground motion prediction equations (GMPE) (Bradley 2010, Bradley 2013, McVerry et al. 2006). Region-specific modification factors based on relaxing the conventional ergodic assumption in GMPE development were developed for the Bradley (2010) model. Because of the observed biases with magnitude and source-to-site distance for the McVerry et al. (2006) model it is not possible to develop region-specific modification factors in a reliable manner. The theory of non-ergodic empirical ground motion prediction was presented, and applied to the 10 event dataset to determine systematic effects in the between- and within-event residuals which lead to modifications in the predicted median and standard deviation of the GMPE. By examining these systematic effects over sub-regions containing a total of 20 strong motion stations within the Canterbury area, modification factors for use in region-specific ground motion prediction were proposed. These modification factors, in particular, are suggested for use with the Bradley et al. (2010) model in Canterbury-specific probabilistic seismic hazard analysis (PSHA) to develop revised design response, particularly for long vibration periods.

6. References

Anderson, J. G., J. N. Brune. Probabilistic seismic hazard analysis without the ergodic assumption, *Seismological Research Letters*, 70, 19-28.

Atik, L. A., N. Abrahamson, J. J. Bommer, F. Scherbaum, F. Cotton, N. Kuehn, (2010). The Variability of Ground-Motion Prediction Models and Its Components, *Seismological Research Letters*, 81, 794-801. 10.1785/gssrl.81.5.794

Bradley, B. A., (2010). NZ-specific pseudo-spectral acceleration ground motion prediction equations based on foreign models, Department of Civil and Natural Resources Engineering, University of Canterbury, Christchurch, New Zealand. 324 pp. http://ir.canterbury.ac.nz/handle/10092/5126

Bradley, B. A., (2012a). Ground motion and seismicity aspects of the 4 September 2010 and 22 February 2011 Christchurch earthquakes, *Technical Report Prepared for the Canterbury Earthquakes Royal Commission* 62 pp.

Bradley, B. A., (2012b). Strong ground motion characteristics observed in the 4 September 2010 Darfield, New Zealand earthquake, *Soil Dynamics and Earthquake Engineering*, 42, 32-46. 10.1016/j.soildyn.2012.06.004

Bradley, B. A., (2013). A New Zealand-specific pseudo-spectral acceleration ground-motion prediction equation for active shallow crustal earthquakes based on foreign models, *Bulletin of the Seismological Society of America*, 103. doi: 10.1785/0120120021

Bradley, B. A., M. Cubrinovski, (2011). Near-source Strong Ground Motions Observed in the 22 February 2011 Christchurch Earthquake, *Seismological Research Letters*, 82, 853-865. 10.1785/gssrl.82.6.853

Bradley, B. A., M. Cubrinovski, R. P. Dhakal, G. A. MacRae, (2009). Probabilistic seismic performance and loss assessment of a bridge-foundation-soil system, *Soil Dynamics and Earthquake Engineering*, 30, 395-411. 10.1016/j.soildyn.2009.12.012

Cubrinovski, M., K. Ishihara, (1998). State concept and modified elastoplasticity for sand modelling, *Soils and Foundations*, 38, 213-225.

Lin, P.-S., B. Chiou, N. Abrahamson, M. Walling, C.-T. Lee, C.-T. Cheng, (2011). Repeatable Source, Site, and Path Effects on the Standard Deviation for Empirical Ground-Motion Prediction Models, *Bulletin of the Seismological Society of America*, 101, 2281-2295. 10.1785/0120090312

McVerry, G. H., J. X. Zhao, N. A. Abrahamson, P. G. Somerville, (2000). Crustal and subduction zone attenuation relations for New Zealand earthquakes, in *12th World Conference on Earthquake Engineering*: Auckland, New Zealand. 8.

McVerry, G. H., J. X. Zhao, N. A. Abrahamson, P. G. Somerville, (2006). New Zealand acceleration response spectrum attenuation relations for crustal and subduction zone earthquakes, *Bulletin of the New Zealand Society for Earthquake Engineering*, 39, 1-58.

Rodriguez-Marek, A., G. A. Montalva, F. Cotton, F. Bonilla, (2011). Analysis of Single-Station Standard Deviation Using the KiK-net Data, *Bulletin of the Seismological Society of America*, 101, 1242-1258. 10.1785/0120100252

Smyrou, E., P. Tasiopoulou, I. E. Bal, G. Gazetas, (2011). Ground Motions versus Geotechnical and Structural Damage in the February 2011 Christchurch Earthquake, *Seismological Research Letters*, 82, 882-892. 10.1785/gssrl.82.6.882

Walling, M., (2009). Non-ergodic probabilistic seismic hazard analysis and spatial simulation of variation in ground motion. University of California, Berkeley. 263.

Appendix 1: GMPE comparisons for all 10 events

Bradley (2010) model

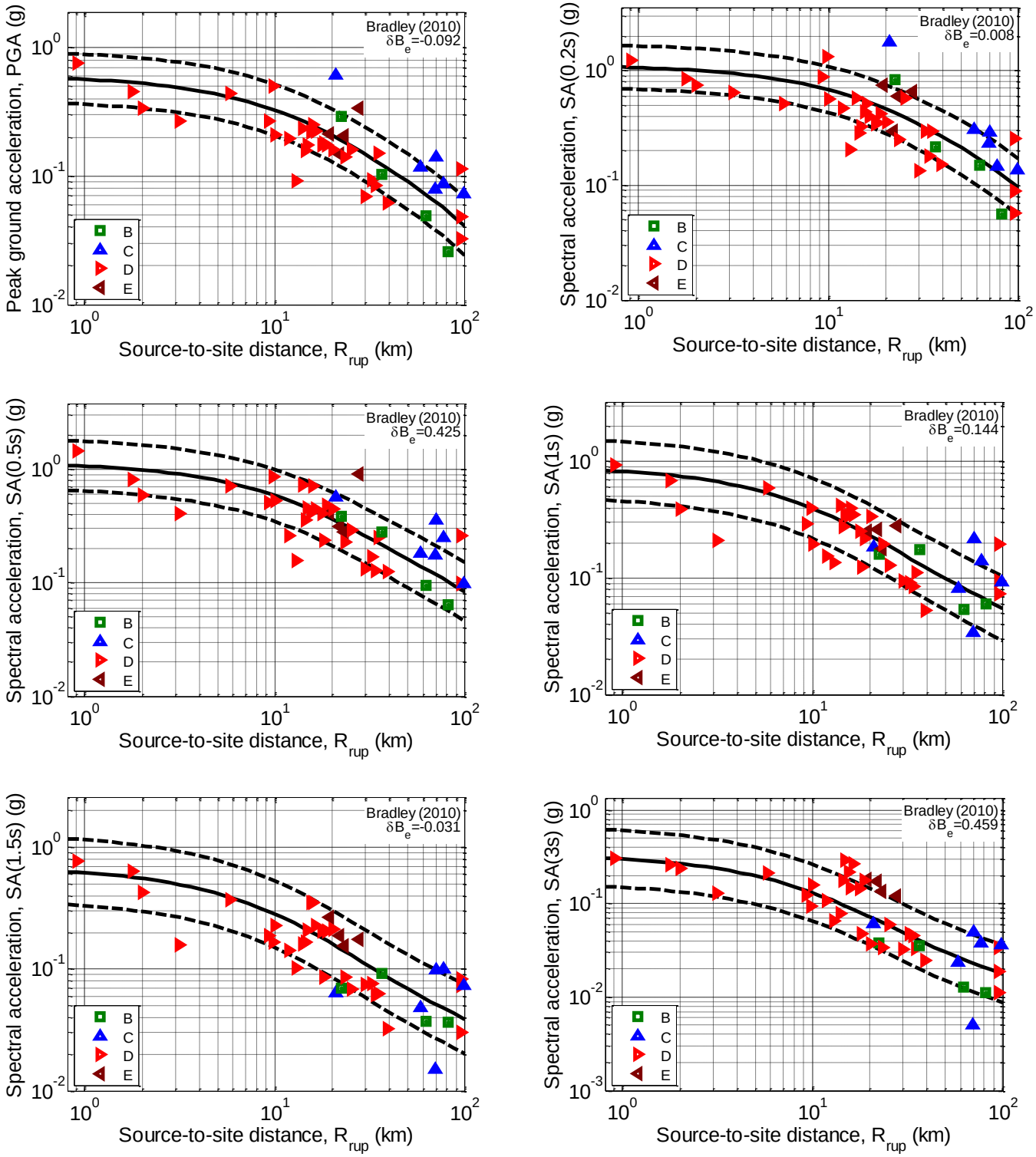

Figure 18: Comparison of the Bradley (2010) prediction (for site class D) and observations for the 4 September 2010 earthquake: (a) PGA; (b) SA(0.2); (c) SA(0.5); (d) SA(1.0); (e) SA(1.5); and (f) SA(3.0).

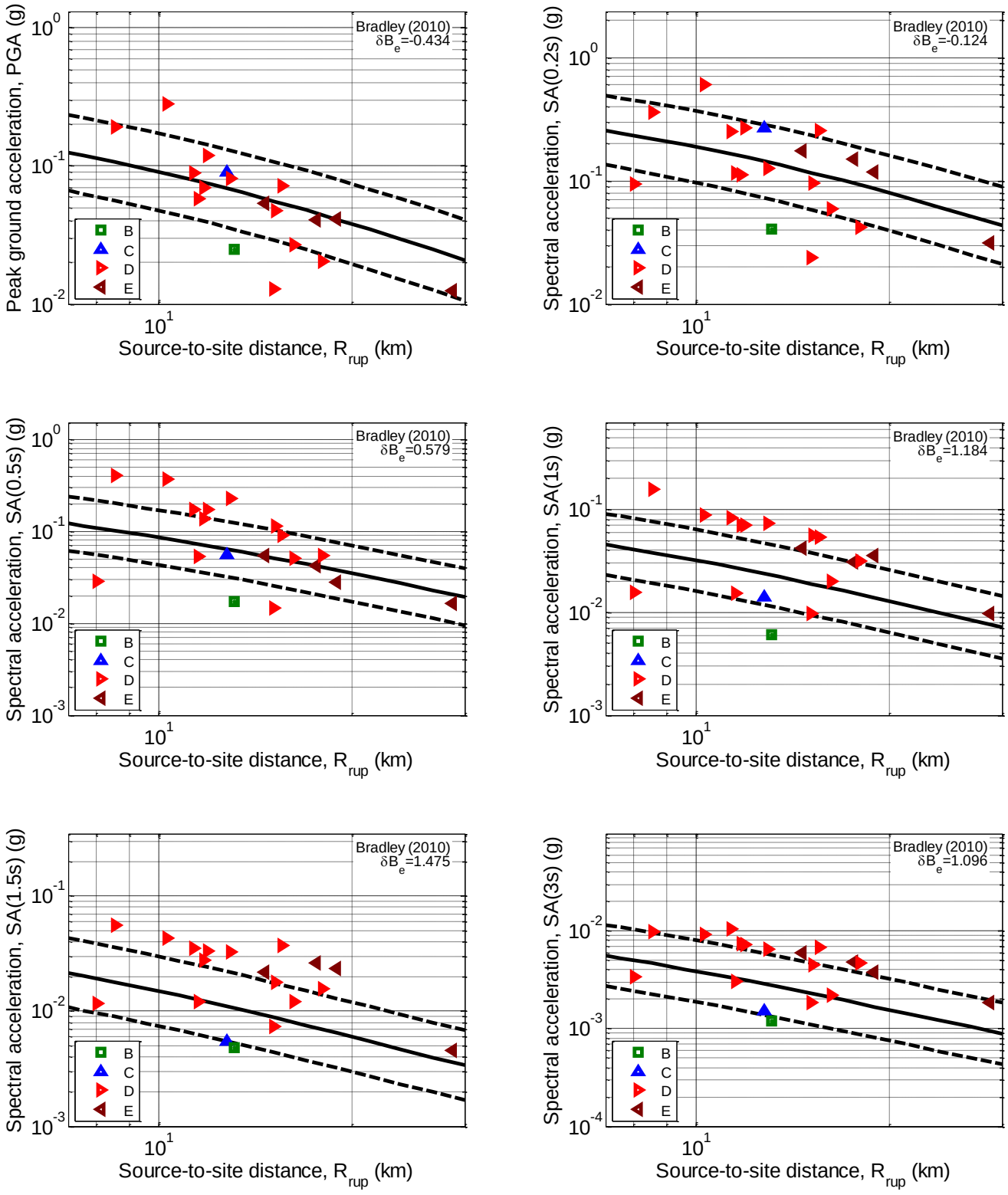

Figure 19: Comparison of the Bradley (2010) prediction (for site class D) and observations for the 19 October 2010 earthquake: (a) PGA; (b) SA(0.2); (c) SA(0.5); (d) SA(1.0); (e) SA(1.5); and (f) SA(3.0).

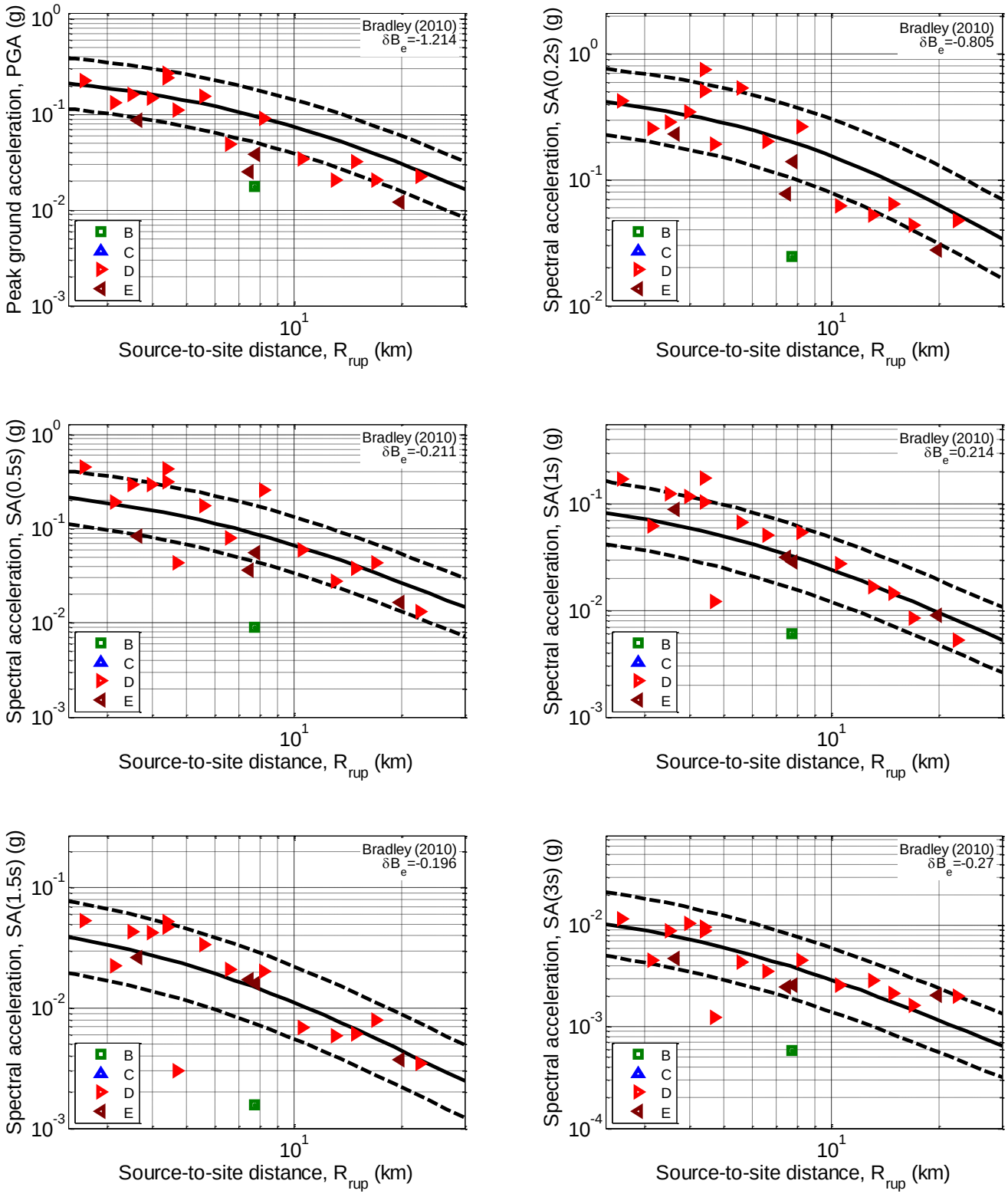

Figure 20: Comparison of the Bradley (2010) prediction (for site class D) and observations for the 26 December 2010 earthquake: (a) PGA; (b) SA(0.2); (c) SA(0.5); (d) SA(1.0); (e) SA(1.5); and (f) SA(3.0).

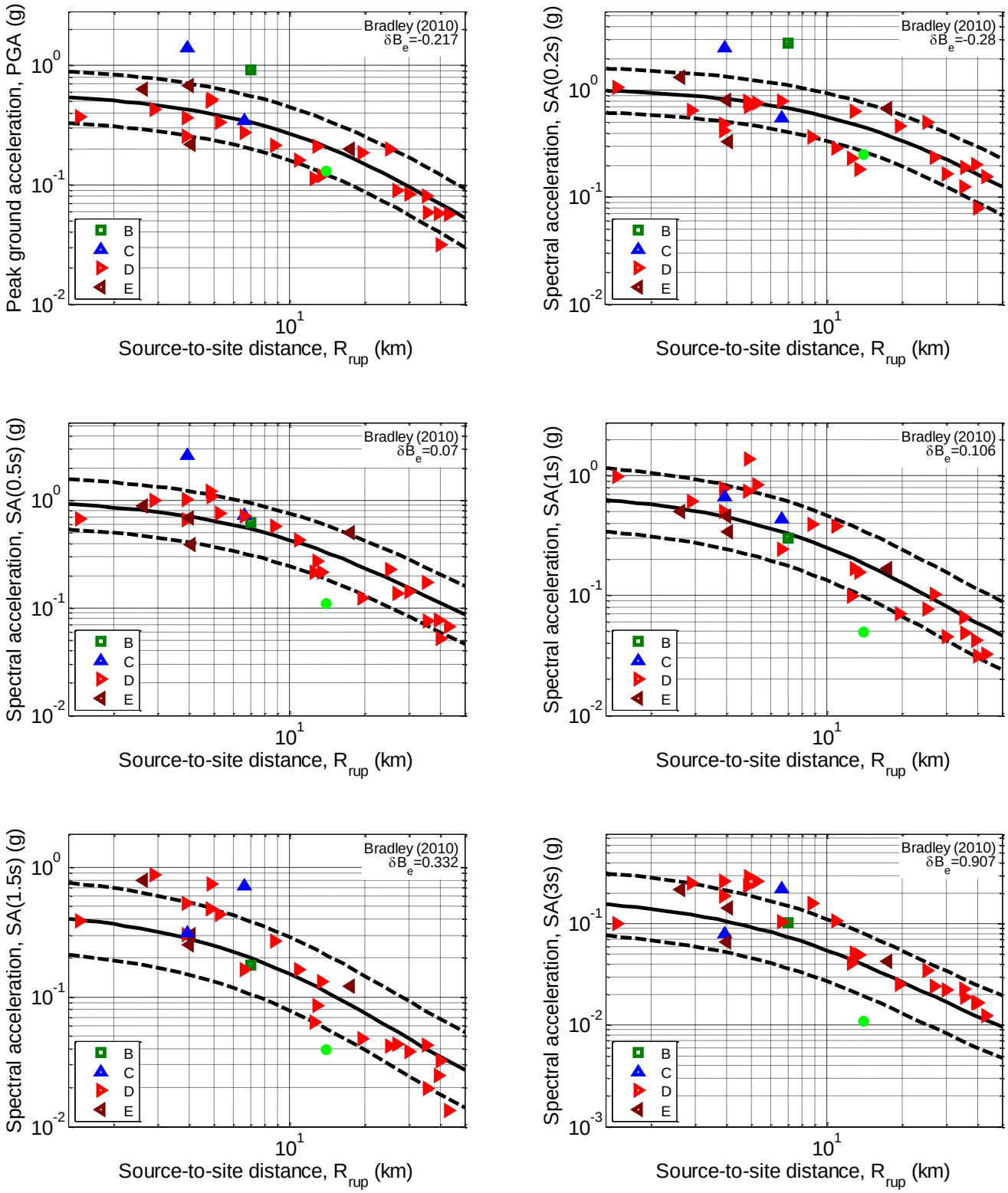

Figure 21: Comparison of the Bradley (2010) prediction (for site class D) and observations for the 22 February 2011 earthquake: (a) PGA; (b) SA(0.2); (c) SA(0.5); (d) SA(1.0); (e) SA(1.5); and (f) SA(3.0).

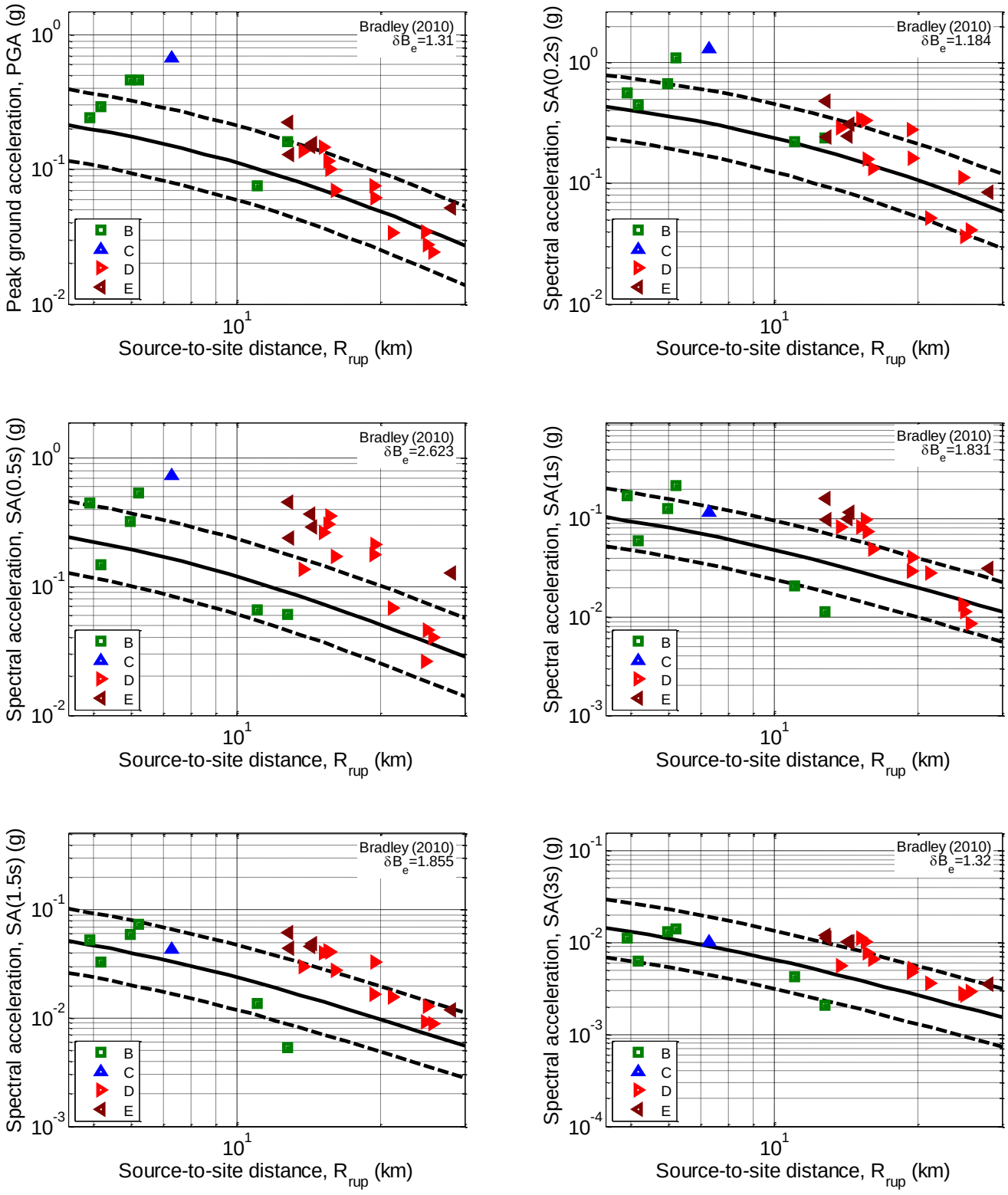

Figure 22: Comparison of the Bradley (2010) prediction (for site class D) and observations for the 16 April 2011 earthquake: (a) PGA; (b) SA(0.2); (c) SA(0.5); (d) SA(1.0); (e) SA(1.5); and (f) SA(3.0).

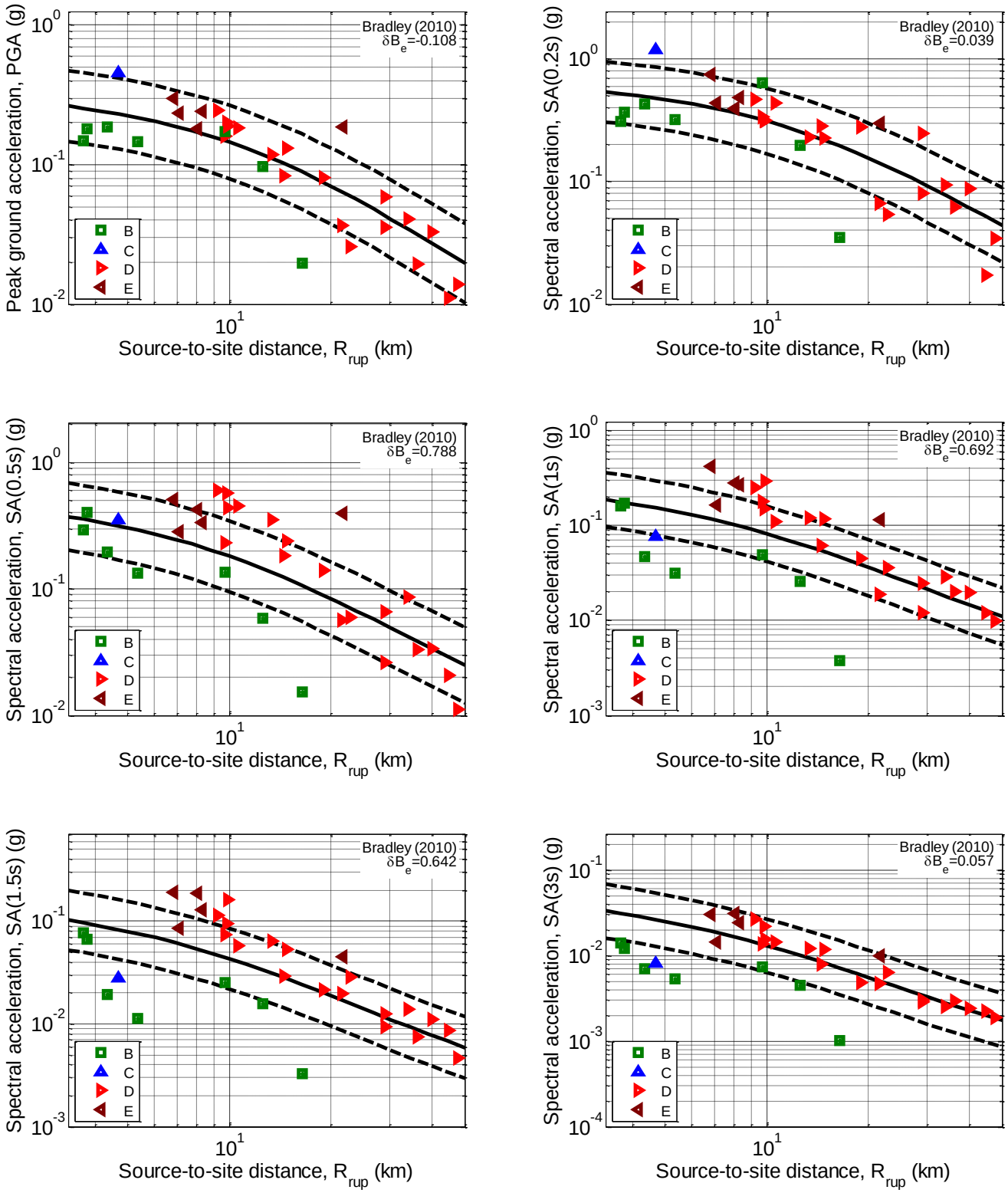

Figure 23: Comparison of the Bradley (2010) prediction (for site class D) and observations for the 13 June 2011 (1:01pm) 2011 earthquake: (a) PGA; (b) SA(0.2); (c) SA(0.5); (d) SA(1.0); (e) SA(1.5); and (f) SA(3.0).

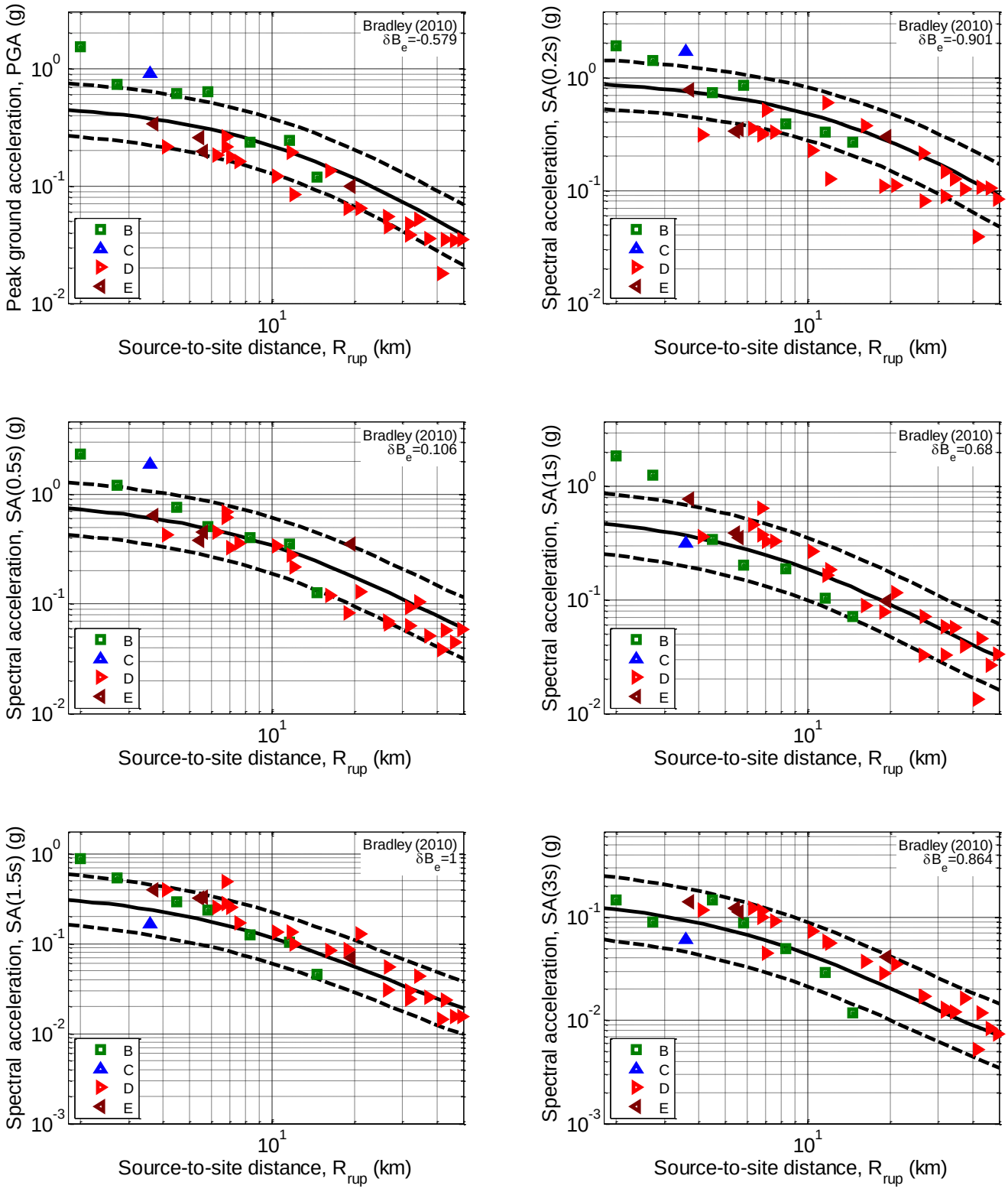

Figure 24: Comparison of the Bradley (2010) prediction (for site class D) and observations for the 13 June 2011 (2:20pm) 2011 earthquake: (a) PGA; (b) SA(0.2); (c) SA(0.5); (d) SA(1.0); (e) SA(1.5); and (f) SA(3.0).

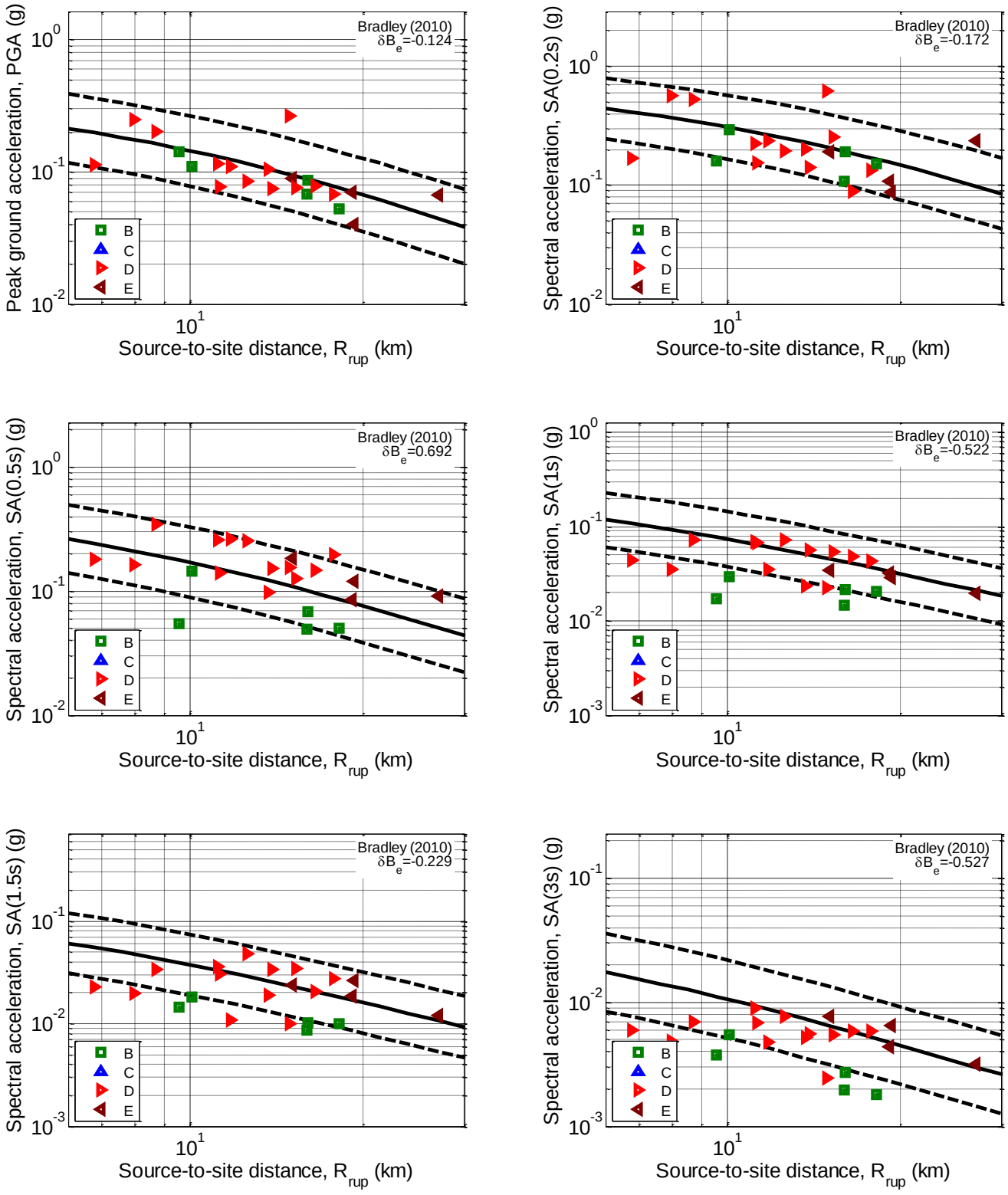

Figure 25: Comparison of the Bradley (2010) prediction (for site class D) and observations for the 21 June 2011 earthquake: (a) PGA; (b) SA(0.2); (c) SA(0.5); (d) SA(1.0); (e) SA(1.5); and (f) SA(3.0).

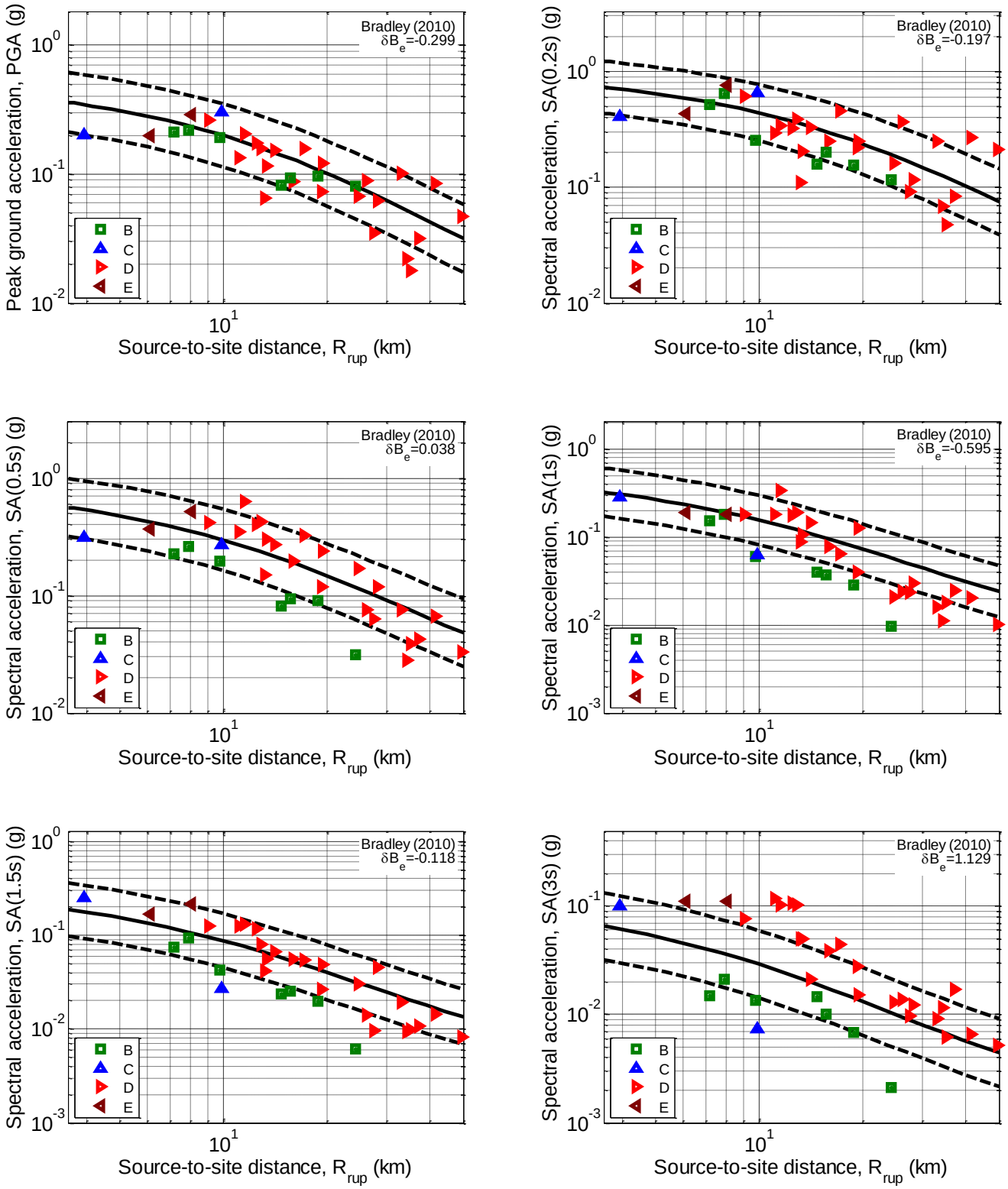

Figure 26: Comparison of the Bradley (2010) prediction (for site class D) and observations for the 23 December 2011 (12:58pm) earthquake: (a) PGA; (b) SA(0.2); (c) SA(0.5); (d) SA(1.0); (e) SA(1.5); and (f) SA(3.0).

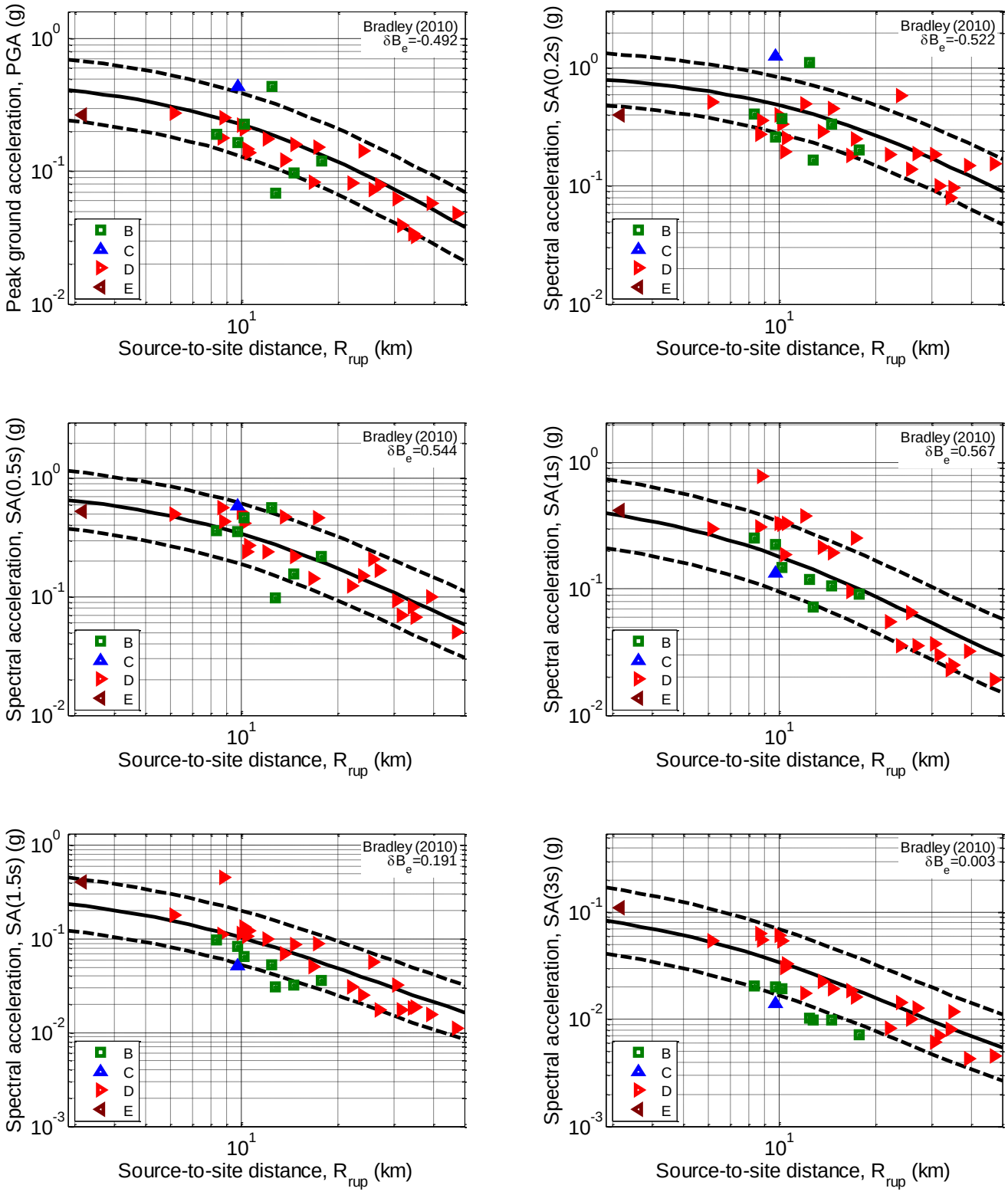

Figure 27: Comparison of the Bradley (2010) prediction (for site class D) and observations for the 23 December 2011 (1:18pm) earthquake: (a) PGA; (b) SA(0.2); (c) SA(0.5); (d) SA(1.0); (e) SA(1.5); and (f) SA(3.0).

McVerry et al. (2006) model

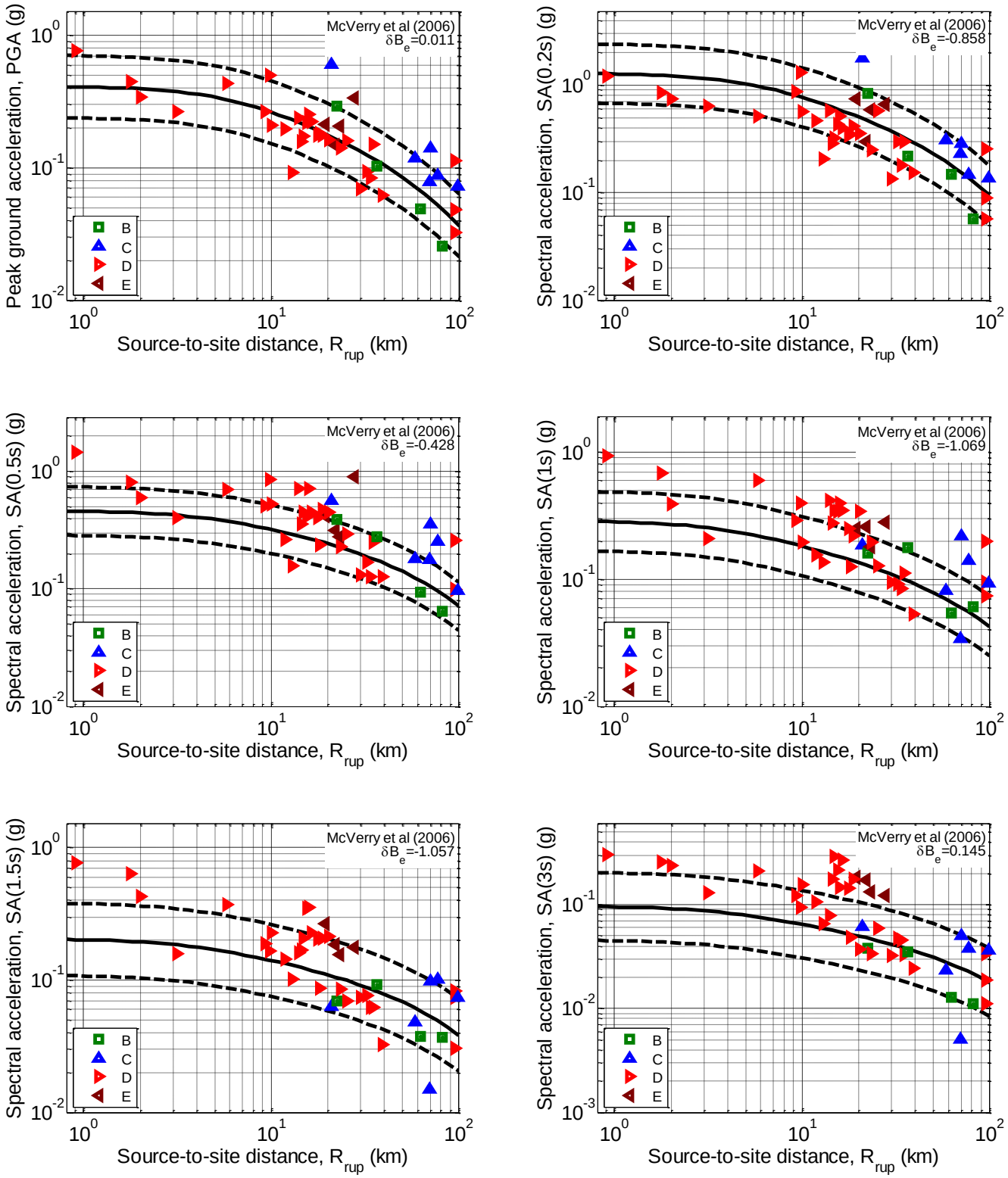

Figure 28: Comparison of the McVerry et al. (2006) prediction (for site class D) and observations for the 4 September 2010 earthquake: (a) PGA; (b) SA(0.2); (c) SA(0.5); (d) SA(1.0); (e) SA(1.5); and (f) SA(3.0).

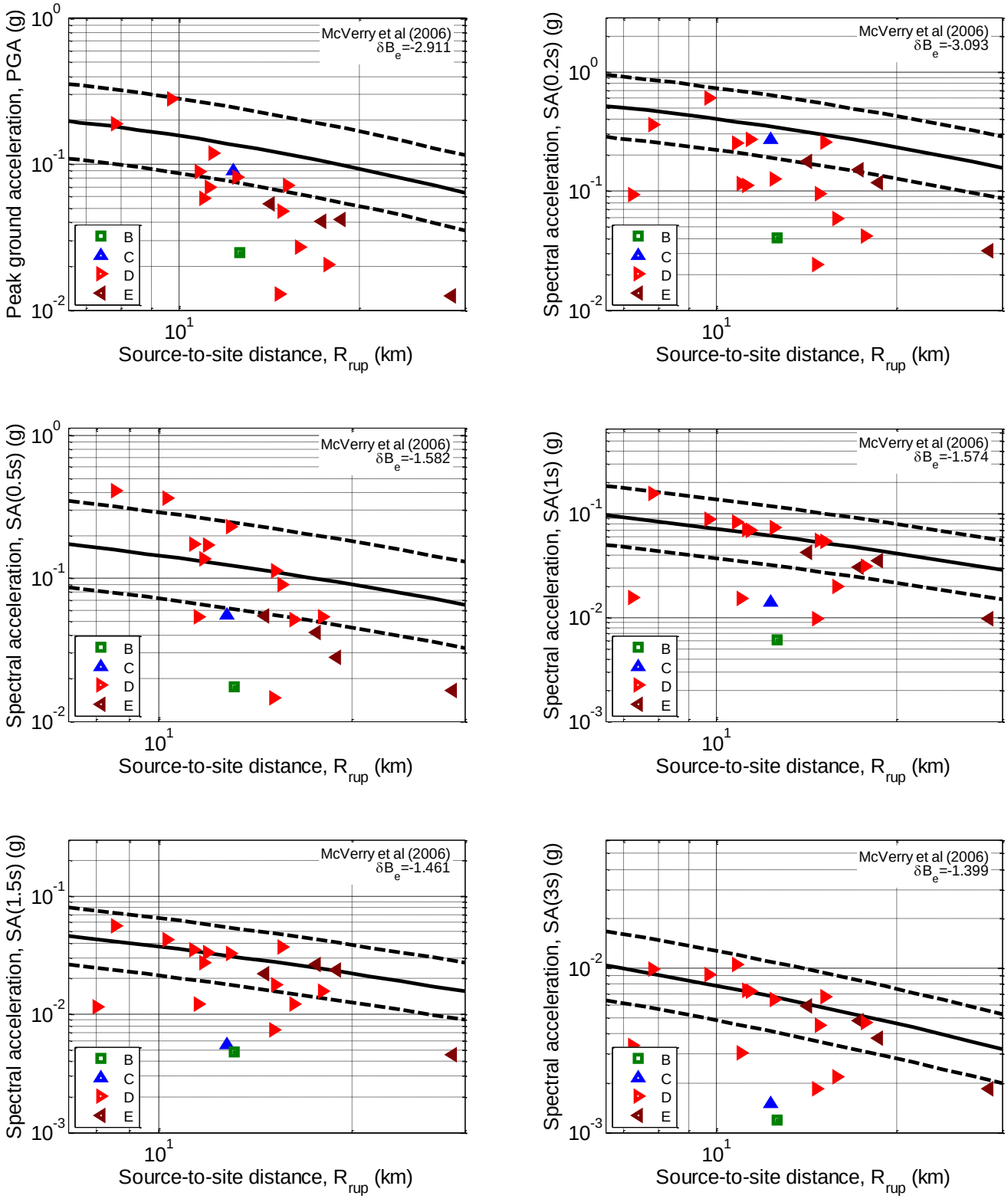

Figure 29: Comparison of the McVerry et al. (2006) prediction (for site class D) and observations for the 19 October 2010 earthquake: (a) PGA; (b) SA(0.2); (c) SA(0.5); (d) SA(1.0); (e) SA(1.5); and (f) SA(3.0).

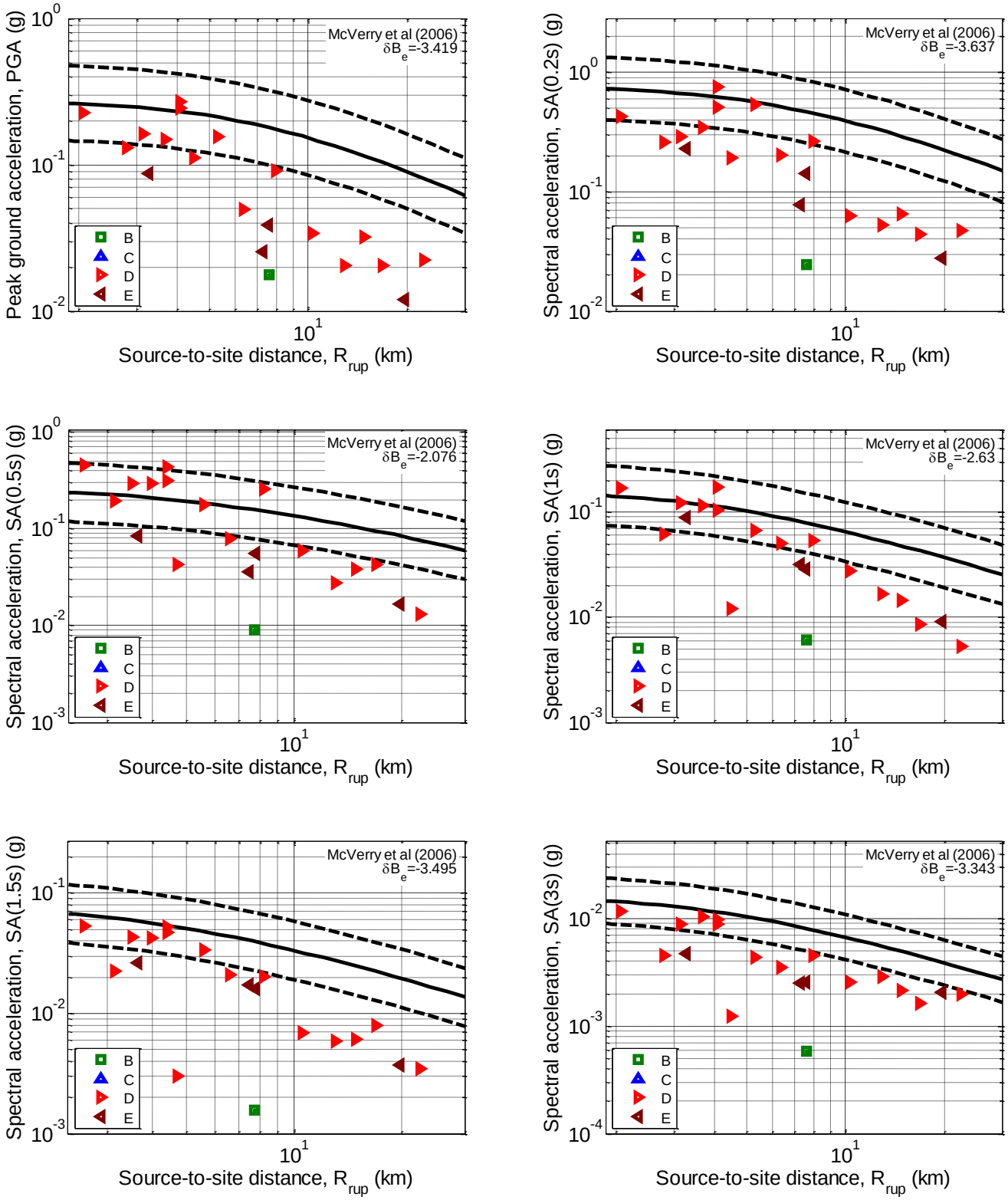

Figure 30: Comparison of the McVerry et al. (2006) prediction (for site class D) and observations for the 26 December 2010 earthquake: (a) PGA; (b) SA(0.2); (c) SA(0.5); (d) SA(1.0); (e) SA(1.5); and (f) SA(3.0).

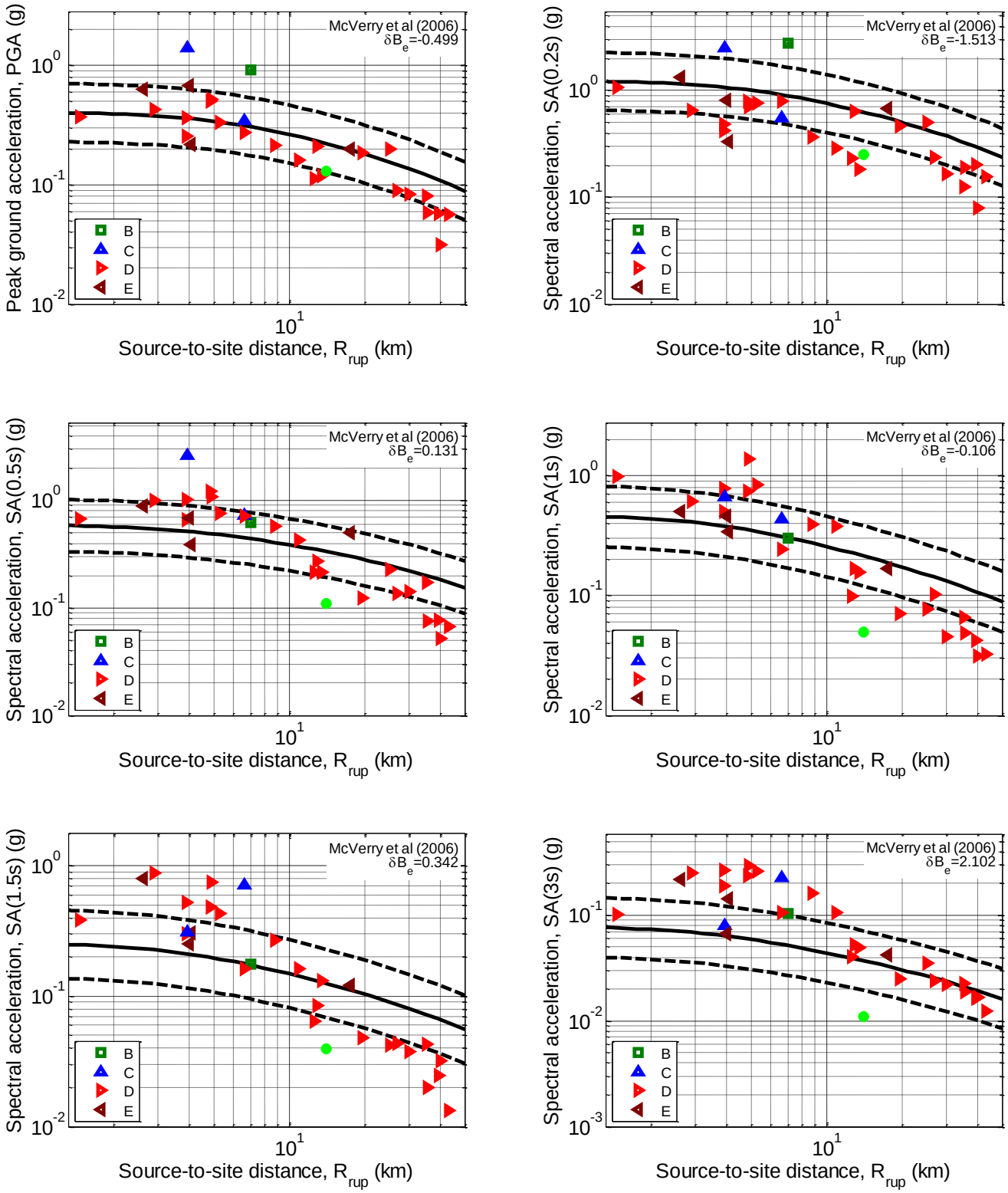

Figure 31: Comparison of the McVerry et al. (2006) prediction (for site class D) and observations for the 22 February 2011 earthquake: (a) PGA; (b) SA(0.2); (c) SA(0.5); (d) SA(1.0); (e) SA(1.5); and (f) SA(3.0).

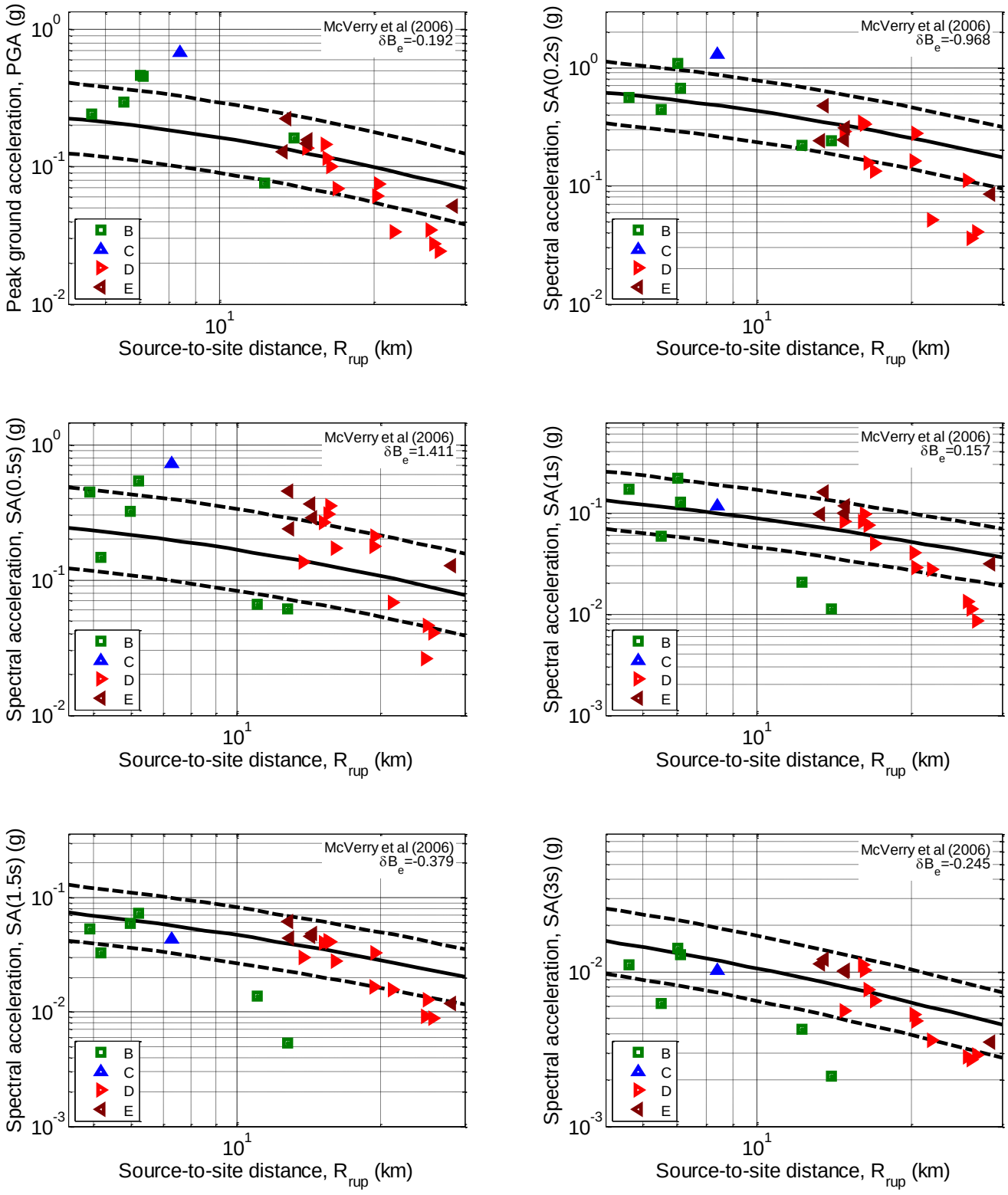

Figure 32: Comparison of the McVerry et al. (2006) prediction (for site class D) and observations for the 16 April 2011 earthquake: (a) PGA; (b) SA(0.2); (c) SA(0.5); (d) SA(1.0); (e) SA(1.5); and (f) SA(3.0).

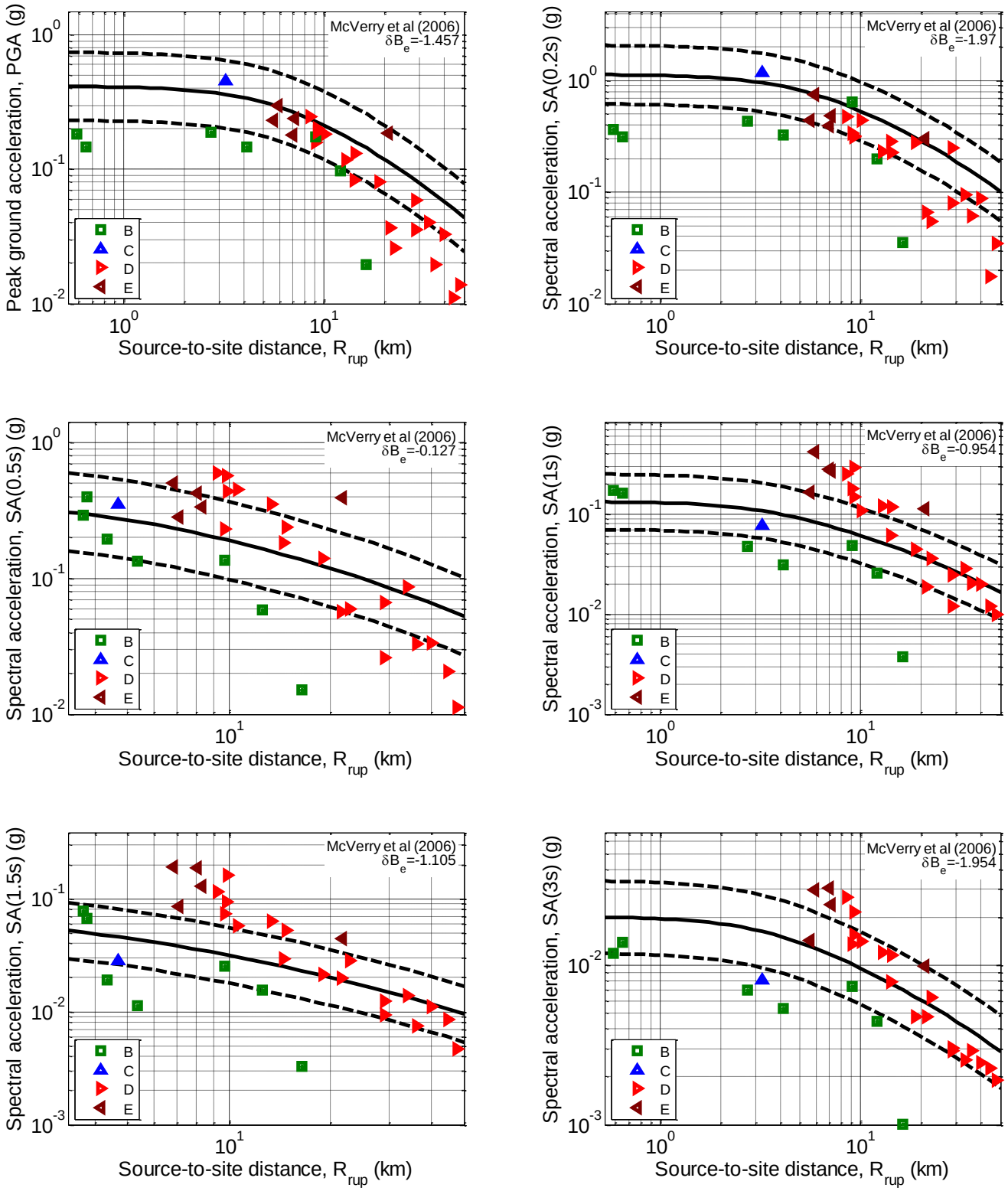

Figure 33: Comparison of the McVerry et al. (2006) prediction (for site class D) and observations for the 13 June 2011 (1:01pm) 2011 earthquake: (a) PGA; (b) SA(0.2); (c) SA(0.5); (d) SA(1.0); (e) SA(1.5); and (f) SA(3.0).

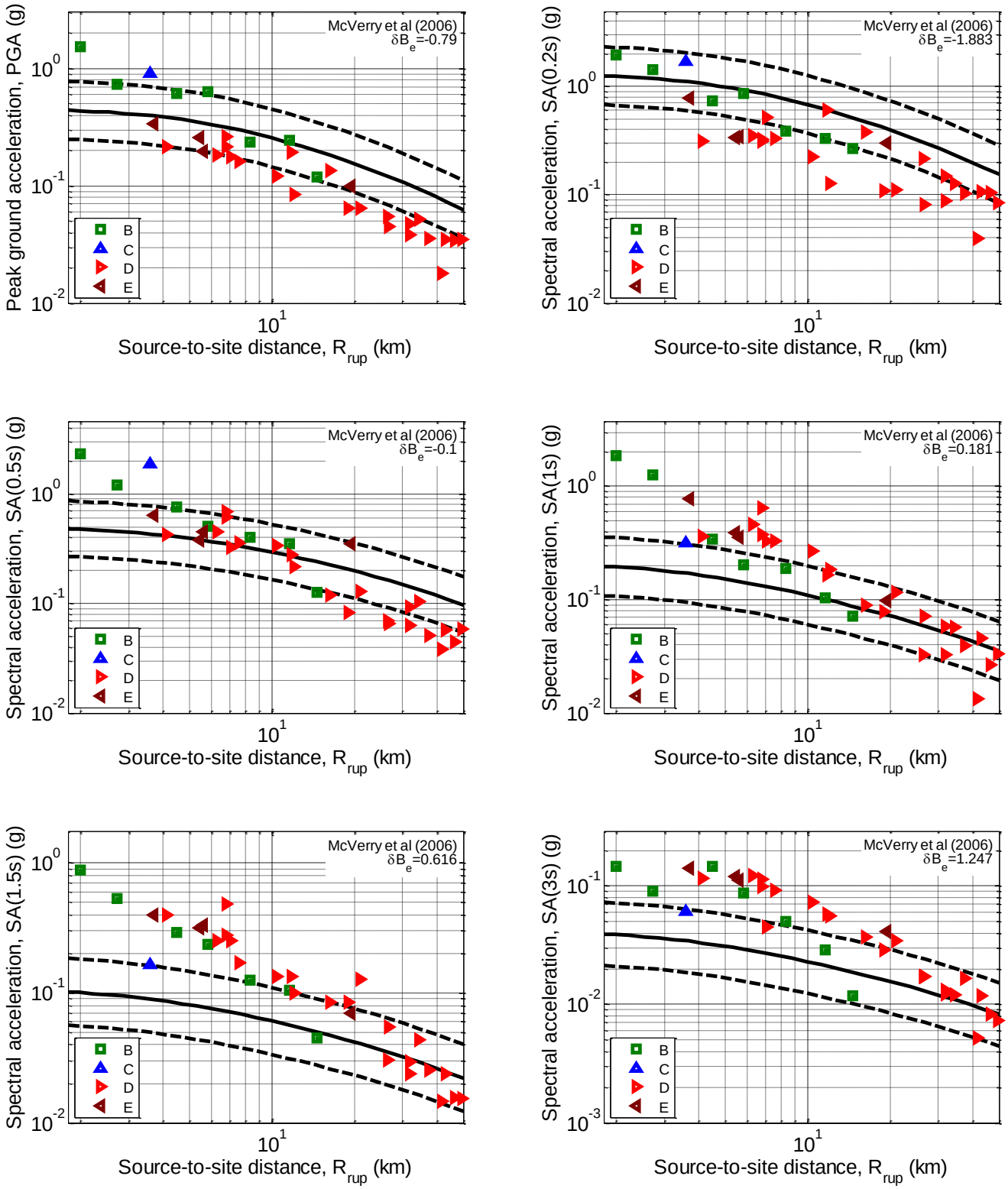

Figure 34: Comparison of the McVerry et al. (2006) prediction (for site class D) and observations for the 13 June 2011 (2:20pm) 2011 earthquake: (a) PGA; (b) SA(0.2); (c) SA(0.5); (d) SA(1.0); (e) SA(1.5); and (f) SA(3.0).

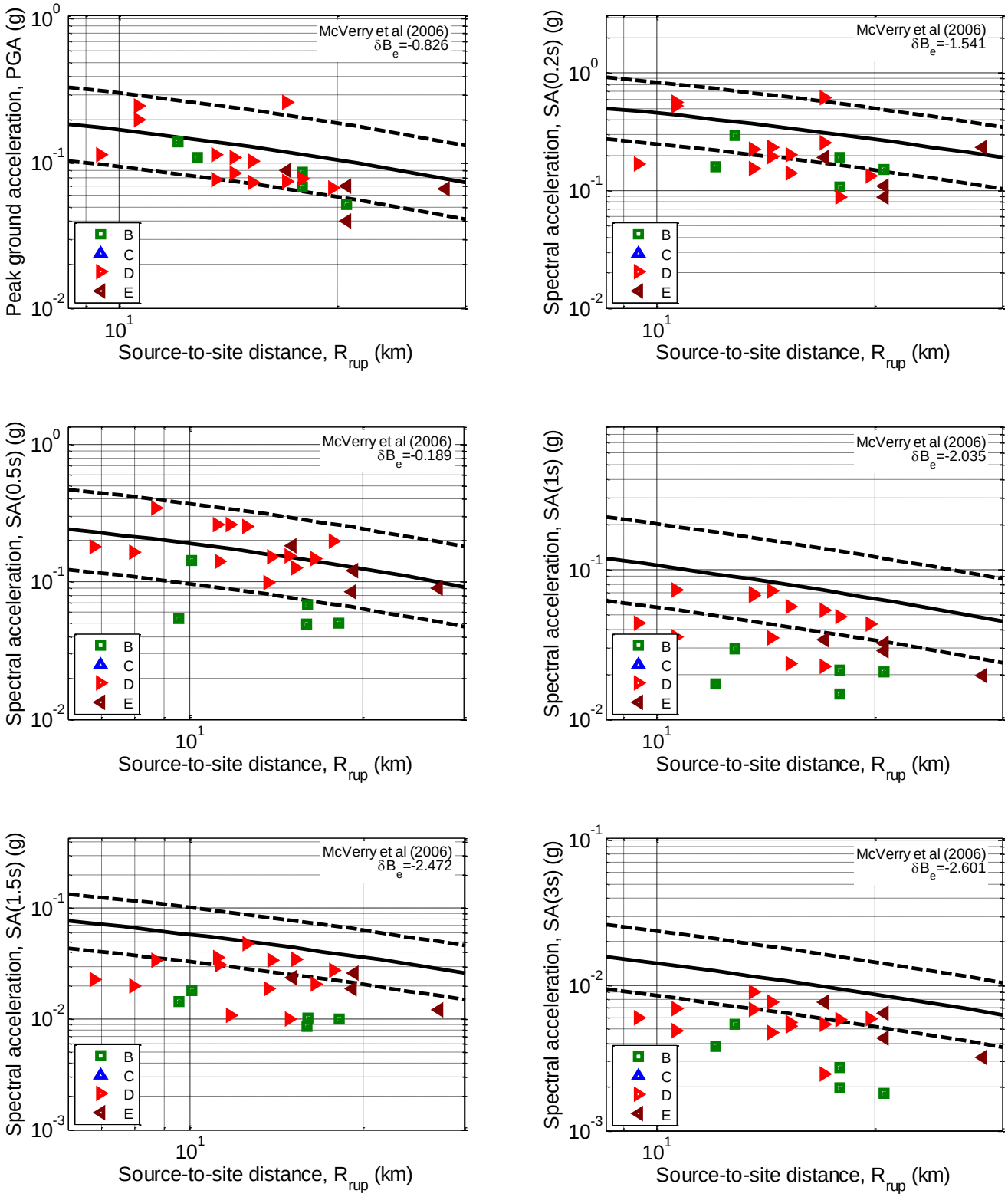

Figure 35: Comparison of the McVerry et al. (2006) prediction (for site class D) and observations for the 21 June 2011 earthquake: (a) PGA; (b) SA(0.2); (c) SA(0.5); (d) SA(1.0); (e) SA(1.5); and (f) SA(3.0).

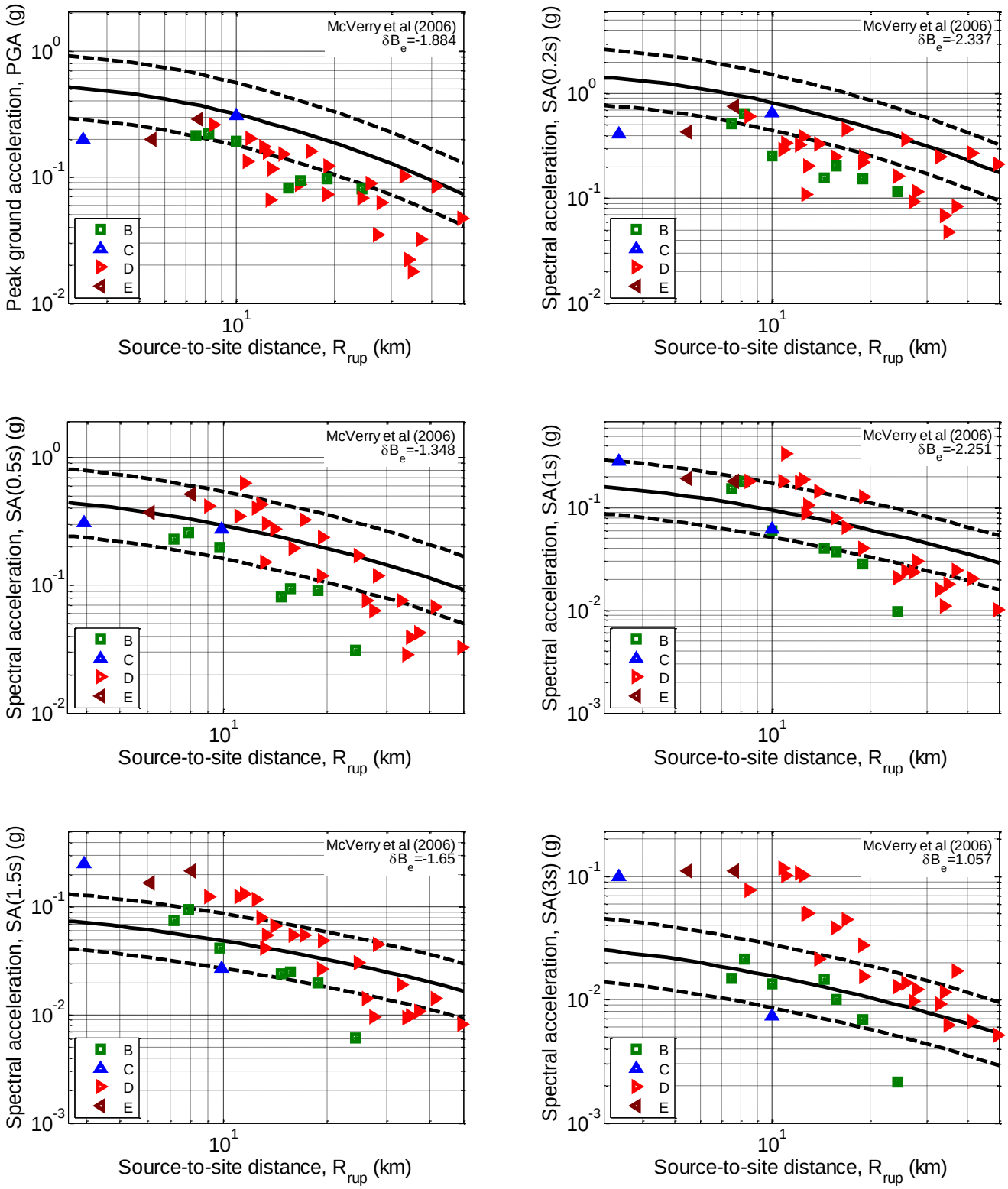

Figure 36: Comparison of the McVerry et al. (2006) prediction (for site class D) and observations for the 23 December 2011 (12:58pm) earthquake: (a) PGA; (b) SA(0.2); (c) SA(0.5); (d) SA(1.0); (e) SA(1.5); and (f) SA(3.0).

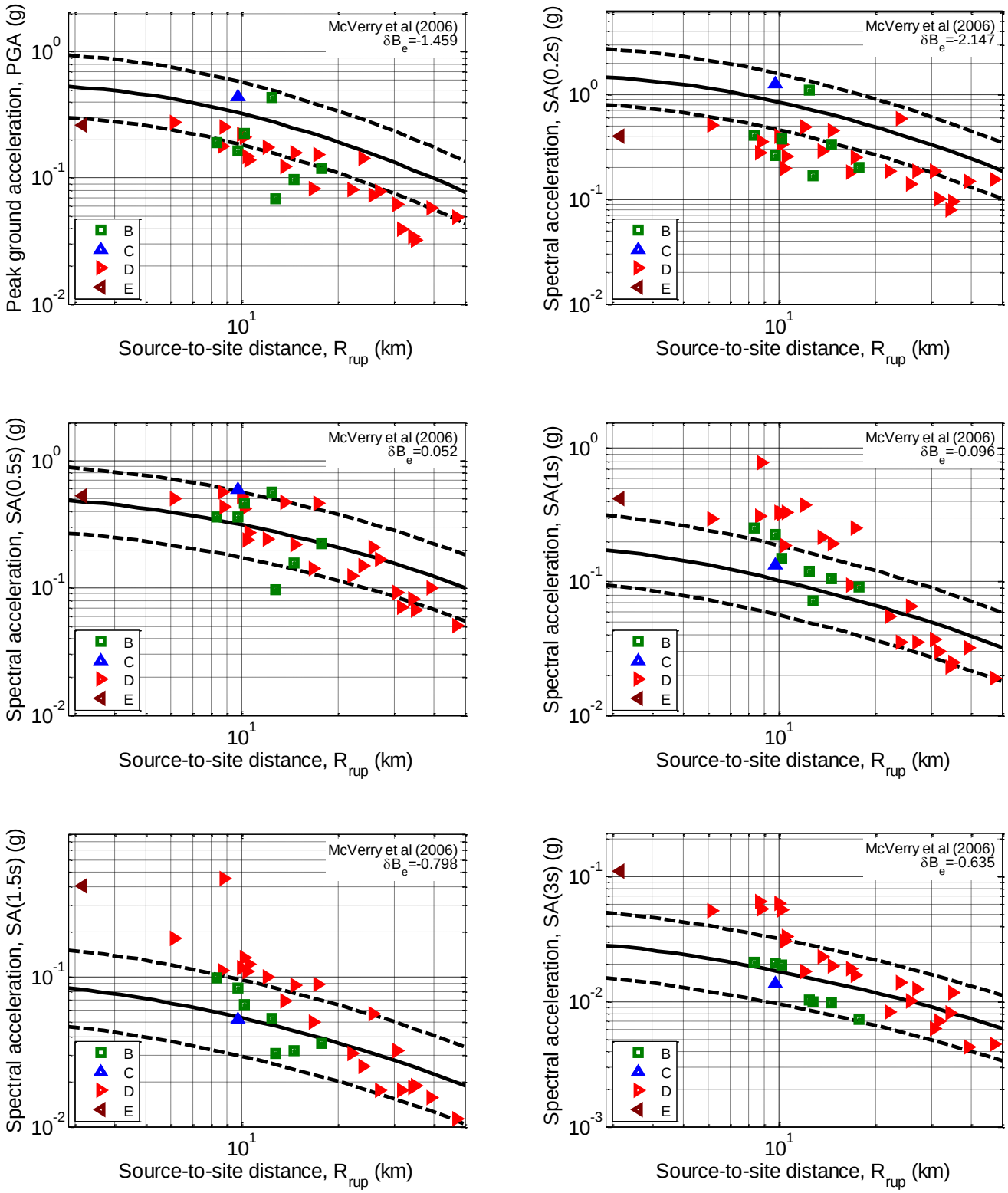

Figure 37: Comparison of the McVerry et al. (2006) prediction (for site class D) and observations for the 23 December 2011 (1:18pm) earthquake: (a) PGA; (b) SA(0.2); (c) SA(0.5); (d) SA(1.0); (e) SA(1.5); and (f) SA(3.0).

Appendix 2: Insight from site response numerical simulations

The Christchurch region has both a relatively deep basin of sedimentary soils and also very soft surficial soils which easily liquefy. Significant long period SA amplitudes were recorded at locations in the Christchurch central business district during several of the Canterbury earthquakes and the local soil stratigraphy is postulated to have contributed to these observations.

Smyrou et al. (2011) attempted to illustrate the role of the deep and shallow geotechnical layers via a 1D effective stress analysis, that has also been independently performed, and is presented here. The 1D analyses utilized the LPCC rock motion, and a 400m deep column of finite elements comprised of 3 layers. The base gravel layer ranged from 25m to 400m depth, while two overlying layers ranging from depths 0m – 7.5m – 25m were based on the soil profile at Fitzgerald Bridge (Bradley et al. 2009). The gravel layer was modelled as a Drucker-Prager material, while the Stress-Density model (Cubrinovski and Ishihara 1998) was used for modelling the two sandy soil layers. Figure 38 and Figure 39 illustrate in linear and log scales, respectively, the acceleration response spectrum of the simulated ground motions at the top of the gravel layer (25m depth) and at the surface, in comparison to the observed ground motion SA amplitudes at CHHC and CBGS. It can be seen that while the observations and predictions are obviously different that the simulations clearly capture the significant amplification in long period ground motion due to the large depth of gravel layers; and also the significant reduction in high frequency ground motion ($T < 1s$) in the shallow sandy soil layers as a result of significant nonlinear response and liquefaction.

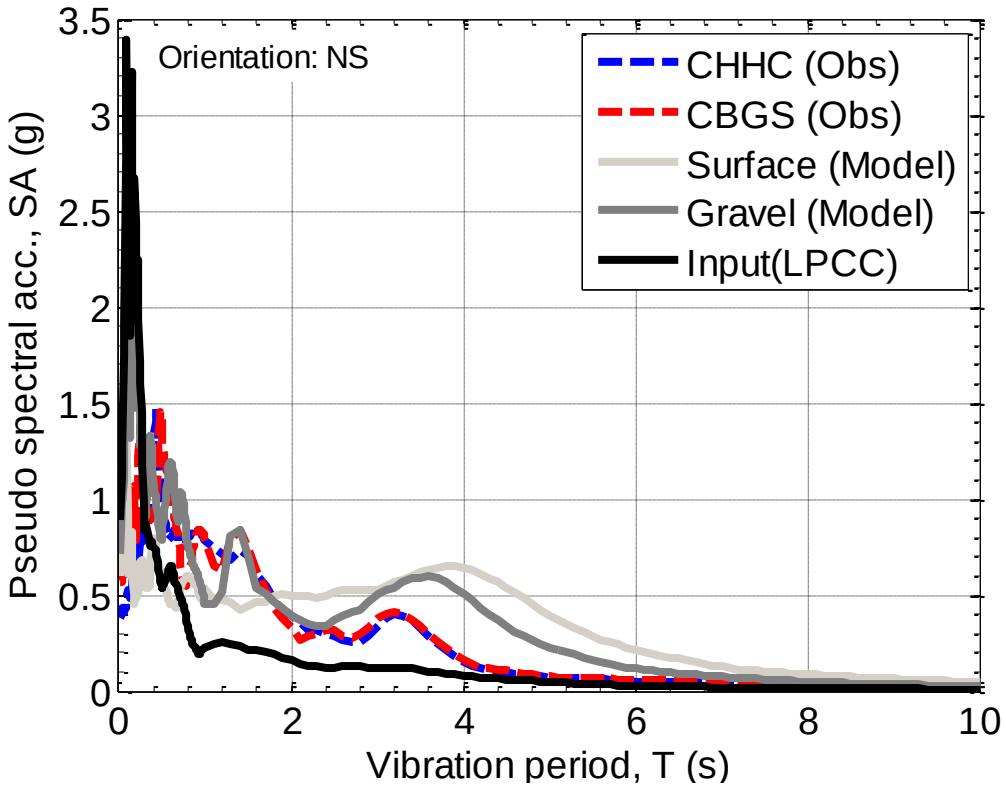

Figure 38: Acceleration response spectra obtained from the 1D site response model as compared with observations at CBGS and CHHC.

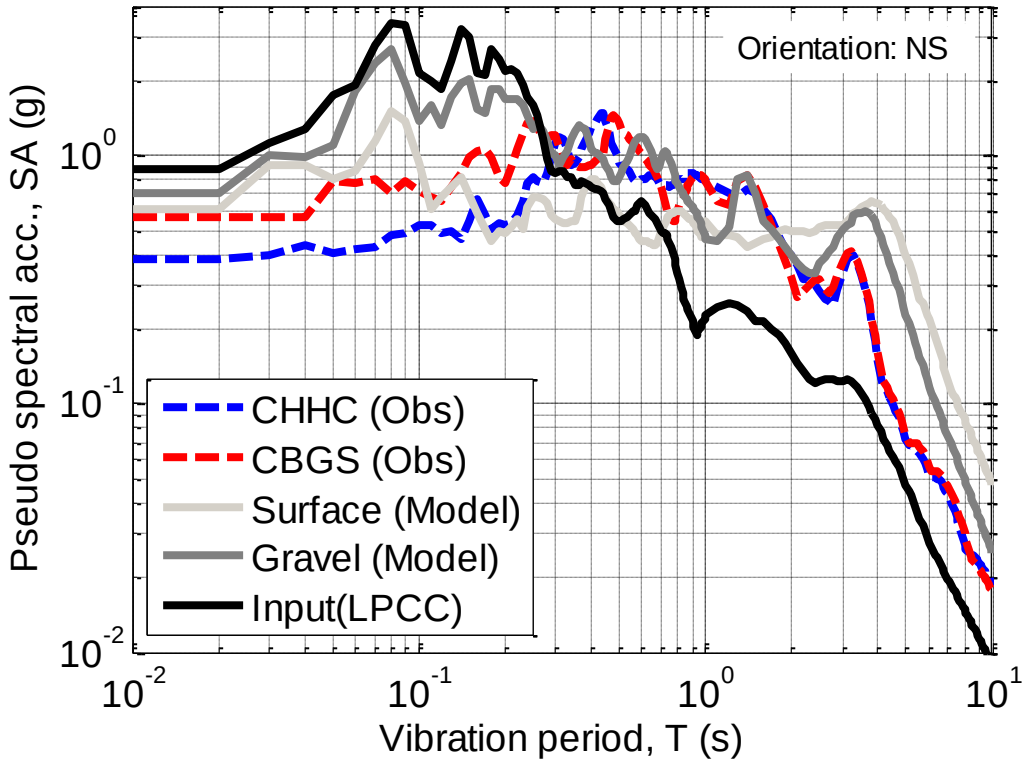

Figure 39: As for Figure 38, but in log-log scale.

Appendix 3: Within-event residuals for individual sites

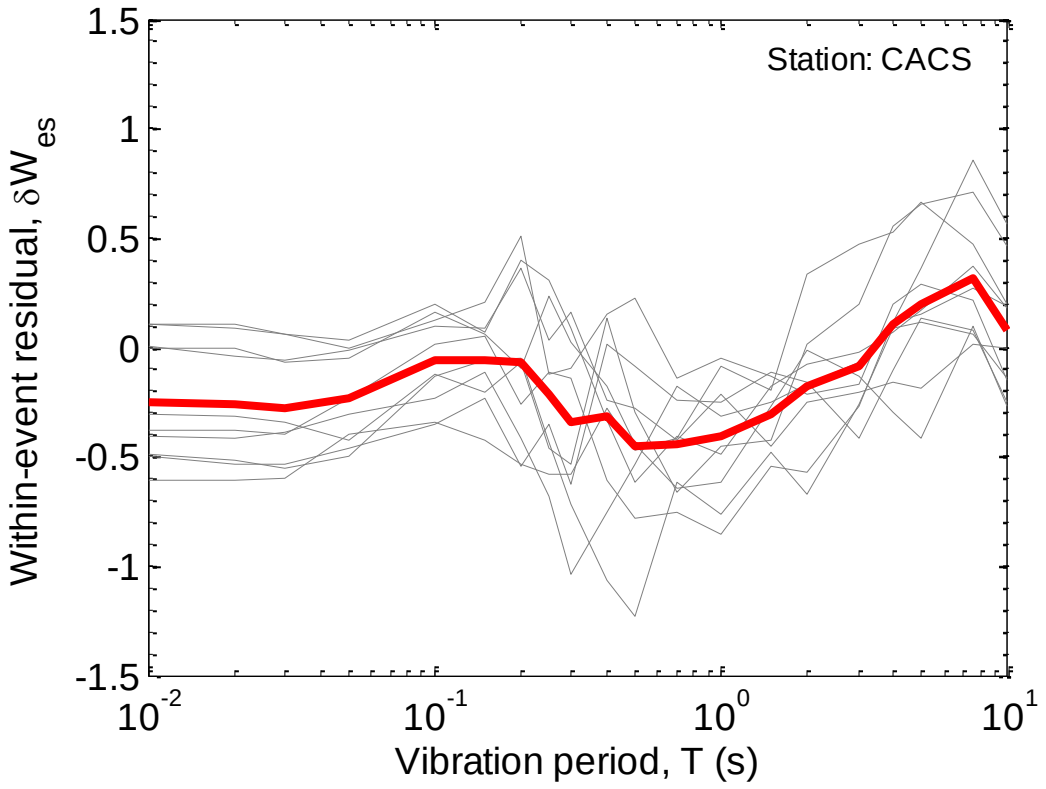

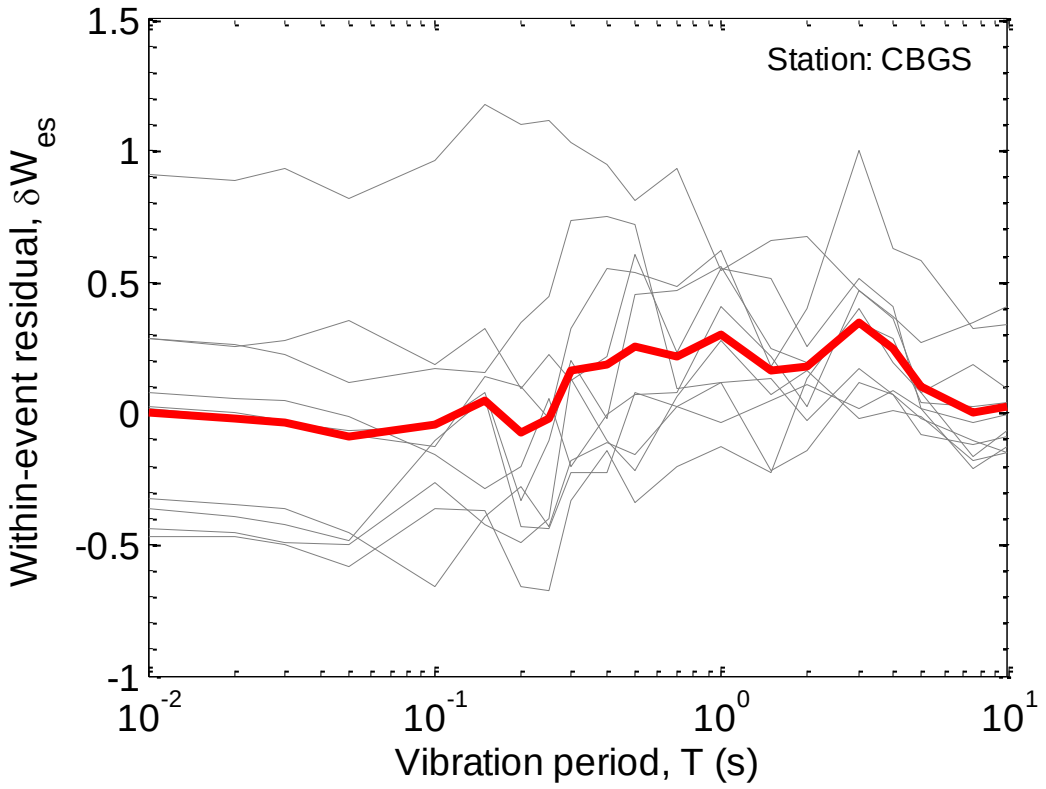

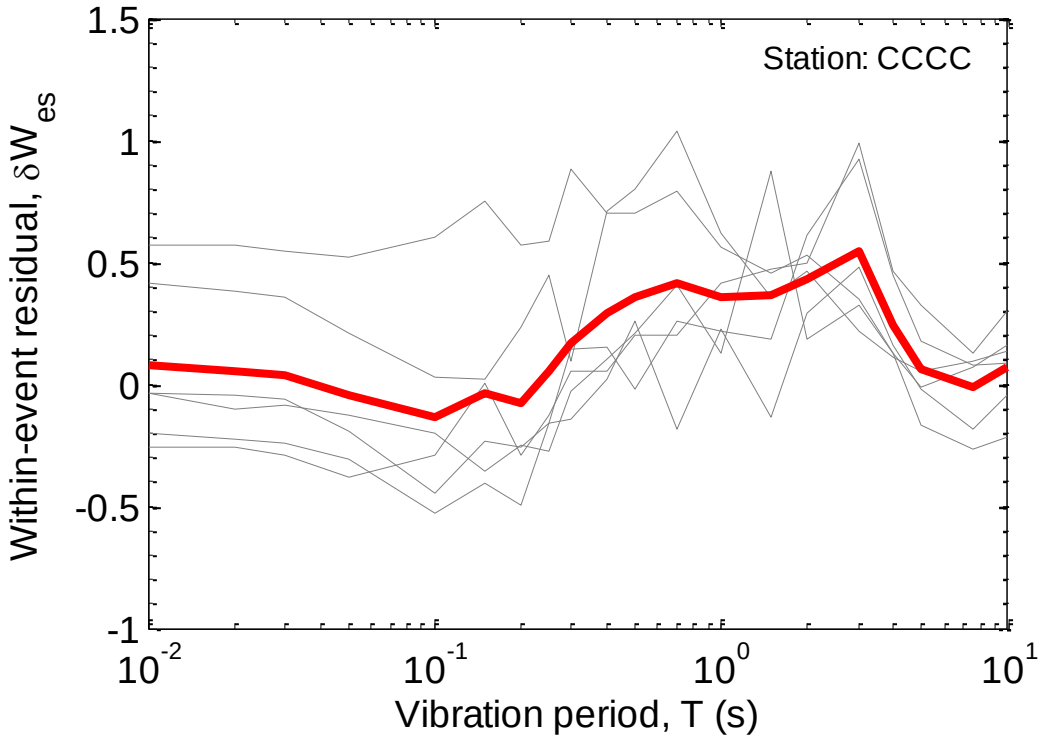
Station: CCCC
Within-event residual, δW_es
1.5
1
0.5
0
-0.5
-1
10^-2
10^-1
10^0
10^1
Vibration period, T (s)

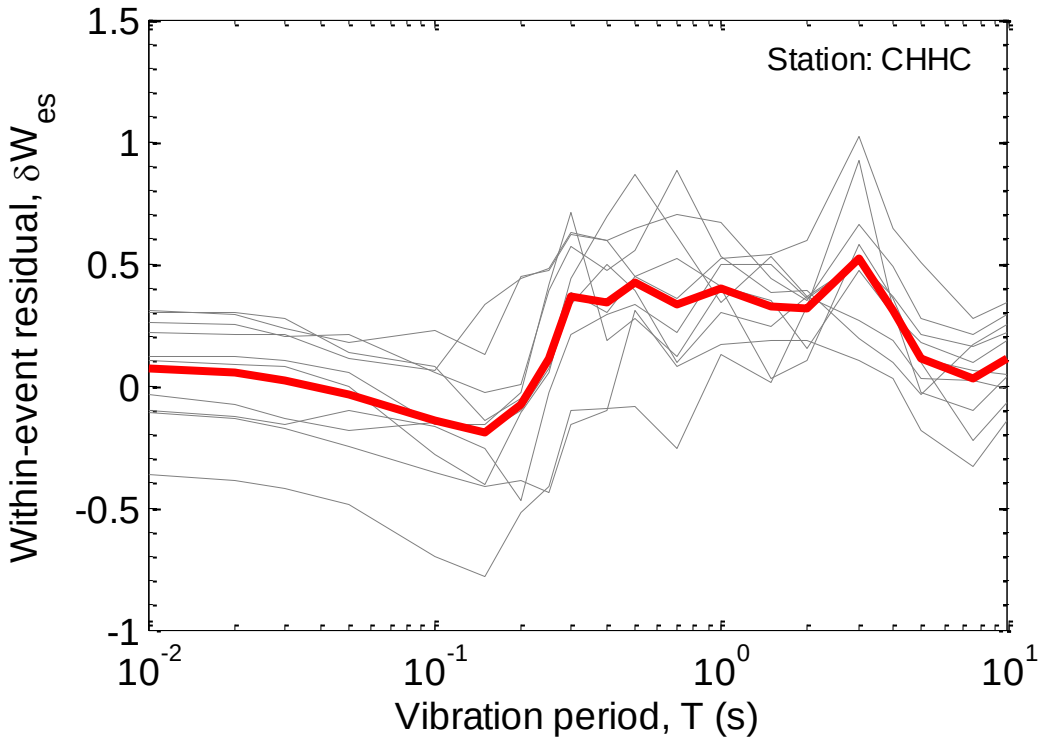
Station: CHHC
Within-event residual, δW_es
1.5
1
0.5
0
-0.5
-1
10^-2
10^-1
10^0
10^1
Vibration period, T (s)

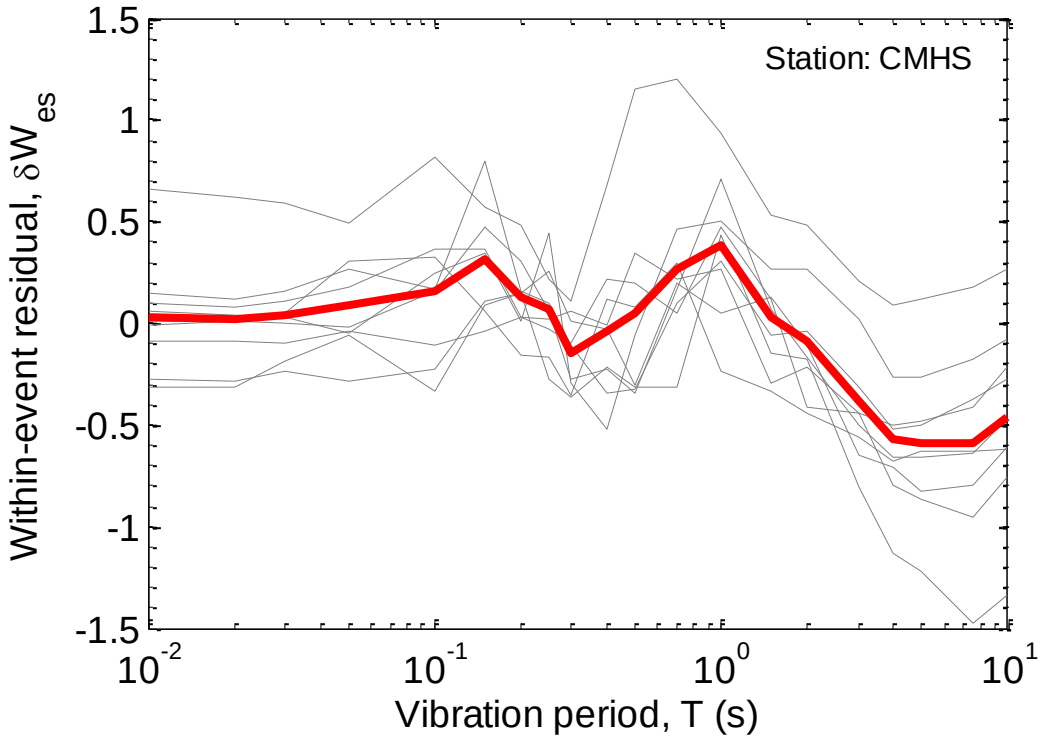
Station: CMHS
Within-event residual, δW_es
Vibration period, T (s)
1.5
1
0.5
0
-0.5
-1
-1.5
10^-2
10^-1
10^0
10^1

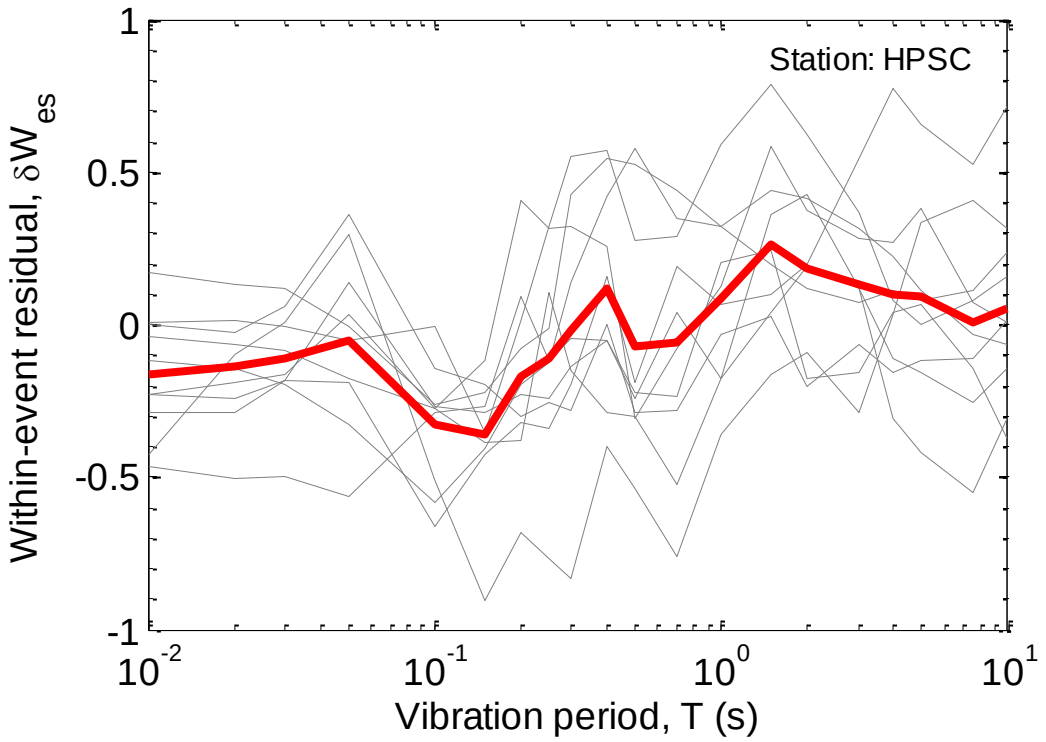
Station: HPSC
Within-event residual, δW_es
Vibration period, T (s)
1
0.5
0
-0.5
-1
10^-2
10^-1
10^0
10^1

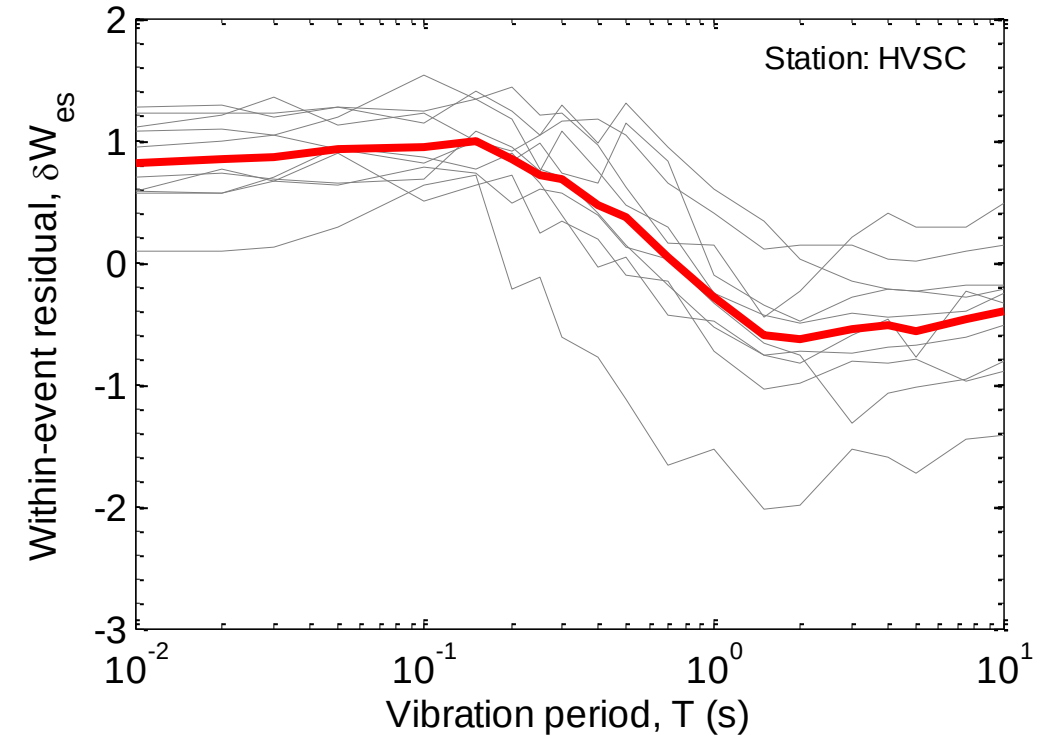
Station: HVSC
Within-event residual, δW_es
Vibration period, T (s)
2
1
0
-1
-2
-3
10^-2
10^-1
10^0
10^1

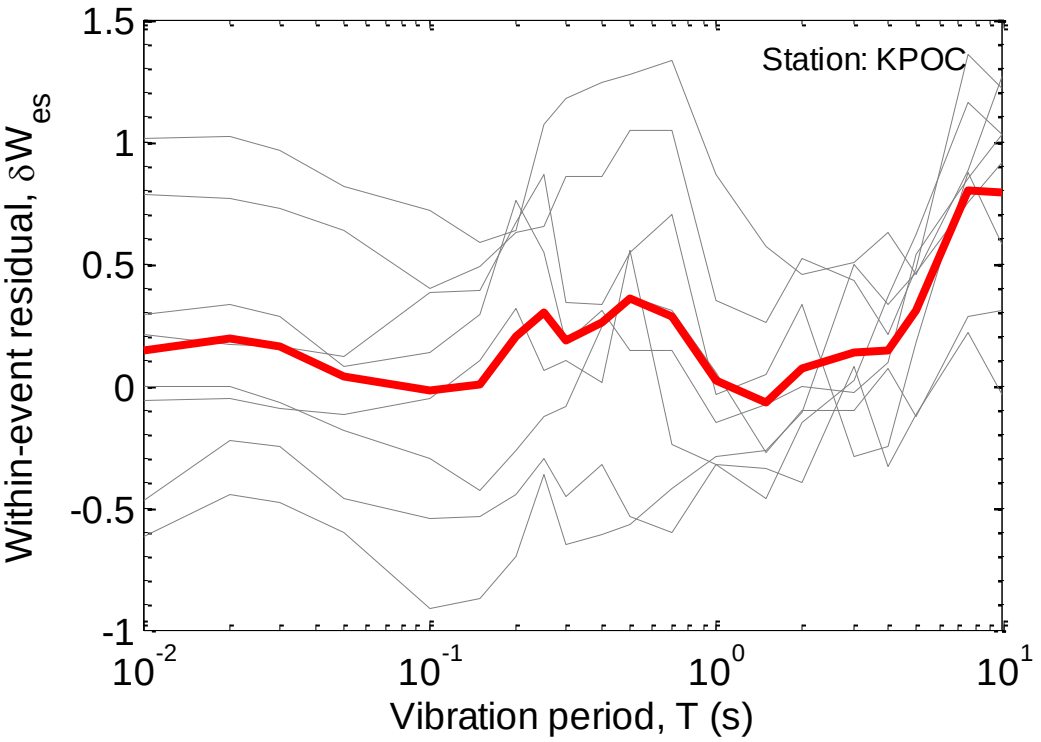
Station: KPOC
Within-event residual, δW_es
Vibration period, T (s)
1.5
1
0.5
0
-0.5
-1
10^-2
10^-1
10^0
10^1

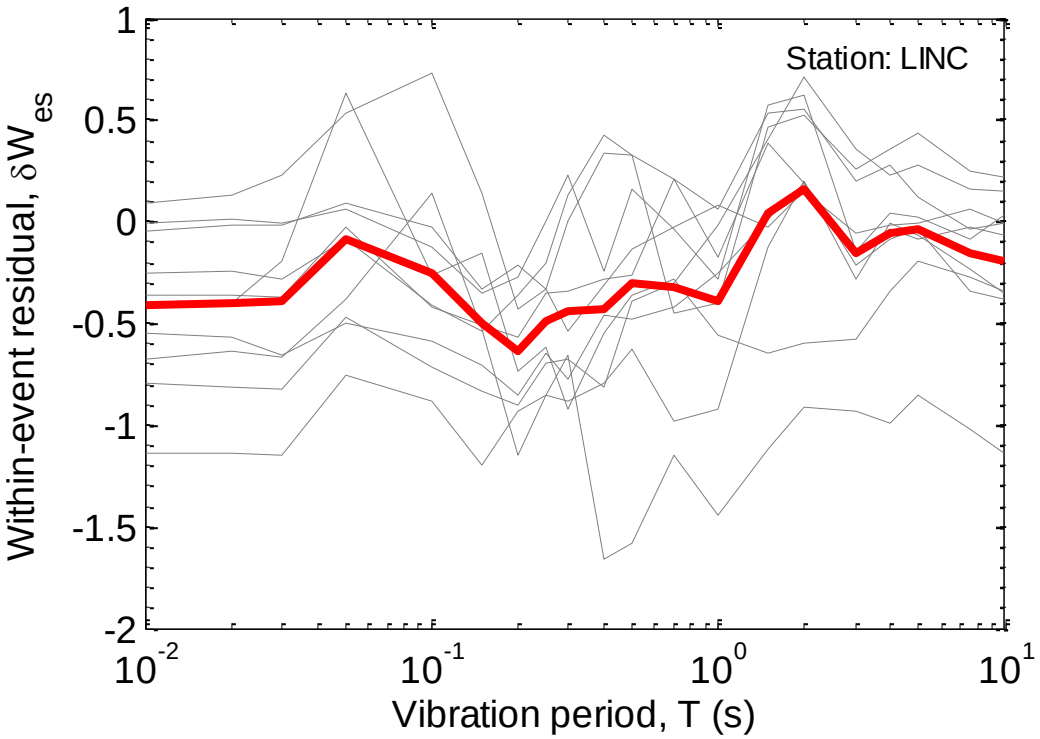
Station: LINC
Within-event residual, δW_es
Vibration period, T (s)
1
0.5
0
-0.5
-1
-1.5
-2
10^-2
10^-1
10^0
10^1

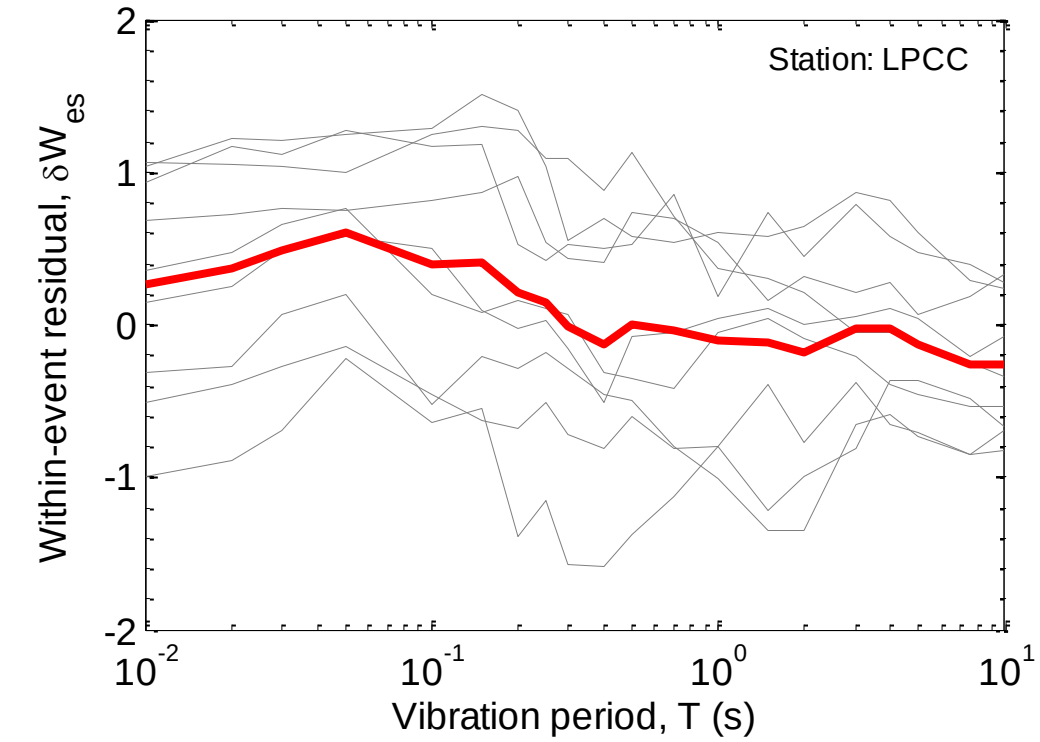
Station: LPCC
Within-event residual, δW_es
Vibration period, T (s)
2
1
0
-1
-2
10^-2
10^-1
10^0
10^1

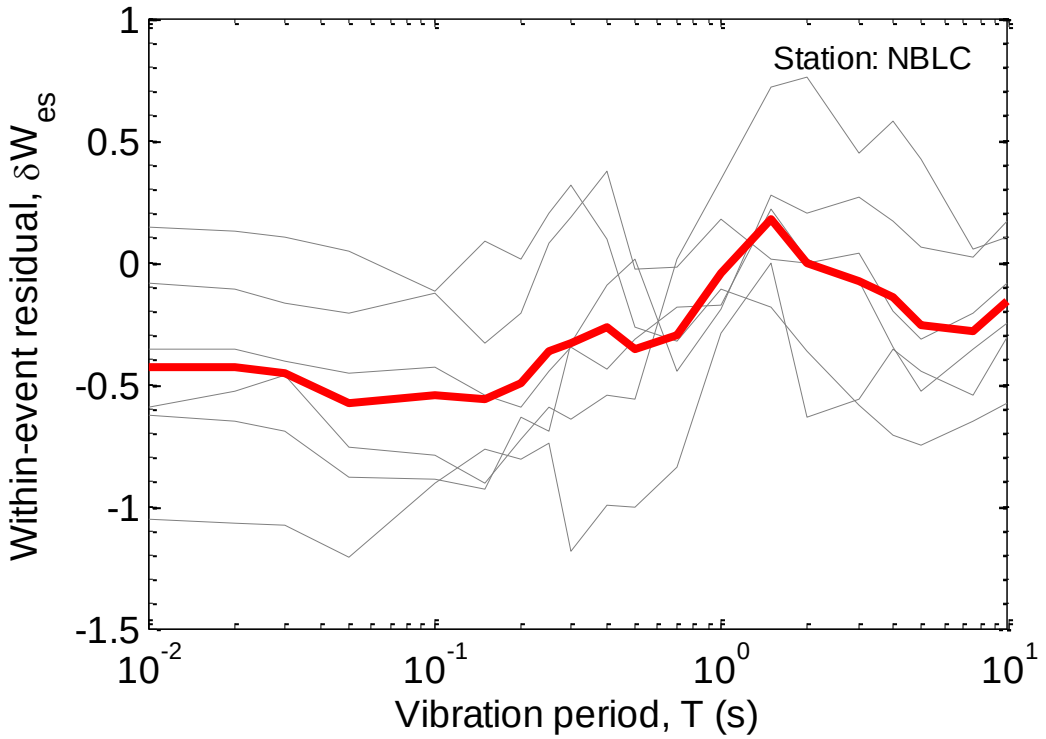
Station: NBLC
Within-event residual, δW_es
1
0.5
0
-0.5
-1
-1.5
10^-2
10^-1
10^0
10^1
Vibration period, T (s)

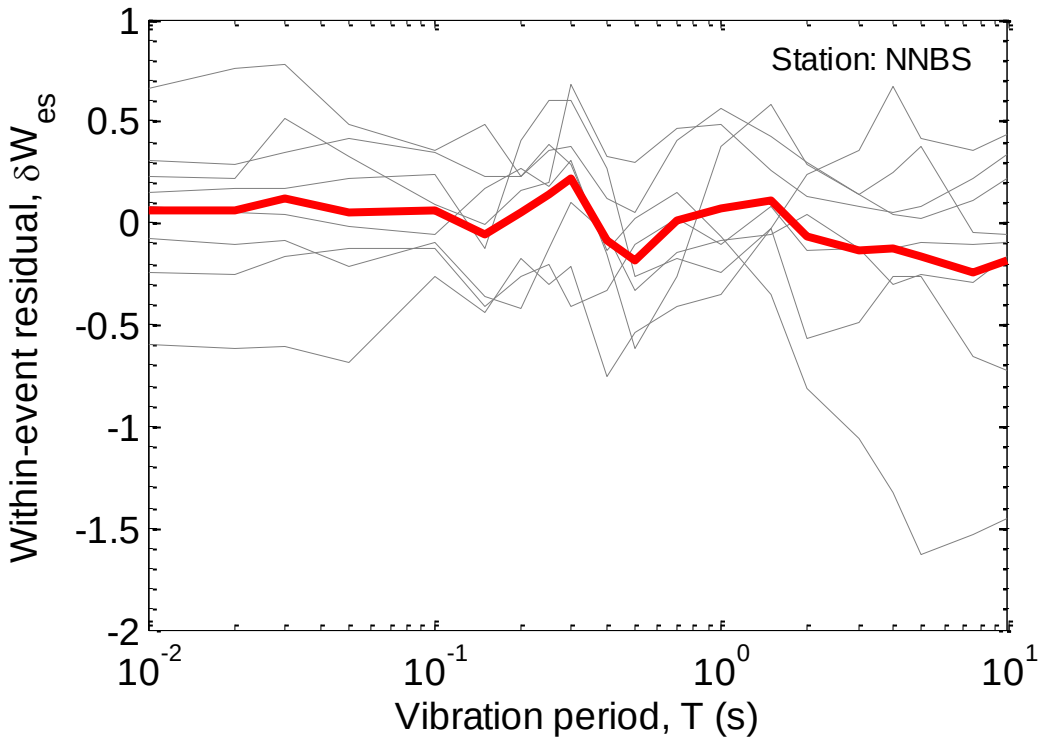
Station: NNBS
Within-event residual, δW_es
1
0.5
0
-0.5
-1
-1.5
-2
10^-2
10^-1
10^0
10^1
Vibration period, T (s)

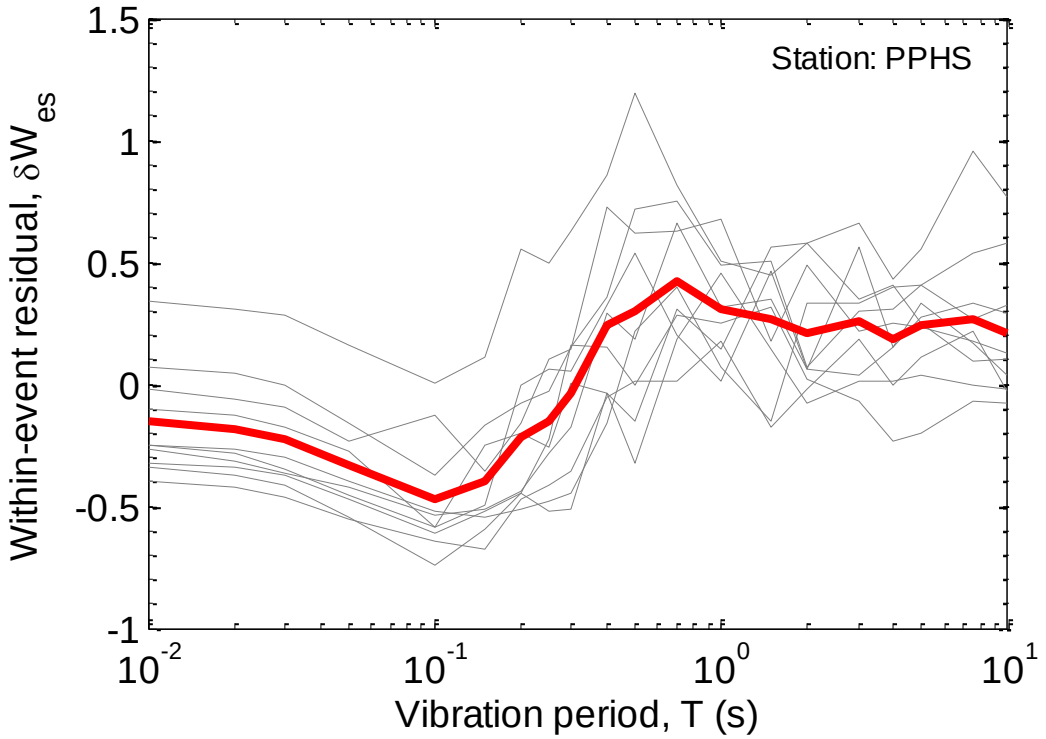
Station: PPHS
Within-event residual, δW_es
1.5
1
0.5
0
-0.5
-1
10^-2
10^-1
10^0
10^1
Vibration period, T (s)

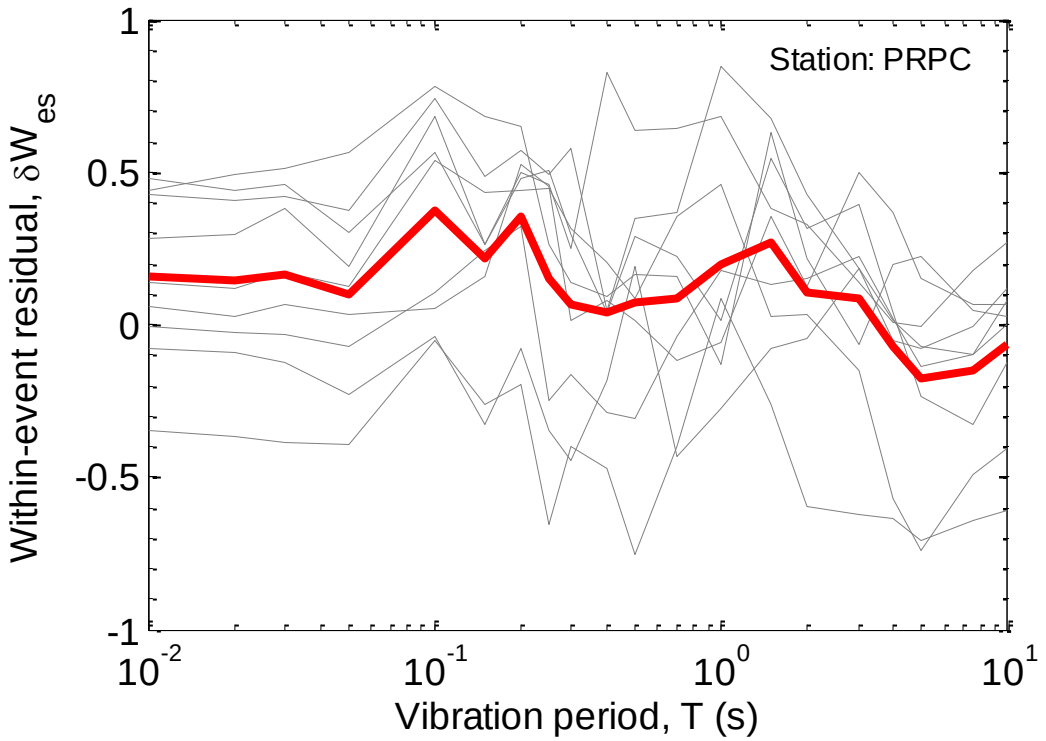
Station: PRPC
Within-event residual, δW_es
1
0.5
0
-0.5
-1
10^-2
10^-1
10^0
10^1
Vibration period, T (s)

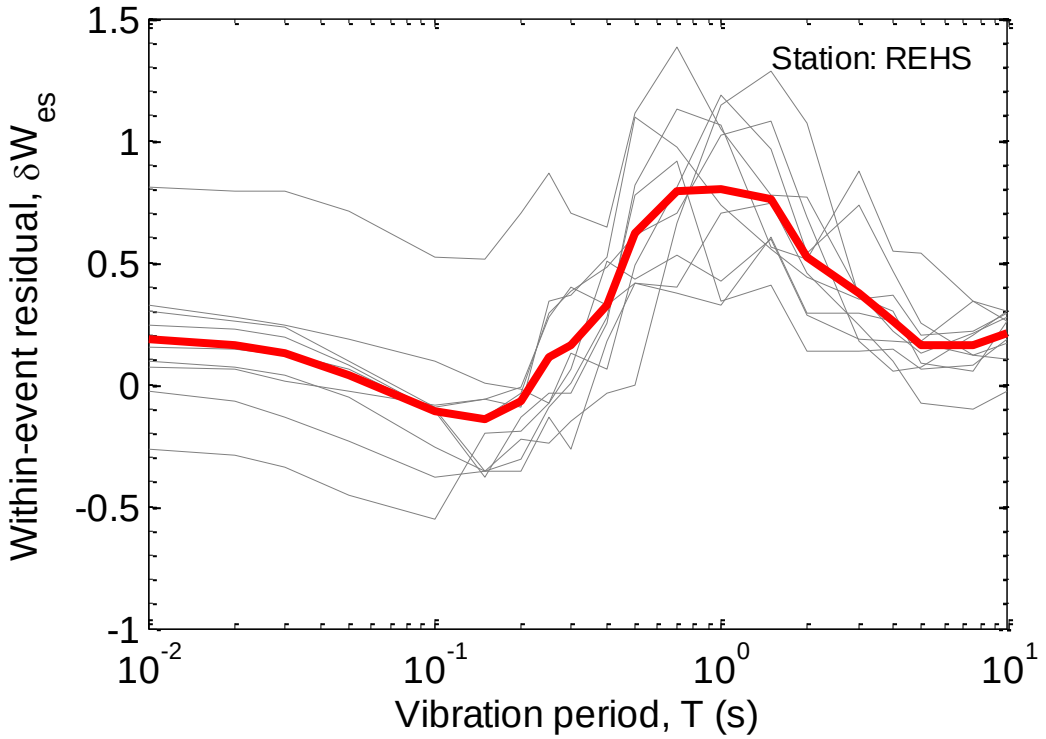
Station: REHS
Within-event residual, δW_es
1.5
1
0.5
0
-0.5
-1
10^-2
10^-1
10^0
10^1
Vibration period, T (s)

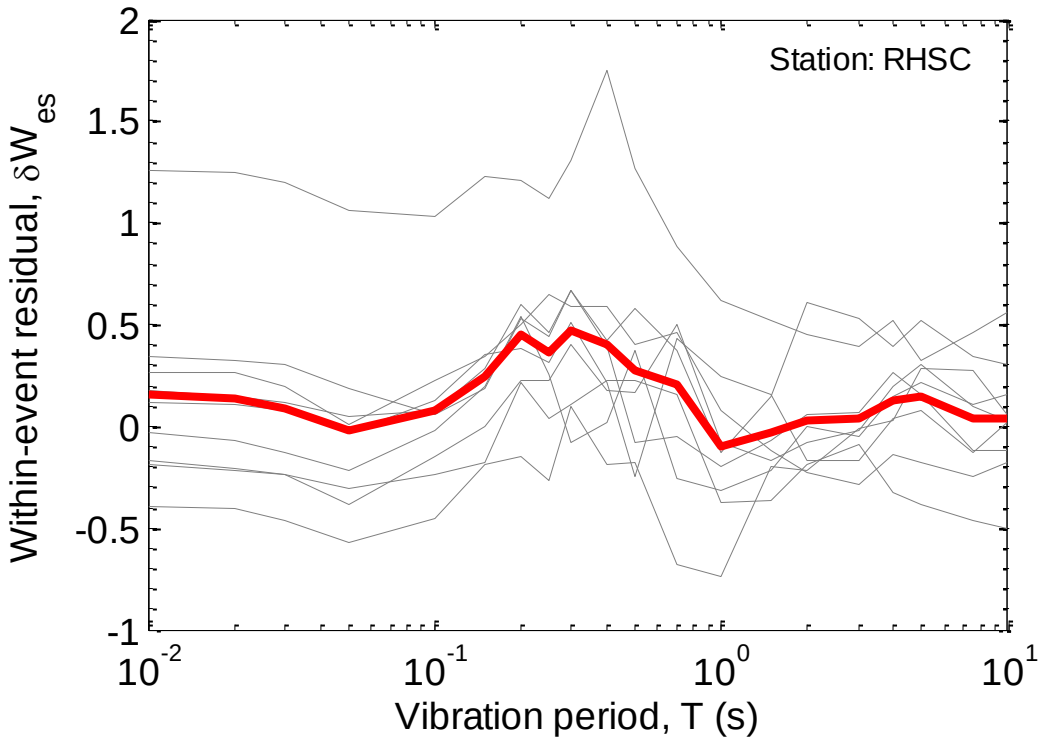
Station: RHSC
Within-event residual, δW_es
2
1.5
1
0.5
0
-0.5
-1
10^-2
10^-1
10^0
10^1
Vibration period, T (s)

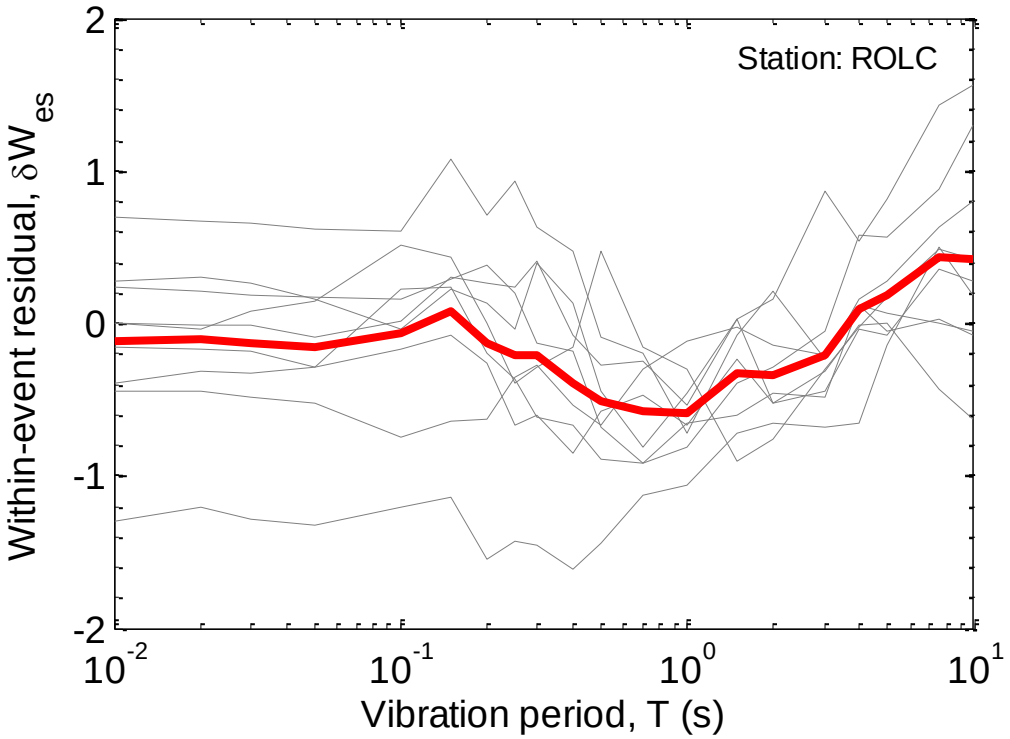
Station: ROLC
Within-event residual, δW_es
2
1
0
-1
-2
10^-2
10^-1
10^0
10^1
Vibration period, T (s)

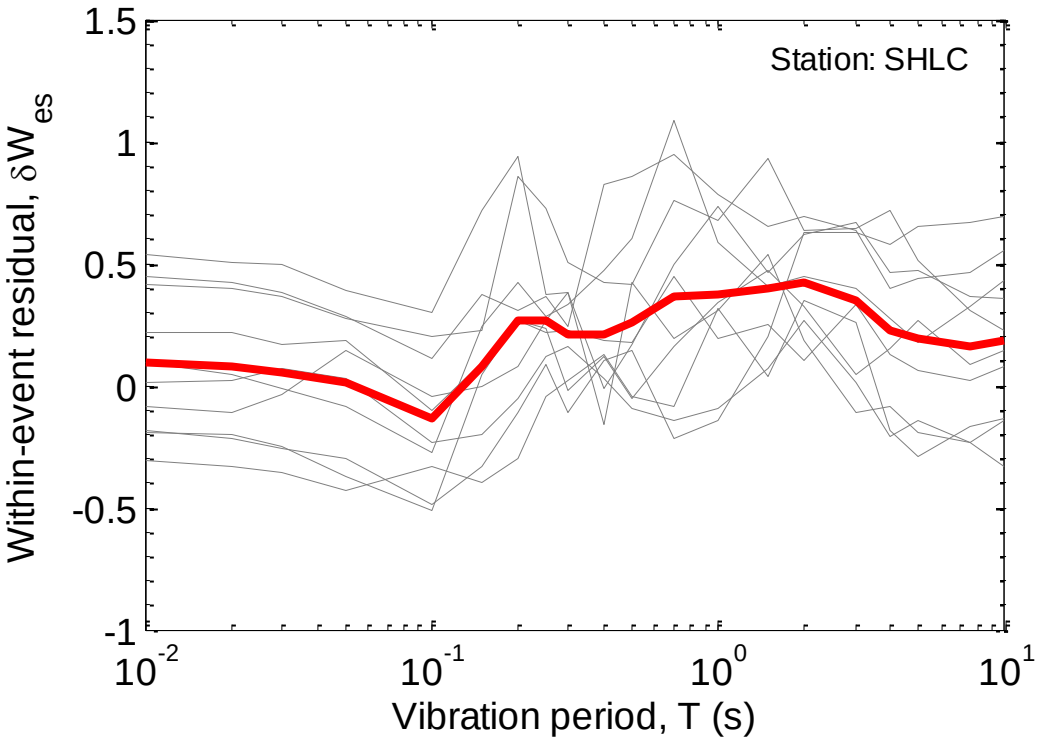
Station: SHLC
Within-event residual, δW_es
1.5
1
0.5
0
-0.5
-1
10^-2
10^-1
10^0
10^1
Vibration period, T (s)

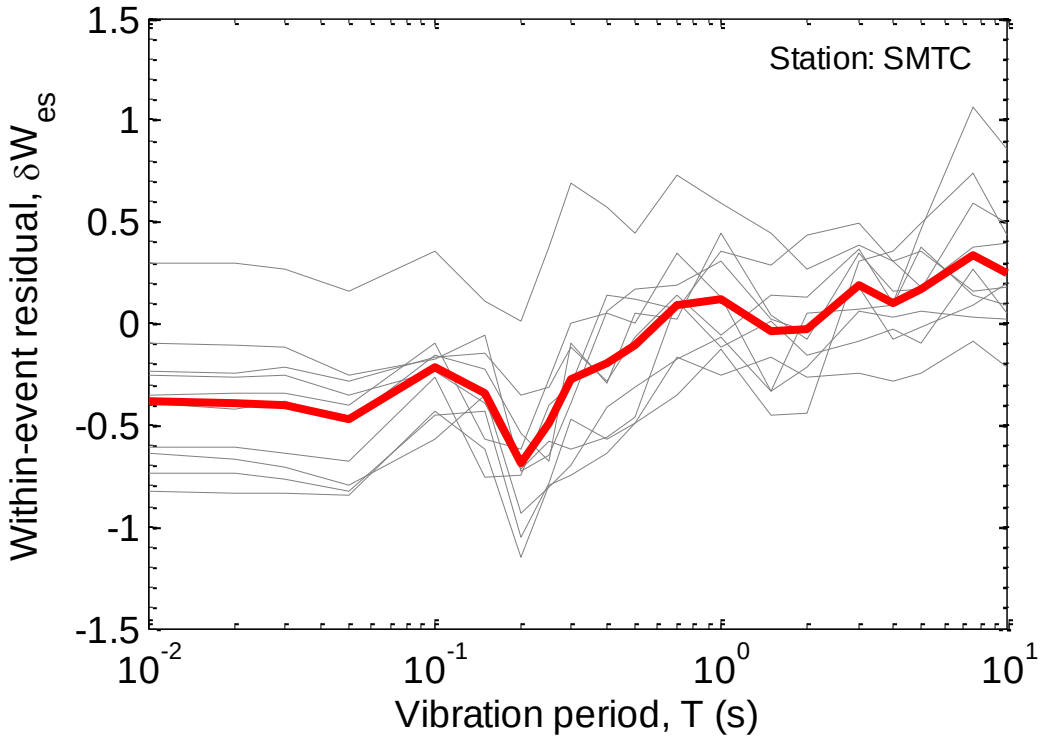
Station: SMTC
Within-event residual, δW_es
1.5
1
0.5
0
-0.5
-1
-1.5
10^-2
10^-1
10^0
10^1
Vibration period, T (s)

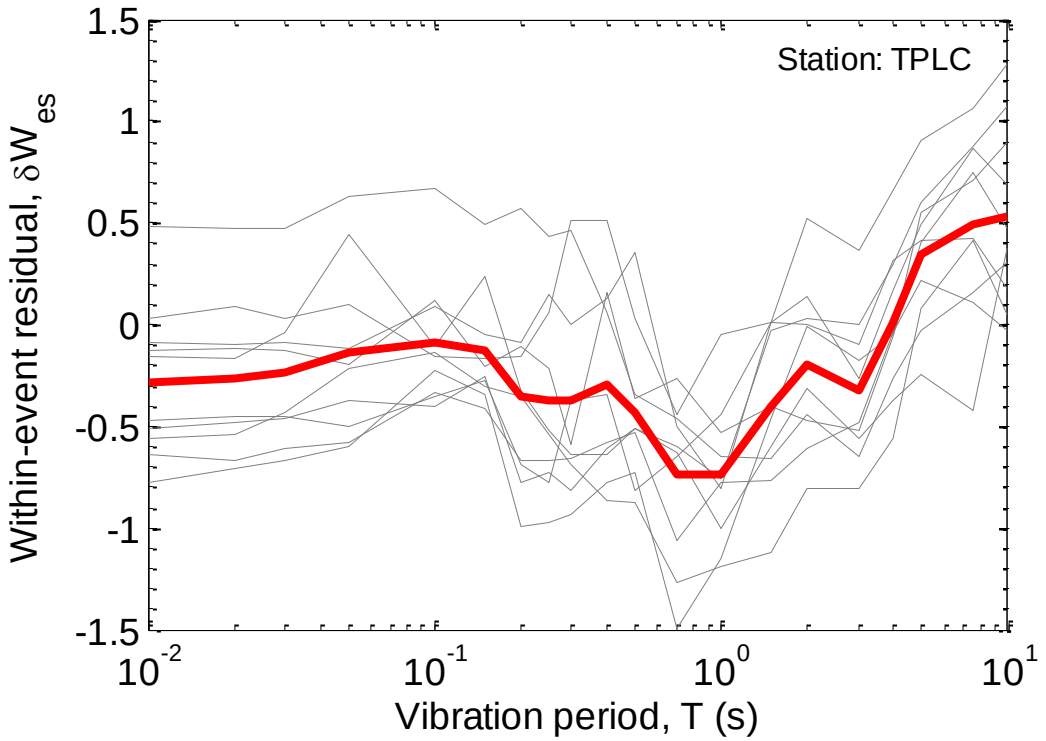
Station: TPLC
Within-event residual, δW_es
1.5
1
0.5
0
-0.5
-1
-1.5
10^-2
10^-1
10^0
10^1
Vibration period, T (s)